1992

RPH preliminary design, trend analysis and initial analysis of the NPS Hummingbird.

Vandiver, James L.

Monterey, California. Naval Postgraduate School

REPORT DOCUMENTATION PAGE

1a. REPORT SECURITY CLASSIFICATION UNCLASSIFIED		1b. RESTRICTIVE MARKINGS	
2a. SECURITY CLASSIFICATION AUTHORITY		3. DISTRIBUTION/AVAILABILITY OF REPORT Approved for public release; distribution is unlimited.	
2b. DECLASSIFICATION/DOWNGRADING SCHEDULE			
4. PERFORMING ORGANIZATION REPORT NUMBER(S)		5. MONITORING ORGANIZATION REPORT NUMBER(S)	
6a. NAME OF PERFORMING ORGANIZATION Naval Postgraduate School	6b. OFFICE SYMBOL *(If applicable)* 31	7a. NAME OF MONITORING ORGANIZATION Naval Postgraduate School	
6c. ADDRESS (*City, State, and ZIP Code*) Monterey, CA 93943-5000		7b. ADDRESS (*City, State, and ZIP Code*) Monterey, CA 93943-5000	
8a. NAME OF FUNDING/SPONSORING ORGANIZATION	8b. OFFICE SYMBOL *(If applicable)*	9. PROCUREMENT INSTRUMENT IDENTIFICATION NUMBER	
8c. ADDRESS (*City, State, and ZIP Code*)		10. SOURCE OF FUNDING NUMBERS	
		Program Element No.	Project No.	Task No.	Work Unit Accession Number

11. TITLE *(Include Security Classification)*
RPH Preliminary Design, Trend Analysis and Initial Analysis of the NPS Hummingbird

12. PERSONAL AUTHOR(S) Vandiver, James L.

13a. TYPE OF REPORT	13b. TIME COVERED	14. DATE OF REPORT *(year, month, day)*	15. PAGE COUNT
Master's Thesis	From To	1992 September 24	104

16. SUPPLEMENTARY NOTATION
The views expressed in this thesis are those of the author and do not reflect the official policy or position of the Department of Defense or the U.S. Government.

17. COSATI CODES			18. SUBJECT TERMS *(continue on reverse if necessary and identify by block number)*
FIELD	GROUP	SUBGROUP	RPH, DESIGN

19. ABSTRACT *(continue on reverse if necessary and identify by block number)*

The Department of Aeronautics and Astronautics at the Naval Postgraduate School (NPS) is expanding its helicopter research capabilities in order to facilitate present and future research demands. The rapidly changing needs have already out paced available assets. Therefore it was necessary to design and develop a new remotely piloted helicopter (RPH) that would meet present needs, NOTAR and HHC, and be flexible enough to meet future needs. The research efforts encompassed by this thesis are defining the present needs, investigating what type/size of RPH would fulfill these needs, procuring this asset, and analyzing its capabilities. Based on a defined payload, helicopter trends are analyzed to determine an estimate of the overall RPH size (gross weight) and engine size required. A preliminary design process validates these figures. Choosing to procure an RPH instead of building one, a detailed performance analysis is conducted on the main rotor system. This analysis includes blade vibration analysis, retreating blade stall analysis, and power required analysis. Modification of the RPH's main rotor hub, drive train, and landing gear are studied and recommendations presented. This research effort is a continuation of a long-term program to provide NPS with robust assets to support present and future rotorcraft research efforts.

20. DISTRIBUTION/AVAILABILITY OF ABSTRACT	21. ABSTRACT SECURITY CLASSIFICATION	
☐ UNCLASSIFIED/UNLIMITED ☐ SAME AS REPORT ☐ DTIC USERS	Unclassified	
22a. NAME OF RESPONSIBLE INDIVIDUAL E. Roberts Wood	22b. TELEPHONE *(Include Area code)* (408) 646-2897	22c. OFFICE SYMBOL AAWD

Approved for public release; distribution is unlimited.

RPH Preliminary Design,Trend Analysis
and
Initial Analysis of
the NPS Hummingbird

by

James L. Vandiver
Lieutenant , United States Navy
B.S., United States Naval Academy

Submitted in partial fulfillment
of the requirements for the degree of

MASTER OF SCIENCE IN AERONAUTICAL ENGINEERING

from the

NAVAL POSTGRADUATE SCHOOL
September 1992

ABSTRACT

The Department of Aeronautics and Astronautics at the Naval Postgraduate School (NPS) is expanding its helicopter research capabilities in order to facilitate present and future research demands. The rapidly changing needs have already out paced available assets. Therefore it was necessary to design and develop a new remotely piloted helicopter (RPH) that would meet present needs, NOTAR and HHC, and be flexible enough to meet future needs. The research efforts encompassed by this thesis are defining the present needs, investigating what type/size of RPH would fulfill these needs, procuring this asset, and analyzing its capabilities. Based on a defined payload, helicopter trends are analyzed to determine an estimate of the overall RPH size (gross weight) and engine size required. A preliminary design process validates these figures. Choosing to procure an RPH instead of building one, a detailed performance analysis is conducted on the main rotor system. This analysis includes blade vibration analysis, retreating blade stall analysis, and power required analysis. Modification of the RPH's main rotor hub, drive train, and landing gear are studied and recommendations presented. This research effort is a continuation of a long- term program to provide NPS with robust assets to support present and future rotorcraft research efforts.

TABLE OF CONTENTS

I. INTRODUCTION

Helicopter research in the Department of Aeronautics and Astronautics at the Naval Postgraduate School (NPS) is rapidly accelerating. This fast pace has created a need for expanding the capabilities of the department's Remotely Piloted Vehicles (RPV). Valuable research has been accomplished through the employment of the existing RPVs. The GMP Legend, a commercially produced radio controlled (RC) helicopter, was used to produce baseline vibration analysis and to validate measurement techniques. The results from this work will be of great value in subsequent Higher Harmonic Control (HHC) research. The Bruiser, a limited production, 20 pound payload RPV developed by Pacific RPV, was used in a shake test to obtain an airframe modal analysis.

The preceding research has been of great value to the department, but in order to advance beyond proof of concept and into scale model analysis, a new helicopter was required. Incorporated in the requirements were a helicopter with a tip speed and chord which produced a Reynolds number that was within an acceptable range for comparison with a full scale helicopter; a helicopter of a size large enough to carry a No-Tail-Rotor (NOTAR) tail boom

that would also be testable in the quarter scale (14 by 22 foot) wind tunnel at NASA Langley; and a helicopter with enough flexibility to be adaptable to future research needs. This impetus developed the challenge of designing a suitable RPV for the department.

A critical amount of background knowledge and direction was obtained on a research trip to the Aerostructures Directorate at NASA Langley. They were heavily involved in the design, manufacture and test of their own Free-Flight Rotorcraft Research Vehicle (FFRRV), which was directly along the same lines of interest of NPS. Their RPV was twice the size and considerably more complex than that desired by NPS. The head of the directorate, Arthur E. Phelps III, was invaluable in passing on their corporate knowledge, saving untold hours in achieving the NPS goal.

II. BACKGROUND

A. HIGHER HARMONIC CONTROL (HHC)

The control of vibrations has always been of great concern to both the helicopter designer and to the helicopter pilot. It has been a continuing source of agitation throughout the years and a focus of enormous amounts of research assets. The current means by which the vibrations are reduced are through passive devices which either isolate the source of vibration (isolators) or diffuse the vibration level (absorbers). These vibration absorption mechanisms are usually restricted to a narrow scope of flight conditions and vibratory frequencies. The use of HHC, a relatively new technology, is an active vibration reduction device, vice the passive ones just mentioned. HHC functions by altering the aerodynamic loads on the rotor, and therefore the vibratory forces and moments which cause the airframe to vibrate are reduced. [Ref. 1]

In earlier full scale HHC testing on the Hughes Helicopter OH-6A, it was determined that not only were the vibrations successfully reduced, but the performance of the helicopter was also improved. Other helicopter companies tried to duplicate this resulting improved performance but were unsuccessful. Corroborating this performance

enhancement locally would have great merit. The RPVs on hand did not allow this type of research to be conducted because they could not produce Reynolds numbers over the main rotor blade that would allow data comparison with the data obtained on the OH-6A. A helicopter with a tip speed and chord length that would produce Reynolds numbers on the order of two million was required. This shortcoming provided some of the drive to obtain a new helicopter RPV.

B. NOTAR

Presently, Lt. M. Borno, in conjunction with McDonnell Douglas Helicopter Corporation, is conducting thesis research which will produce a fully operational scale model NOTAR tailboom. The tailboom requirement was that it was to be big enough to test in the quarter scale wind tunnel at NASA Langley. The current RPVs lacked the size to mechanically support and drive a tailboom of this scale. This was a second driver behind acquiring a new helicopter RPV.

C. AUTONOMOUS LANDING AND TAKEOFF SYSTEM (ALTOS)

The United States Navy's growing interest in RPVs and their fleet applications has now reached a point which requires significant background research. As the Navy leans toward fully autonomous RPVs, it lacks experience and expertise in the most effective and efficient means to

launch and recover these vehicles. Recently, Orion Aviation entered into a contract with the United States Navy in conjunction with NPS to develop and test five potential ALTOS concepts and have them analyzed for merit by students at NPS. Once the best ALTOS concept is determined, it will be built by Orion Aviation and then will be demonstrated using an NPS RPV. The expanded capabilities that the new NPS RPV would add to the existing resources would provide greater flexibility in the demonstration and validation phase of the ALTOS program.

III. DEVELOPING SCALE MODEL TRENDS

There is a great deal of documentation for the design of full scale helicopters regardless of weight range, but there exits little or no documentation for design of a scale model helicopter. It was necessary to determine trends for gross weight, takeoff weight, disk loading (DL), rotor radius, solidity (σ), and blade loading (BL) from full scale helicopters in order to determine what the values should be for quarter-scale size. The trends that were developed were typically linear with an adjustment of either the x-intercept or the y-intercept usually required. The adjustment was made assuming the trends held true for all weight ranges, but at the lower weights the line had to be shifted to accommodate scale sizes. The trends that were generated show this assumption to be good.

The first trend determined was between the load a helicopter could carry versus the gross weight of the helicopter. Fig. 1 shows data for thirteen different full scale helicopters plus the Bruiser.

A linear trend analysis produced Eqn. 1:

$$Payload = 270 + \frac{Gross\ Weight}{4.52} \qquad (1)$$

The slope of the line was assumed to be true for all weight ranges, but the y-intercept was decreased for gross weight

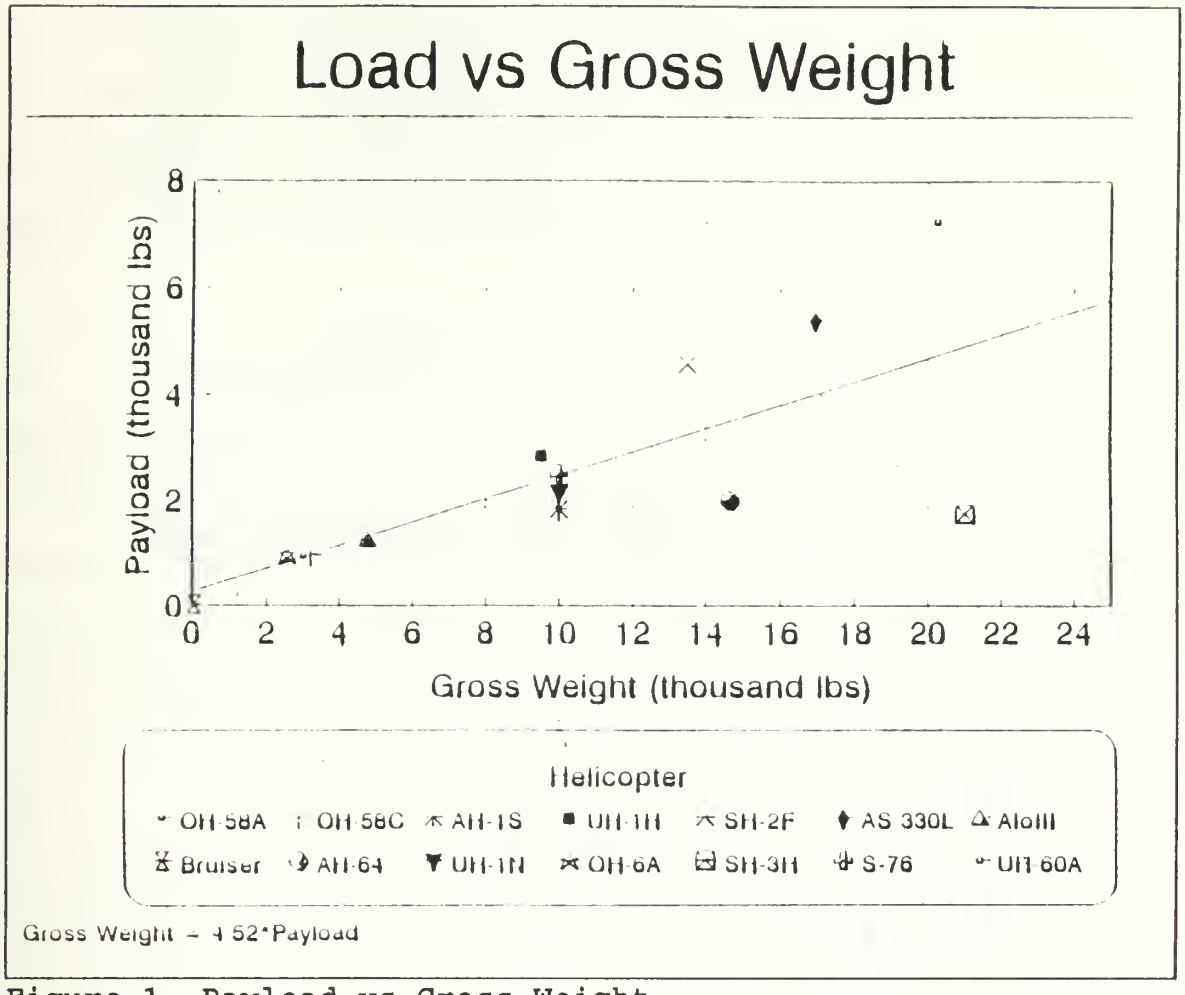

Figure 1 Payload vs Gross Weight

less than 500 pounds. The final equation that was determined is shown in Eqn. 2.

$$Gross\ Weight = 4.52 * Payload \quad (2)$$

The needs as stated in the previous chapter required a payload of between 20 and 30 pounds. This equates to a helicopter between 90 and 135 pounds.

The next trend that was studied was takeoff weight versus usable power. The desire was to use this trend to provide a general idea of what power would be required based on the above weight range. The trend shown in Fig. 2 was used to derive Eqn. 3.

$$Usable\ Power = -70.66 + \frac{Takeoff\ Weight}{7.38} \qquad (3)$$

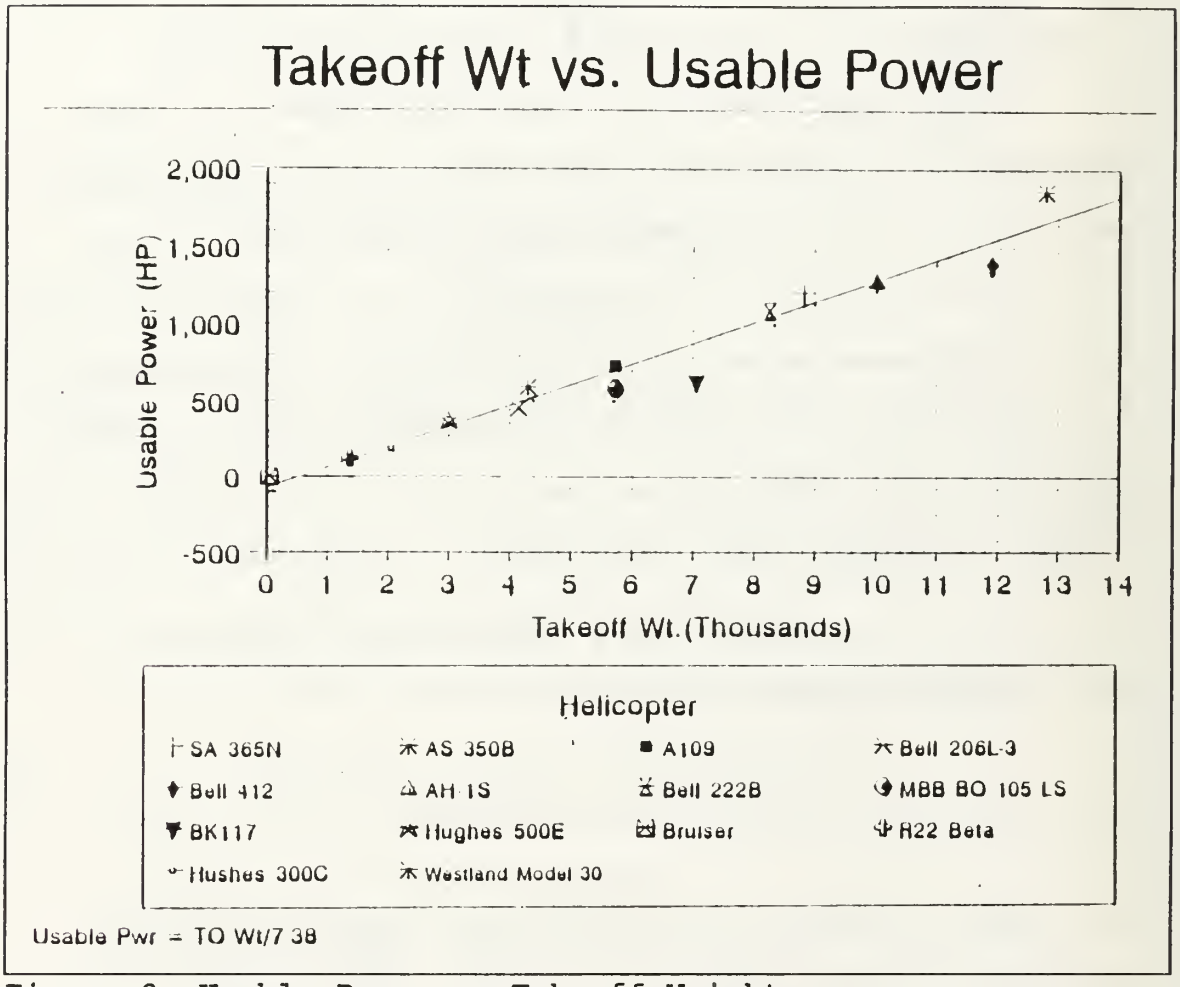

Figure 2 Usable Power vs Takeoff Weight

Again, assuming the slope was accurate over the entire weight range, the intercept point was dropped to zero. The final equation is shown below. This equation shows that power required would range between 12 to 18 horsepower.

$$Usable\ Power = \frac{Takeoff\ Weight}{7.38} \qquad (4)$$

Next, the main rotor blade solidity and blade loading (Ct/σ) versus takeoff weight were compared. Fig. 3 shows that main rotor blade solidity is independent of takeoff weight. The minimum solidity was found to be 0.03 for the Robinson R-22 Beta. The maximum solidity was 0.098 for the Aerospatiale AS 332 L1. The average solidity was approximately 0.07. Fig. 4 shows a similar trend to that of the blade solidity. The blade loading was also independent of takeoff weight. The minimum was 0.05 for the Bell 412. The maximum was 0.095 for
the Aerospatiale SA 365N, and the average was 0.075.

The typical disk loading (DL) for model helicopters is between 1.0 and 2.0. Fig. 5 shows that the model helicopter does not fall within the normal range of full scale helicopters. The minimum full scale DL of 2.8 is that of

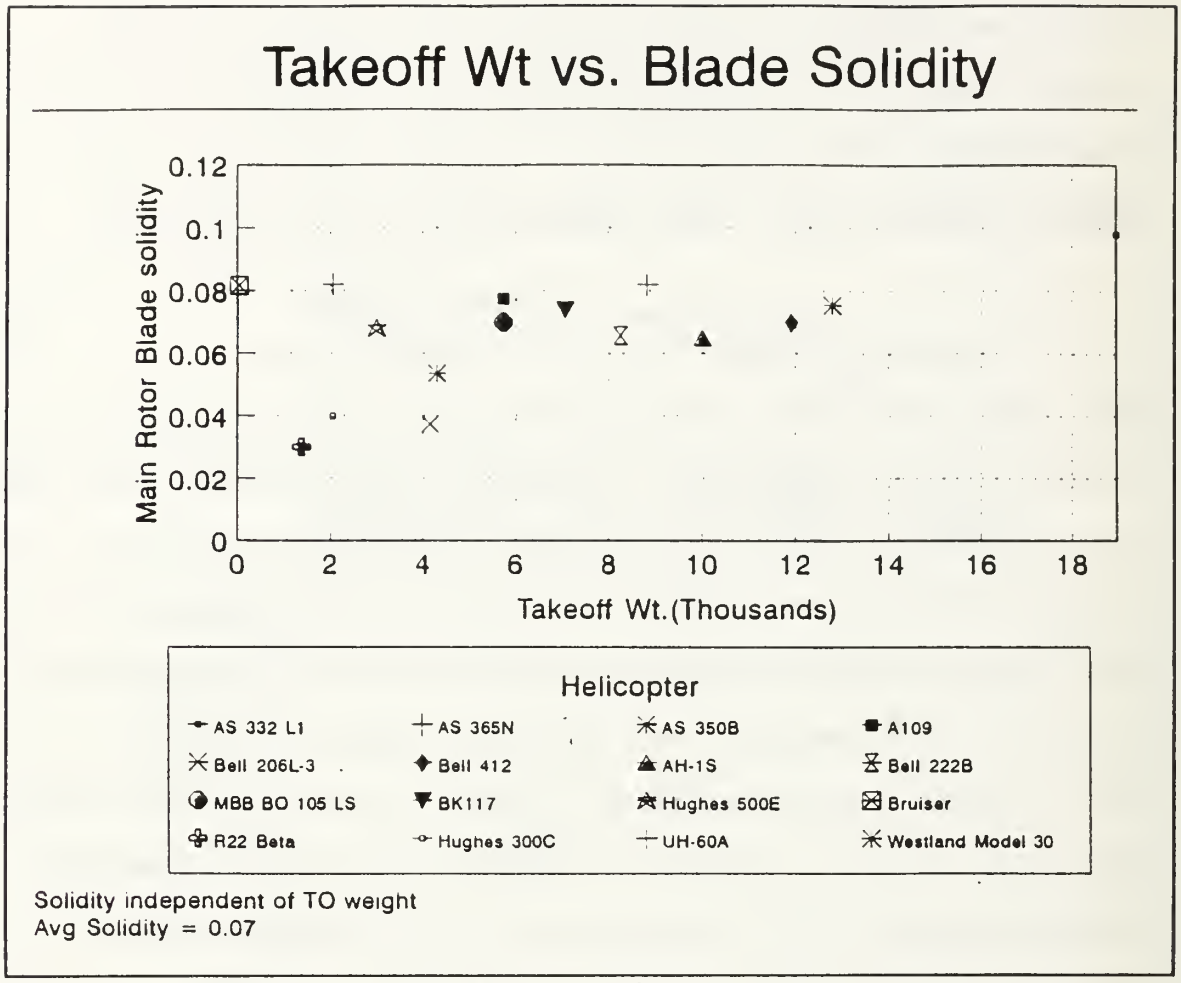

Figure 3 Solidity vs Takeoff Weight

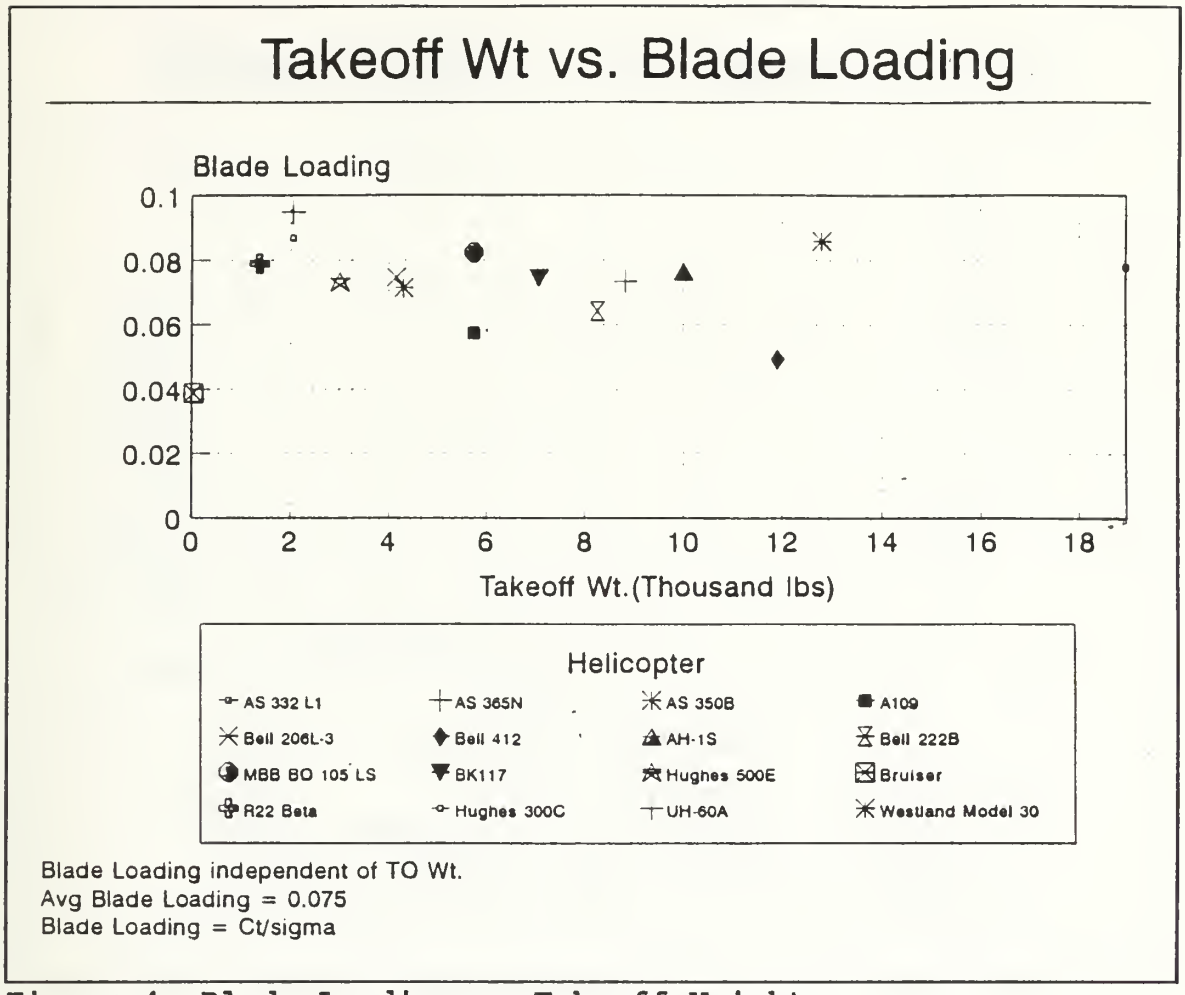

Figure 4 Blade Loading vs Takeoff Weight

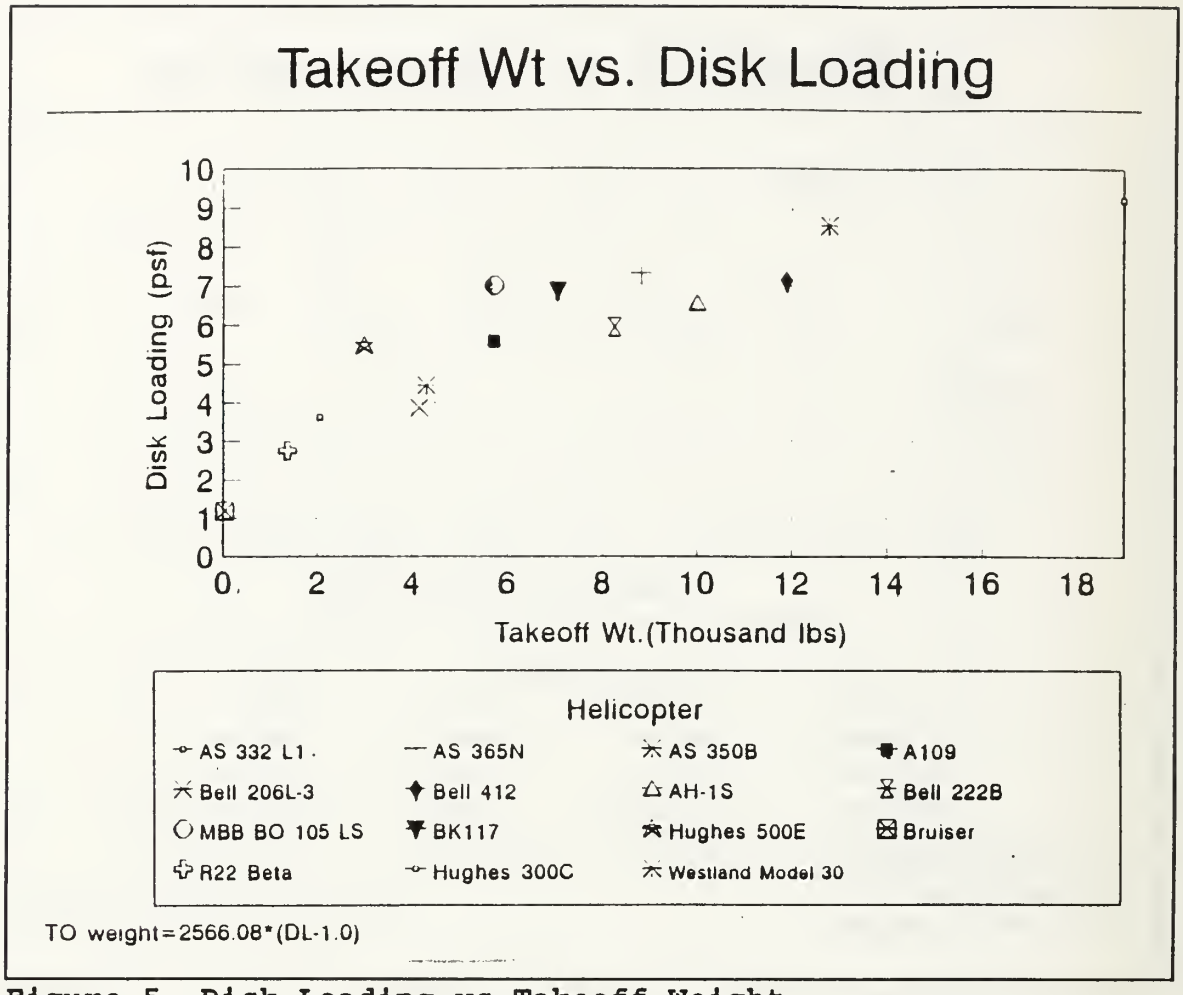

Figure 5 Disk Loading vs Takeoff Weight

the Robinson R-22. Full scale trends were inconclusive in providing guidelines for the model helicopter. Fig. 6 shows how power loading (PL) varies with disk loading. Power loading tells how much weight can be lifted for a given horsepower. The lower the DL, the greater the PL that can be achieved. In summary, the trend analysis shows that a desired payload of 20 to 30 pounds will require a helicopter weight between 90 and 135 pounds. An engine of 12 to 18

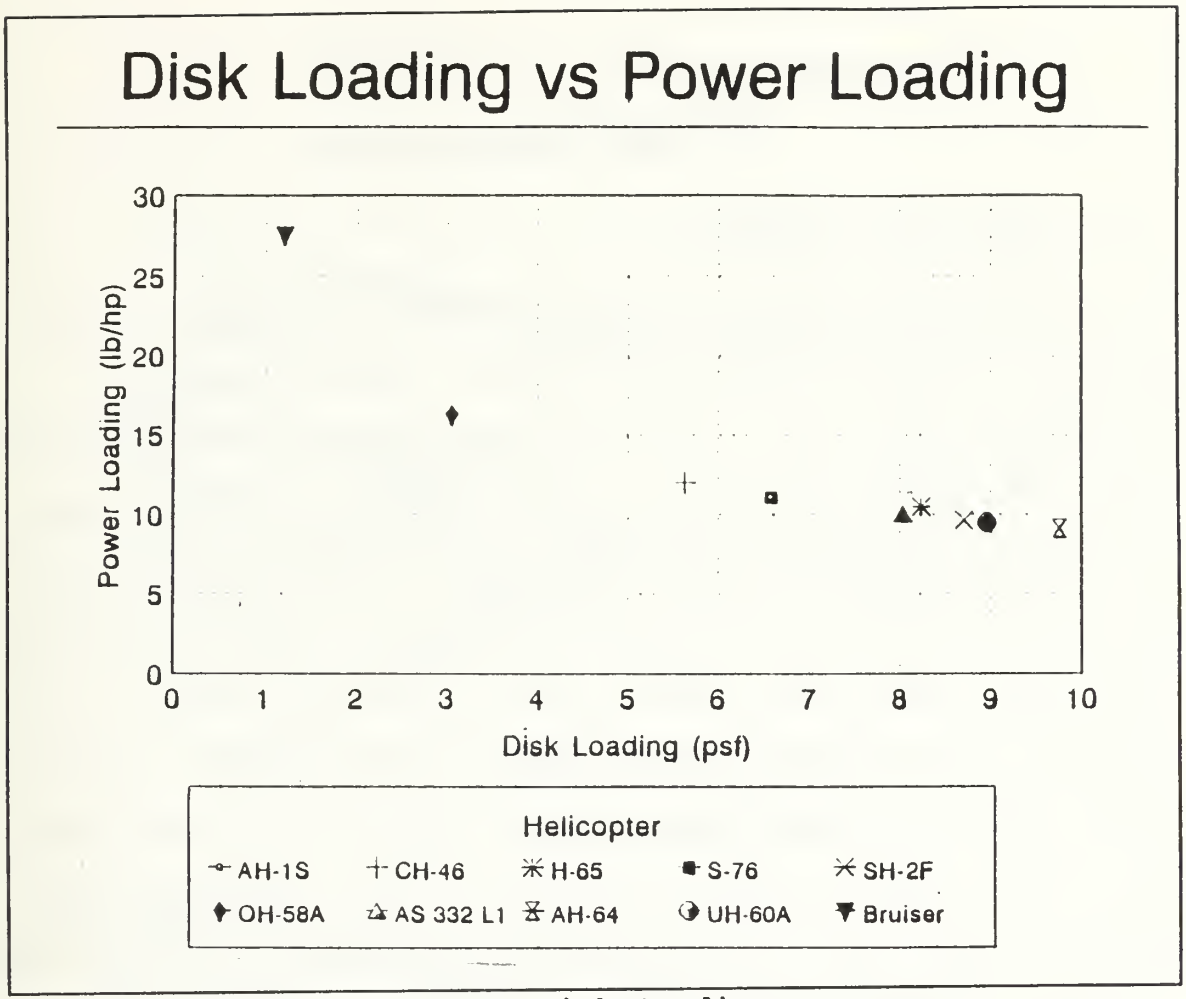

Figure 6 Power Loading vs Disk Loading

horsepower would be required for a helicopter in this weight range. The solidity should be in the vicinity of 0.07 and the BL should be in the vicinity of 0.075. These trends provide a good starting point for the design process and a very good point of comparison for the preliminary design results.

IV. PRELIMINARY DESIGN

A. CONSTRAINT DIAGRAM

The first task to accomplish was to construct a rotor blade tip speed constraint diagram. Based on industry criteria [Ref. 2:p. 90], a tip speed constraint diagram was made using the following limits. The upper boundary can either be set by a noise limit which is 750 fps or a hover tip mach number limit which is M<0.69 (771 fps). The hover tip mach number was used for this constraint diagram. The lower limit is set by requirement to store kinetic energy in the rotor system in case of power failure, in other words an autorotational limit. This limit is set at 400 fps. Two other limits that are important to consider are that of the advancing blade tip mach number limit and the advance ratio (μ) limit. The advancing blade tip mach number limit is set at M<0.8 to avoid compressibility effects on the advancing blade in forward flight. The advance ratio is set at μ<0.4 to avoid retreating blade stall at maximum forward speeds. One additional limit was incorporated to show the lower Reynolds number limit of 1.5 million. Fig. 7 depicts the constraint diagram developed using the above parameters.

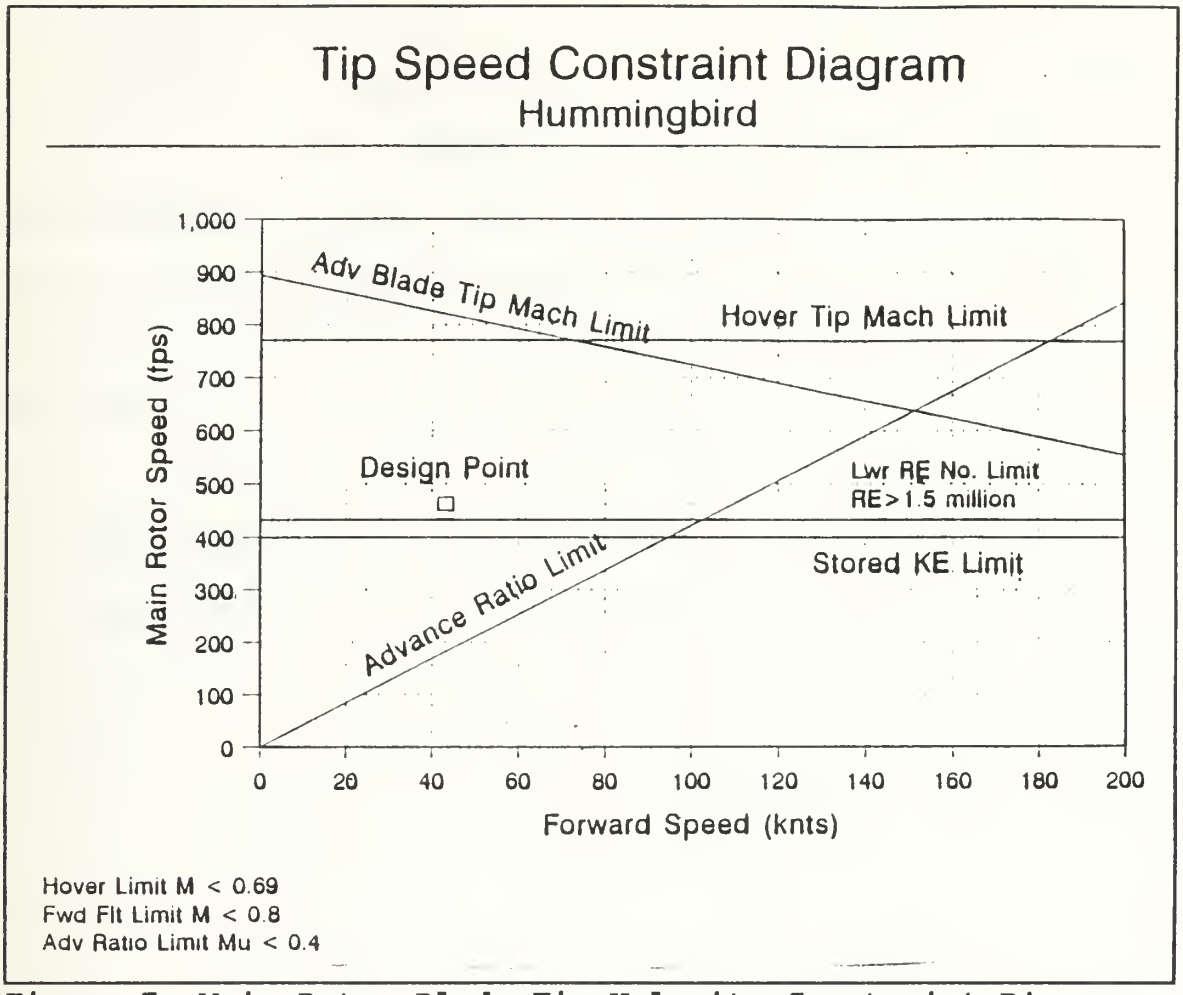

Figure 7 Main Rotor Blade Tip Velocity Constraint Diagram

B. PRELIMINARY ESTIMATES

1. Gross Weight and Blade Radius

Ref. 3 outlines basic steps to quickly estimate the gross weight and rotor radius. Using these steps, the following calculations were made:

Fuel Required

(0.5 lb/hp-hr) Piston Engine

Mission time 60 minutes

Fuel required = (1.0)(25)(0.5)= 12.5 lbs of fuel*

*This is approximately two gallons.

Usable Load (UL)

UL = crew + payload + fuel

UL = 0 + 30 + 12.5 = 42.5 lbs

Assuming 1970 technology, Fig. 8 shows a useful load per gross weight factor of 0.4 [Ref. 3:p. 641].

Gross Weight = 90.6 lbs.

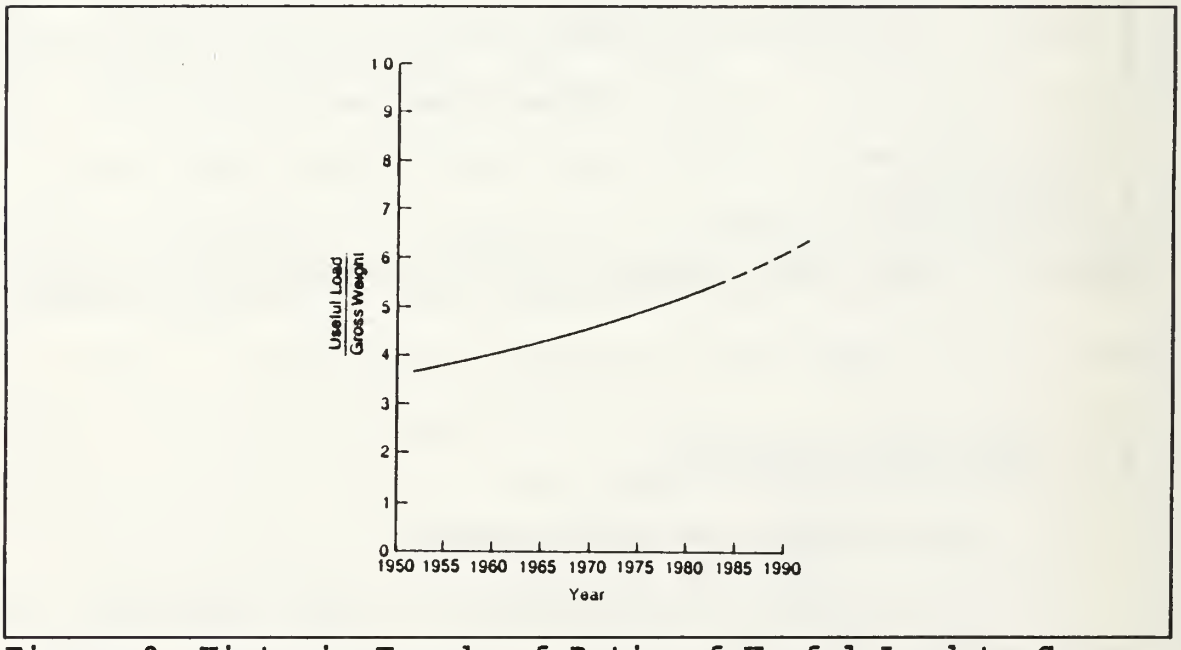

Figure 8 Historic Trends of Ratio of Useful Load to Gross Weight

This number for gross weight falls within the range developed by the trends analysis, though it is on the low side for a payload of 30 pounds. Realizing that the design

weight of any design will grow, it is assumed that the higher weight is more reasonable; therefore, a 130 lb gross weight will be used for the following estimates. Based on this weight and the DL range from 1.0 to 2.0, the rotor radius ranges from 4.55 to 6.43 feet. This rotor radius range is validated by calculation of required blade area as described in Ref. 2. Assuming a maximum forward velocity (V_{max}) of 70 knots, Fig. 9 shows that blade area required is 5.5 square feet, which is 1.83 ft^2 per blade for a three blade system and 1.375 ft^2 for a four blade system. This translates into a radius of 4.9 ft, a DL of 1.74 lb/ft^2 with a chord of 0.375 ft (4.45 in) for the three blade system, and a radius of 4.7 ft, a DL of 1.86 and a chord of 0.292 ft (3.5 inches) for the four blade system.

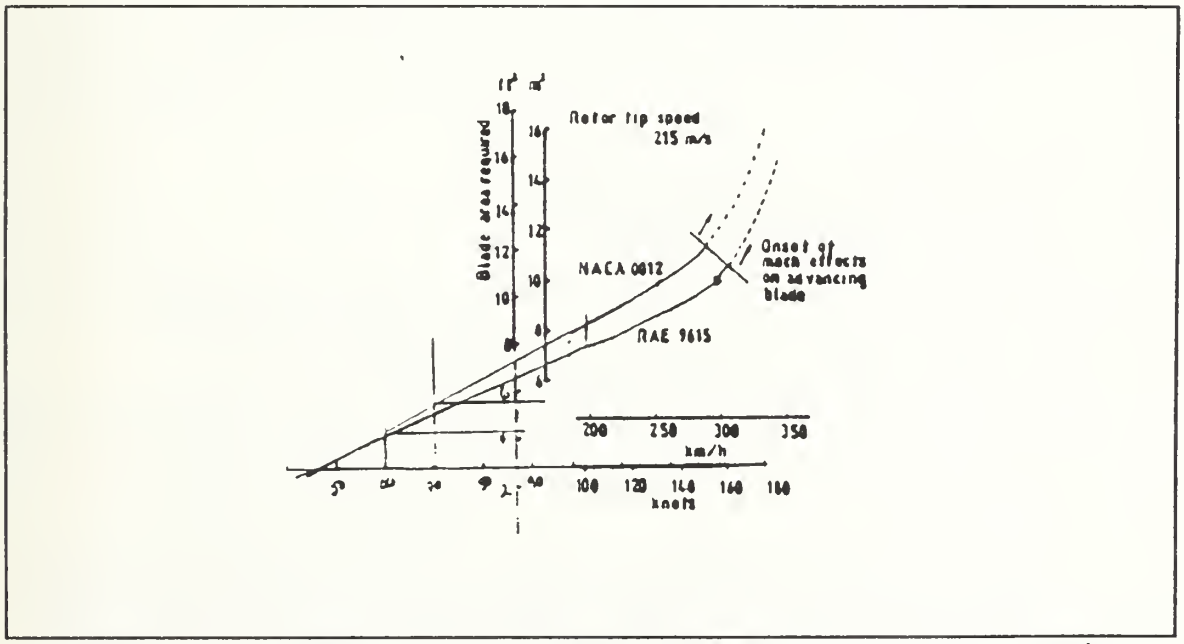

Figure 9 Determination of Blade Area for New Rotor Design

Either of the above systems would be feasible for this design, but the four blade system does have two distinct advantages. First, the blade vibrations in a four blade system are less than those in a three blade system. Second, the aspect ratio (AR) of the three blade system is 13.1 and the AR for the four blade system is 16.1. The normal range for AR is 15 to 20. Any blade below that will have a lower blade efficiency due to tip losses and any blade above that could pose structural problems.

2. One Hour Estimate

In this estimate, there are two constraints: hover out of ground effect (HOGE) and high forward speed flight. The following is a list of the tentative performance requirements:

Payload	20-30 lbs
Crew	0 lbs
Max Speed @ S.L.	70 knots
Cruise Speed ($0.9*V_{max}$)	63 knots
Vertical Rate of Climb	450 fpm @ 4000 ft 95 deg. F

Engine: One - Max continuous rating 25 BHP.

The following calculation as detailed in Ref. 4 will be done using the previous gross weight estimation of 130 lbs. Fig. 10 shows that for a weight of 130 lbs, the equivalent flat plate area (f_e) would be approximately 0.8 ft^2. [Ref. 5:p. 35]

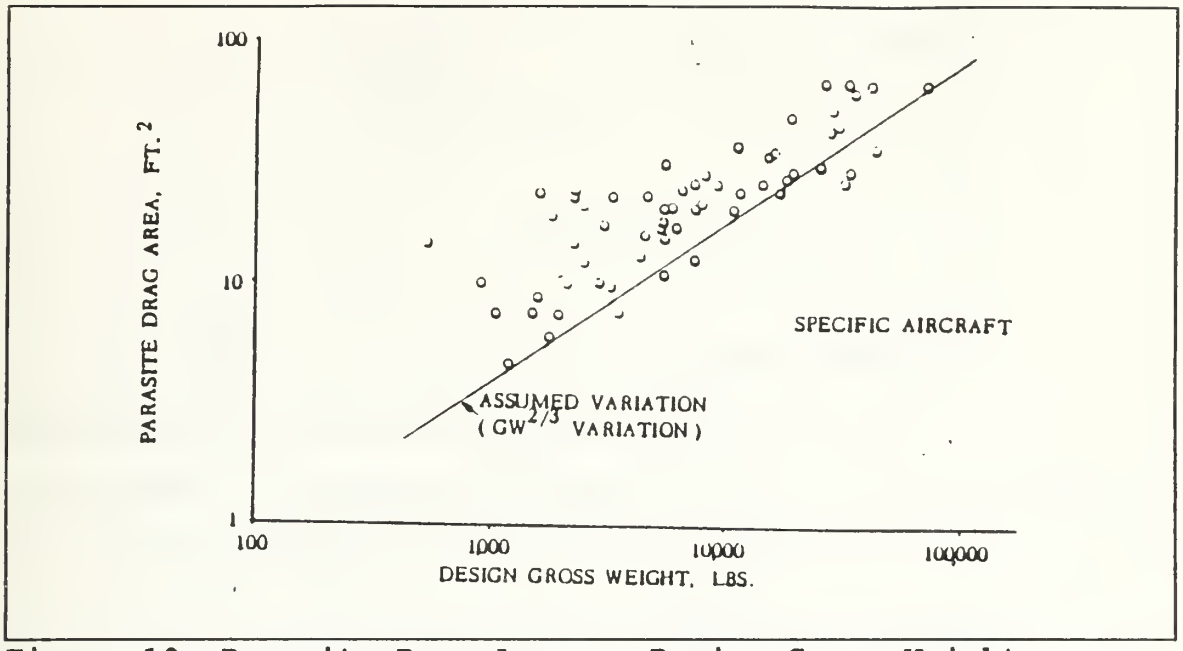

Figure 10 Parasite Drag Area vs Design Gross Weight

a. Maximum Forward Velocity (V_{max})

Assuming seventy percent of installed power is used to overcome parasite drag at high speeds, maximum sea level speed can be calculated.

$$V_{max} = 41 * [\frac{(30 \text{ min } rating\ eng)}{f_e}]^{\frac{1}{3}} \quad (5)$$

Maximum BHP = 25

Assuming Figure of Merit of 70%

THP = 17.5

V_{max} = 114 knots

Based on the assumption that the helicopter was to be derated to a power of 18 HP, the calculations would be changed as follows:

Maximum BHP = 18

Assuming Figure of Merit of 70%

THP = 12.6

V_{max} = 41*[12.6/.8]^(1/3)

V_{max} = 102 knots

b. Rotor Sizing

The preliminary size of the rotor is determined using the rate of climb (ROC) stated earlier. Additional power required to climb 450 fpm is approximately 10% of the power required for HOGE.

ROC 450 fpm @ 4000 ft 95 deg. F (95% of 17.5 THP)

95% of 17.5 hp = 16.63 hp

PL = 130 lb/16.63 hp = 7.82

From Fig. 11 the DL = 3.5 [Ref. 4:p. 8].

DL = Weight/(pi*R^2) = 3.5

R = 3.44 ft

Again assuming a derated engine,

95% of 12.6 hp = 12.0 hp

PL = 130 lb/12.0 hp = 10.83

From Fig. 11

DL = 1.75.

DL = Weight/(pi*R^2) = 1.75

R = 4.86 ft

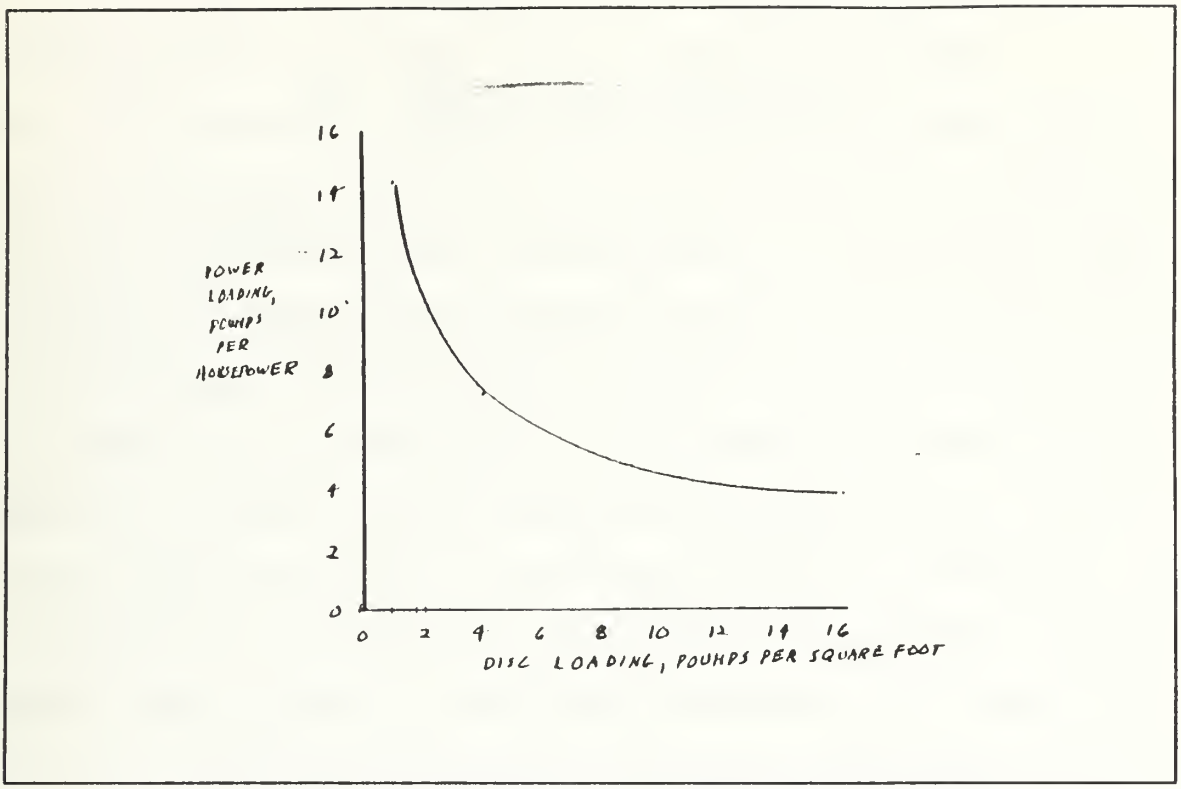

Figure 11 Rotor Performance for Design Conditions

c. Starting Point

The preceding calculations provide a good point at which to begin more in-depth design. In summation, the starting point is

Gross Weight 130 lbs

Empty Weight 87.5 lbs

Payload 30.0 lbs

Fuel Weight 12.5 lbs

Rotor Radius (R) = 4.86

Disk Loading (DL) = 1.75

3. Design from Scratch or Procure

Based on this data, there were two choices to make. First, design a helicopter from scratch which would meet the needs of the Aeronautics and Astronautics Department. While this is definitely an exceptional learning process, the end result would leave the department with a paper helicopter and at least a year's worth of manufacturing. The other path of choice was to look for a helicopter on the open market that closely approached the stated needs. The second alternative, being the most productive and time smart, was chosen. Though the possibility of locating a helicopter that would meet every need was slim, it was the best choice, realizing that the redesign of an existing, flying helicopter was much more frugal financially and time-wise.

V. HUMMINGBIRD ACQUISITION

A. CAPABILITIES

A helicopter of the correct size and payload capability was located at the GMP model helicopter company. The owner and designer, Mr. John Gorham, the lead engineer with Lockheed Corporation on the L-1011, had built ten 165 pound RPVs for the U.S. Army. Their original purpose was to be used as Soviet Hind-D recognition devices. This vehicle was nearly ideal for meeting the needs of the department. There were some shortfalls, which will be mentioned in the next section, but nothing of a critical nature that could not be redesigned or changed. The department purchased one of Mr. Gorham's helicopters, with the desire to purchase a second. The initial RPH was named Hummingbird I. The purpose of buying two helicopters is to allow for concurrent HHC, NOTAR, and ALTOS research. One helicopter would be used in its original configuration for NOTAR and ALTOS research. The other would be converted into a platform capable of HHC research. Fig. 12 contains two pictures of the Hummingbird. Table I contains a list of the Hummingbird characteristics and capabilities as it was received from Mr. Gorham.

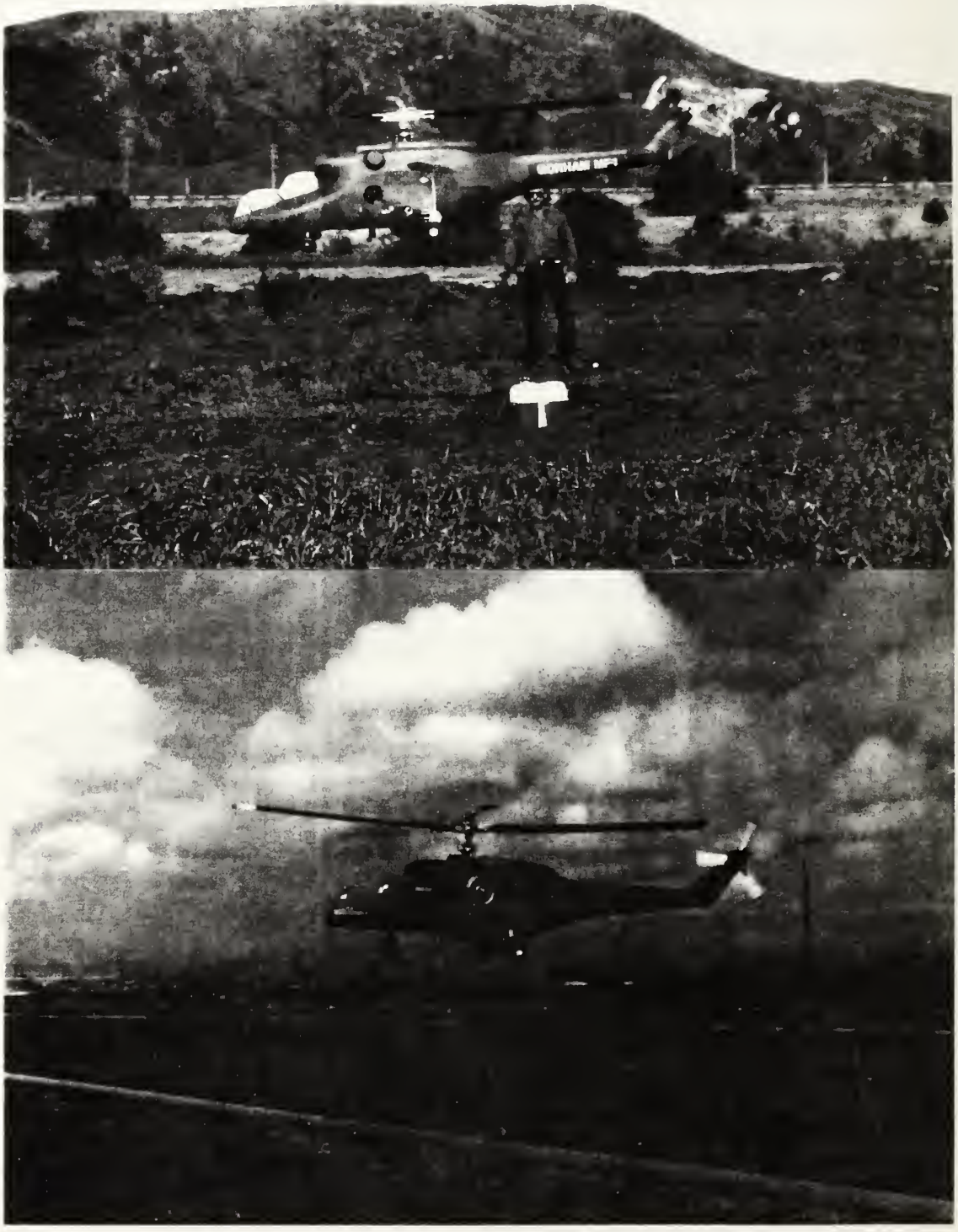

Figure 12 The Hummingbird

Table I HUMMINGBIRD CHARACTERISTICS AND CAPABILITIES

Hummingbird:		
Characteristics		
Weights		
Max Gross Weight	165 lbs	
Empty Weight	115 lbs	
Fuel capacity	6.5 lbs	
Rotor Parameters	**Main**	**Tail**
Radius (R)	5' 3"	12.5"
Chord (c)	6"	2.625"
Solidity (sigma)	0.0061	0.02
No. of blades (b)	2	3
Tip speed	303 fps	241 fps
Twist	-5	0
Hinge offset ration (e/R)	0.127	0.24
Airfoil	NACA 0012	NACA 0012
Engines		
Type	Westlake 342 Series 2100D	
Number	1	
Maximum Usable Power	25 BHP @ 7000 rpm	
Maximum Torque	25 ftlb @ 4000 rpm	

B. SHORTFALLS

The Hummingbird satisfied many of the department's needs; specifically, it was large enough to be developed into a quarter scale model, it had a 50 plus pound payload, and in addition, it had already proven itself in flight test. There were, however, some shortcomings that had to be addressed. These shortfalls included the need for more than

a two blade hub, an RPV that possessed autorotational capabilities and could produce blade Reynolds numbers which would be comparable to full scale helicopters.

1. Two Blade Rotor

In order to have the capability to do HHC research work on the RPV, it was required that the helicopter have at least three rotor blades or more. The reason for this requisite is that the vibratory forces at the rotor blade root are produced by the (n-1)/rev, n/rev, and (n+1)/rev vibrations. The n/rev vertical forces and moments are transmitted to the fixed system at a frequency of n/rev. The (n-1)/rev and (n+1)/rev flapwise blade root shears result in n/rev hub pitching and rolling moments in the airframe. The n/rev flapwise blade root shears feed into the airframe as n/rev vertical forces. The (n-1)/rev and (n+1)/rev chordwise root shears produce n/rev airframe hub forces in the fore and aft and lateral directions. The n/rev chordwise root shears result in n/rev hub yawing moments. Choosing a rotor system with three or more blades therefore will not interfere with the primary 1/rev control inputs. [Ref. 6:p 19] This change alone created a significant amount of work because it includes changing the main rotor hub and redesigning the rotor blades.

2. Lack of Autorotational Capability

The original design never incorporated the ability for the Hummingbird to autorotate, and this was considered unacceptable for the NPS flight research vehicle. The bearings in the drive system do not allow the main rotor to freewheel should the RPV have an engine failure. Presently, should the engine fail it will cause a rapid decay in rotor rpm which will transform the RPV from a flying machine to a projectile. This is a critical redesign requirement which must be accomplished in order to protect the Navy's financial and research investment in the Hummingbird.

3. Low Reynolds Number

In the HHC research, it is not enough to prove that the concept will reduce vibration; that result is sufficiently proved. The desire is to have the ability to test whether HHC also provides performance improvements. This comparison can only be accomplished on helicopters with similar Reynolds numbers.

Reynolds number is the ratio of the inertia to the viscous forces on a volume of fluid (Eqn. 6).

$$Re = \frac{\rho V c}{\mu} \qquad (6)$$

The importance of Reynolds number in the comparison of geometrically similar bodies in incompressible flows can be shown using the Navier-Stokes equations. Eqn. 7 shows the dimensionless Navier-Stokes equation.

$$\frac{Du'}{Dt'} = -\frac{\partial p'}{\partial x'} + \frac{1}{Re}\nabla'^2 u'; \quad \frac{Dv'}{Dt'} = -\frac{\partial p'}{\partial y'} + \frac{1}{Re}\nabla'^2 v'; \quad \frac{Dw'}{Dt'} = -\frac{\partial p'}{\partial z'} + \frac{1}{Re}\nabla'^2 w' \quad (7)$$

These equation show that, given geometrically similar bodies, the equations of motion are identical for the same Reynolds number. The similar bodies includes surface roughness as well as shape. [Ref. 7:p. 304]

The Hummingbird's Reynolds number was on the order of 0.9 million, and it needed to be in the range of 1.5 to 1.8 million to be comparable to that of the OH-6A's Reynolds number equal to 2.4 million.

VI. BLADE DESIGN

A. SPECIFICS

1. Airfoil

The airfoils that were available with the Hummingbird were NACA 0012 and NACA 0013. This type of airfoil is widely used in industry for numerous reasons. First, the airfoil is symmetrical and therefore there is no nose-down pitching moment which is associated with cambered airfoils. Second, it is a relatively thick airfoil which will provide an acceptable maximum lift coefficient. Finally, there is a vast amount of data available on this airfoil, which provides for much easier analysis. This is due to the fact that the NACA 0012 airfoil was selected by Mr. Sikorsky for the VS-300, the world's first truly successful helicopter. It was also the airfoil of choice for almost all early helicopters, including more recent aircraft still in service, such as the Navy H-3.

For improved performance, a more recent advanced technology airfoil worthy of consideration is the NACA 23012. The characteristic drooped nose is an effective method of increasing the maximum lift coefficient. Also, at high lift it has lower drag than a similar six-series airfoil at low mach numbers. [Ref. 3:p. 388]

2. Twist

The twist of a rotor blade enhances two main areas of the helicopter's performance--hover performance and retreating blade stall--but it also produces increased vibration in forward flight. Its most notable adverse effect is to increase blade vibratory stresses and in this way reduce blade fatigue life. Built-in blade twist affects the radial variation of inflow angle from blade tip to blade root. Ideal twist is represented by Eqn. 8.

$$\phi = \phi_t \frac{R}{r} \tag{8}$$

Hovering performance is enhanced with the addition of negative twist by creating a more uniform inflow distribution along the blade span. The larger the amount of twist, the closer it approximates an ideal twist distribution. Generally accepted values of main rotor blade twist are -8 to -14 degrees. Ideal twist yields the minimum induced loss for a given thrust. Retreating blade stall is delayed when twist is employed by unloading the tips, which reduces the tip angle of attack [Ref. 8:p. 57].

These regions of enhanced performance are not critical areas for the Hummingbird. The Hummingbird will operate at relatively slow forward speeds; therefore, retreating blade stall is not a concern. It would be attractive to have highly efficient blades in the hover regime, but with the present payload capability of 50

pounds, it is not critical. If these were critical areas for the Hummingbird, it might be worth the effort to manufacture new blades with twist; but since they are not, simplicity rules, and it was decided not to incorporate twist in the present rotor blade design.

3. Tip Velocity

Determining the tip speed (V_{tip}) for the Hummingbird was a difficult matter because its effects were coupled with so many other areas of the helicopter's performance. The constraint diagram from Chapter II is shown again in Fig 13.

The design point is shown to be in the proximity of V_{max} of 40 knots and V_{tip} of 450 fps. V_{max} was obtained from the Hummingbird original design. The means by which V_{tip} was determined will follow. Low tip speeds have the advantage of low noise and good hovering performance. "High tip speeds have the advantage of low rotor and drive system weights and high stored energy for autorotative entries and flares." [Ref. 3] In the case of the Hummingbird, V_{tip} was the variable used for a tradeoff study. V_{tip} had to be large enough to produce Reynolds numbers which could be compared with full scale helicopters, but small enough to provide a reasonable Figure of Merit (FM).

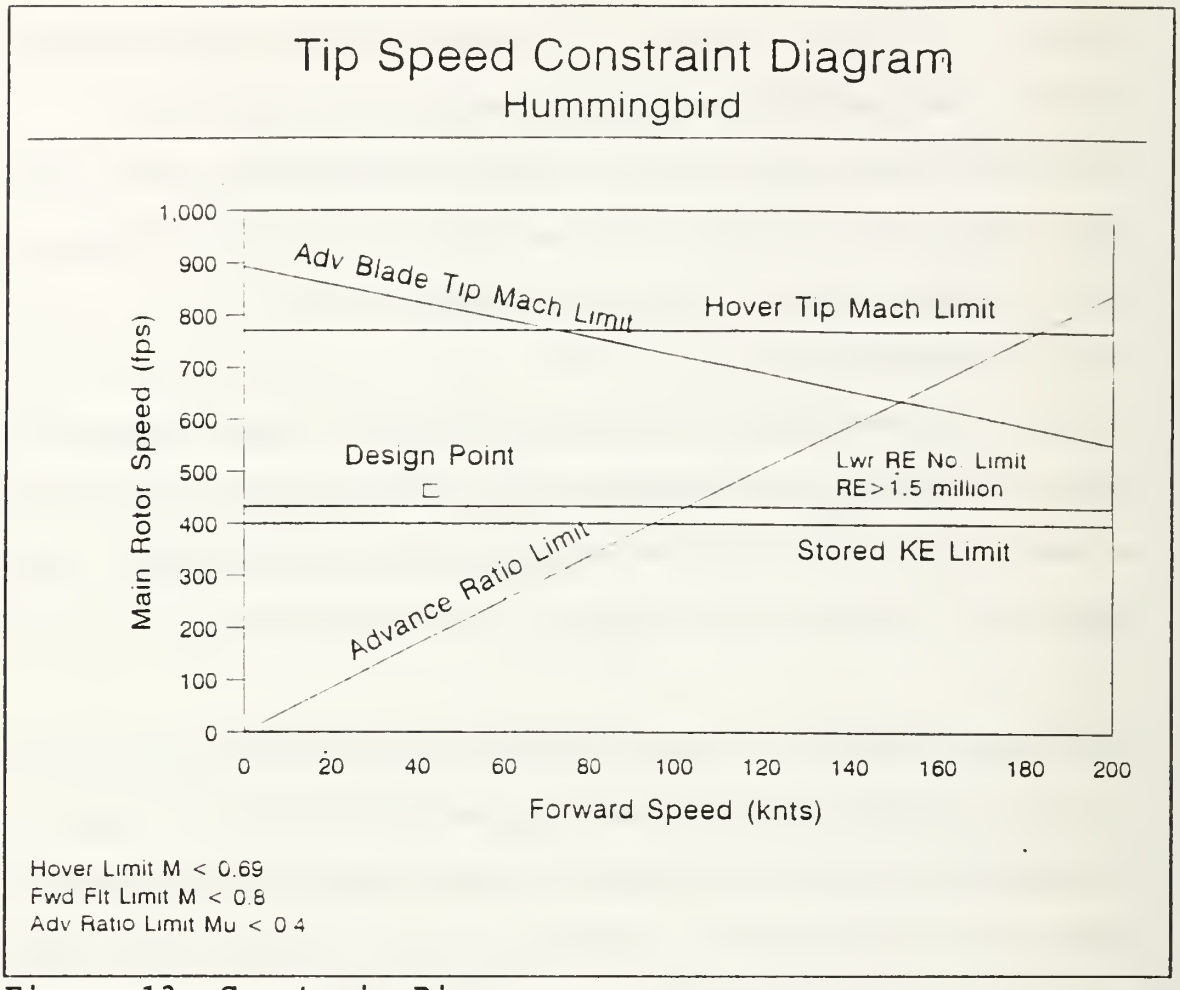

Figure 13 Constrain Diagram

B. TRADEOFF

The need to achieve a Reynolds number in the range mentioned earlier was the source of some consternation. If Reynolds numbers were not considered, it was quite easy to design a rotor blade that would fly efficiently and meet the department needs. The complication begins when the V_{tip}, Reynolds number, Figure of Merit and chord length requirements are all met at the same time. Reynolds number

is a function of V_{tip} and chord length as shown by Eqn. 9.

$$Re = 6400 V_{tip} C \quad (9)$$

Fig. 14 and 15 show this relationship over a certain range

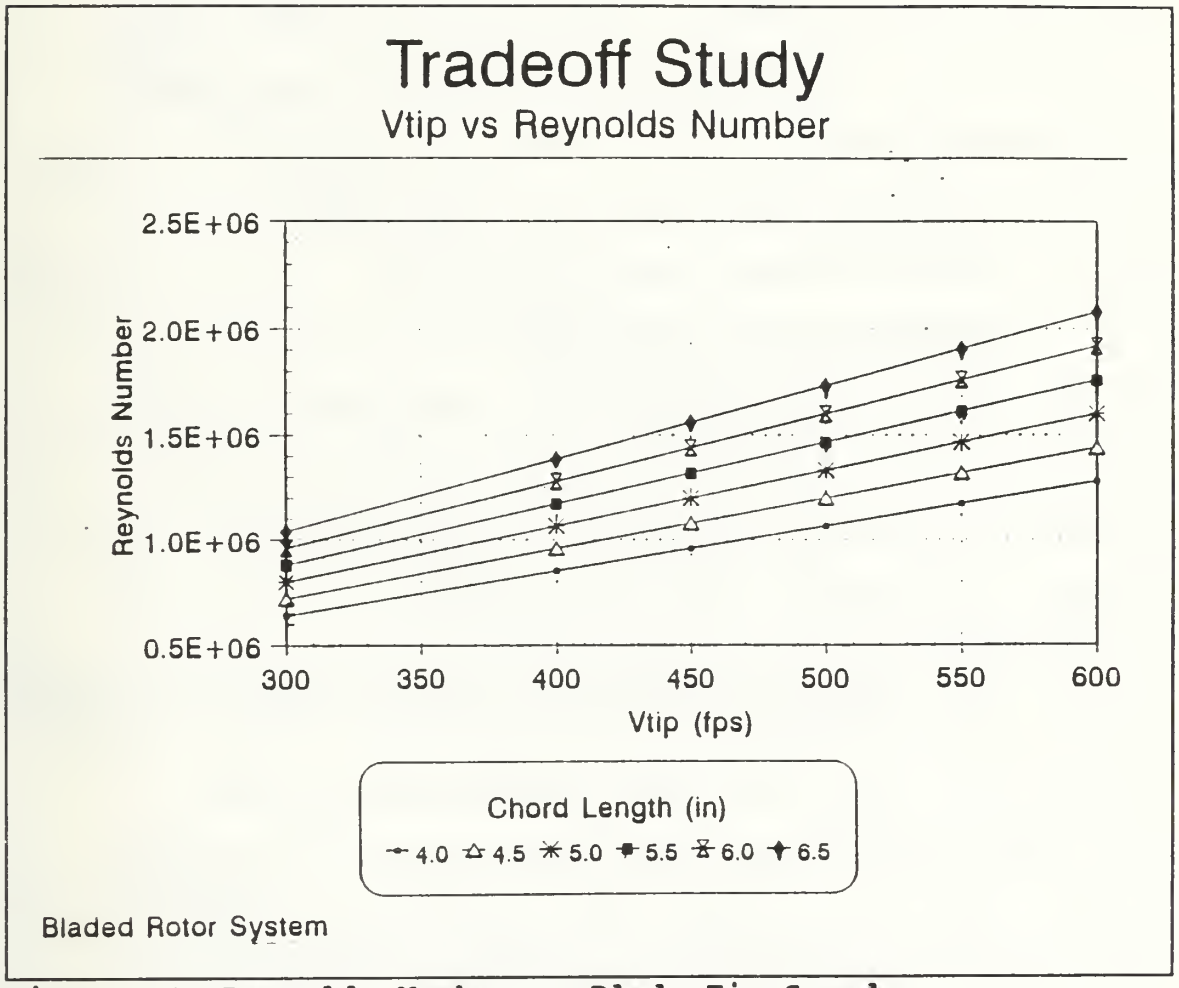

Figure 14 Reynolds Number vs Blade Tip Speed

of V_{tip} and chord length.

Figure of Merit is shown by the relationship in Eqn. 10. Induced power is the power required to overcome the drag due to the generated lift. Total power also includes the power

$$FM = \frac{P_i}{P_{total}} \quad (10)$$

required to move the rotor blades through the air (profile power) and the power required to drag the fuselage through the air (parasite power). Fig. 16 and 17 show this relationship over the same V_{tip} and chord length range.
To link the Figure of Merit and Reynolds number together, lines of constant Reynolds numbers were plotted on the Figure of Merit versus chord length chart. Fig. 18 allowed for the tradeoff to be visualized simultaneously on one graph. The Hummingbird came with three sets of blades. One set was of radius 4.52 feet with a chord of 6 inches. The other two sets were of radius 5.0 feet with a chord of 6.5 inches. To expedite the design process, the available blades were selected versus designing and manufacturing new ones. Since there was a requirement for at least a three bladed rotor, the second set of blades was chosen.
The advantages of this choice are seen in the tradeoff study. Choosing a longer chord length allowed for a slower tip speed for the same Reynolds number. Since profile power is proportional to V_{tip}^3, the slower tip speed increases the FM from 0.48 to 0.54.

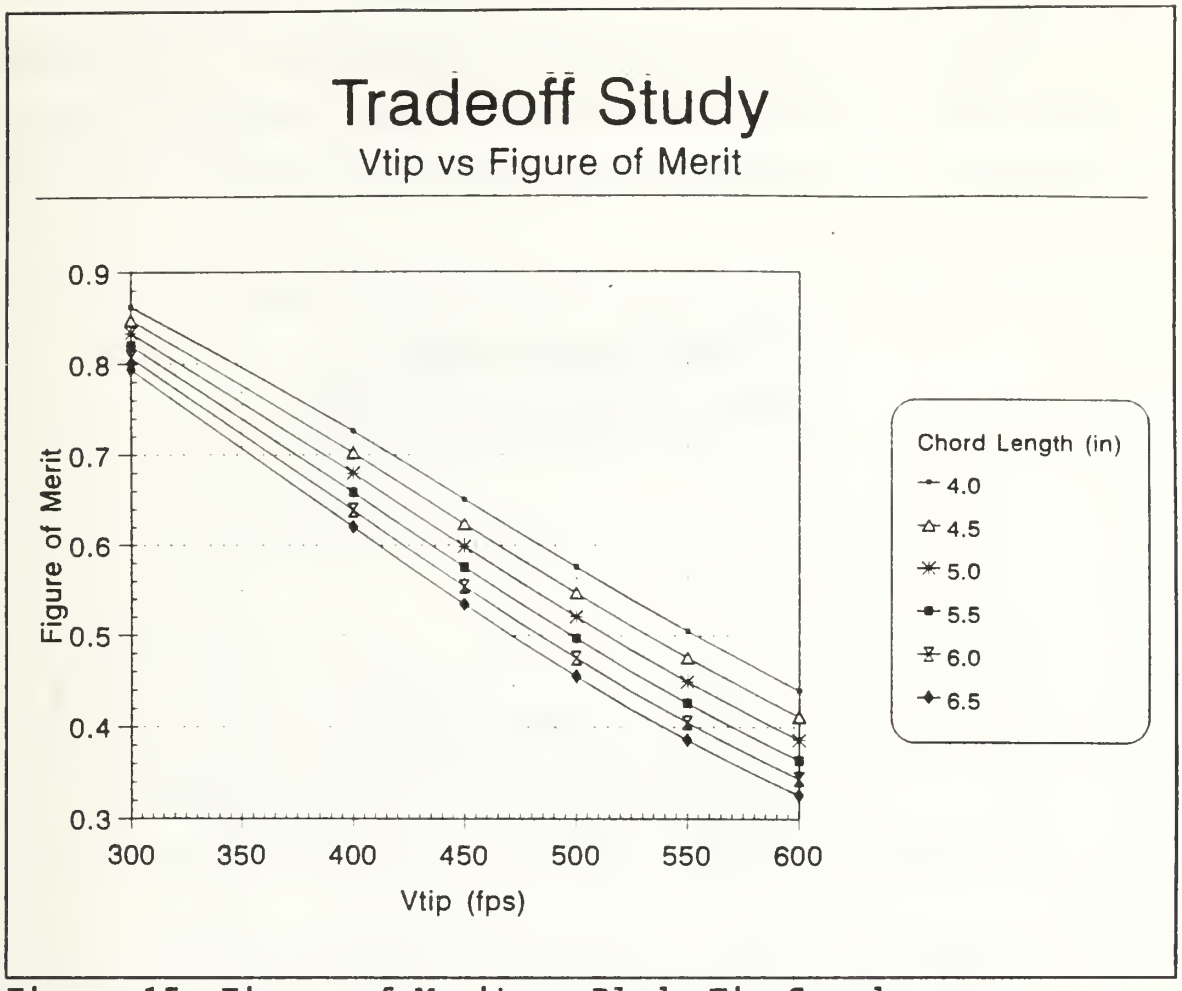

Figure 15 Figure of Merit vs Blade Tip Speed

C. STABILITY

The pitch and roll damping is produced by the tilt of the tip path plane, which lags behind the motion of the shaft by an amount that is proportional to the rate of pitch or roll. Therefore, the aerodynamics on the blade causes the tip path plane to tend to stabilize itself in an equilibrium position with respect to the shaft. "If the

aerodynamic and inertia flapping moment are equated, the following results for the angular displacement of the rotor plane with respect to the shaft per unit tilting velocity of the shaft is obtained for the hovering case:"[Ref. 8:p. 275]

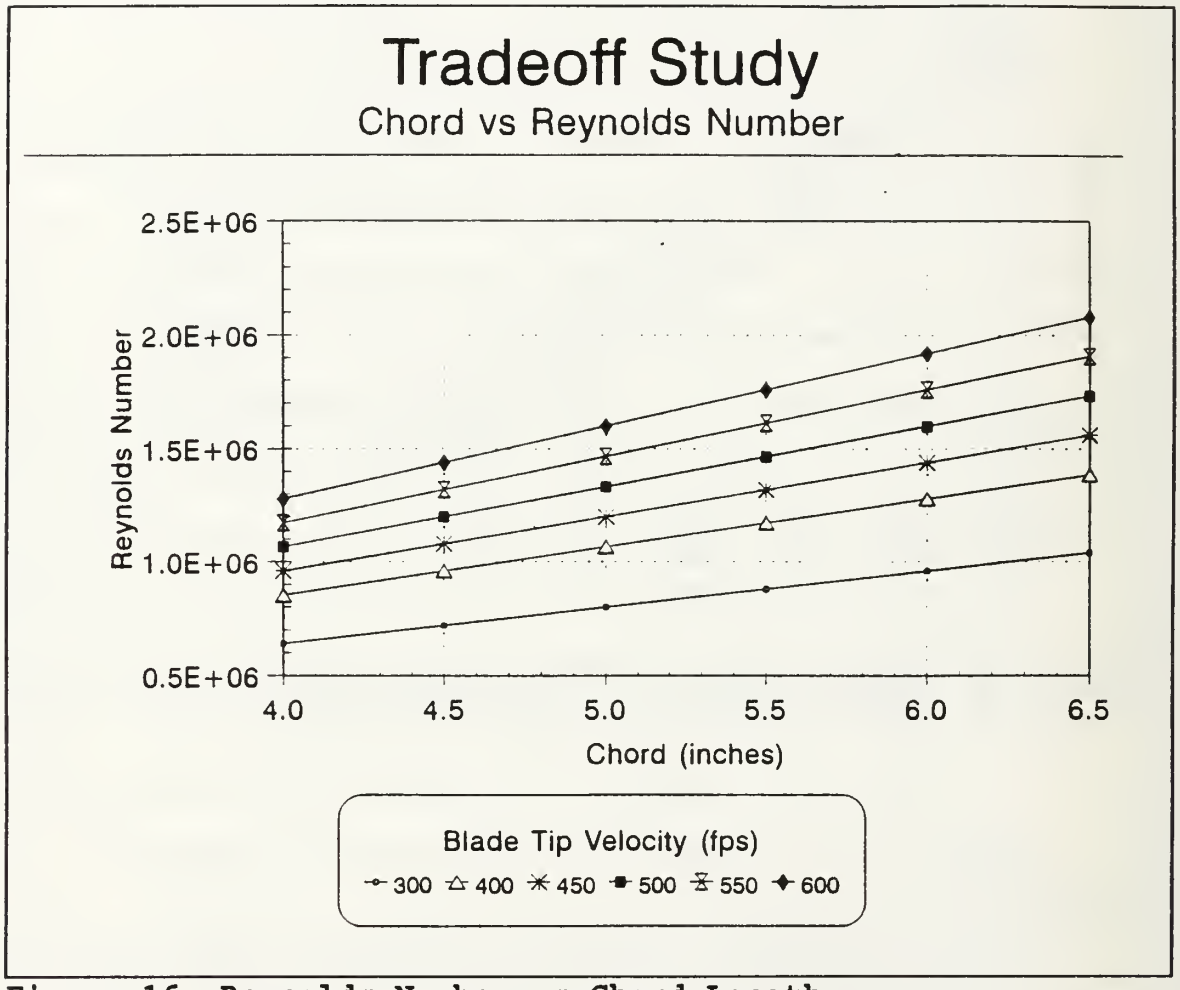

Figure 16 Reynolds Number vs Chord Length

$$\frac{\delta}{\omega} = \frac{16}{\gamma\Omega} \qquad (11)$$

The quantity $16/(\gamma\Omega)$ can be understood more easily by examining its physical interpretation as follows: The thrust

vector lags the rotor shaft by a time constant of $16/(\gamma\Omega)$ seconds if the rotor shaft is tilted with any constant angular velocity. Therefore, the larger the time constant $(16/(\gamma\Omega))$, the greater the system is damped. Lock number

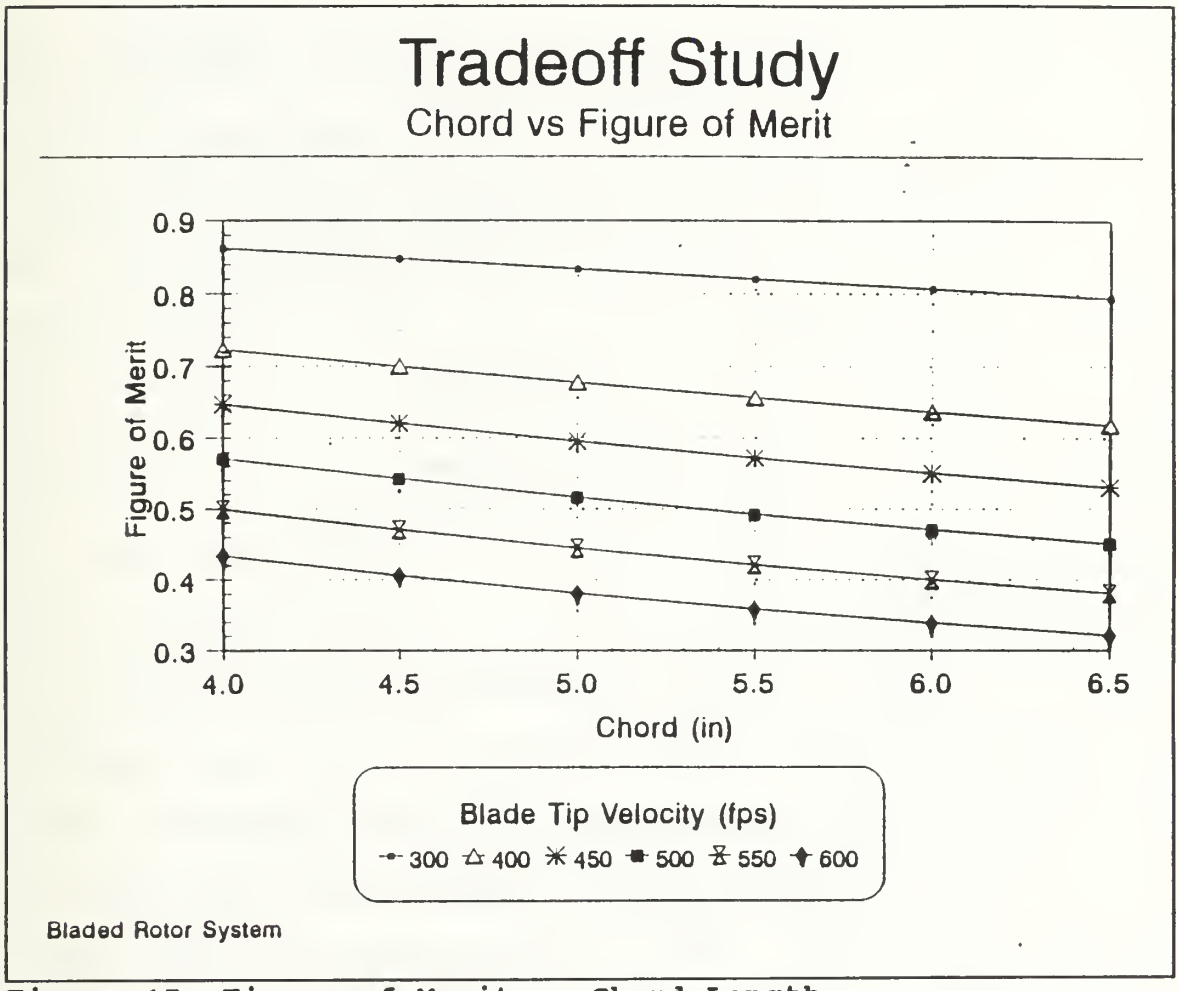

Figure 17 Figure of Merit vs Chord Length

(γ) relates the inertia and aerodynamic characteristics of a blade and is shown in Eqn. 12.

$$\gamma = \frac{c\rho a R^4}{I_b} \qquad (12)$$

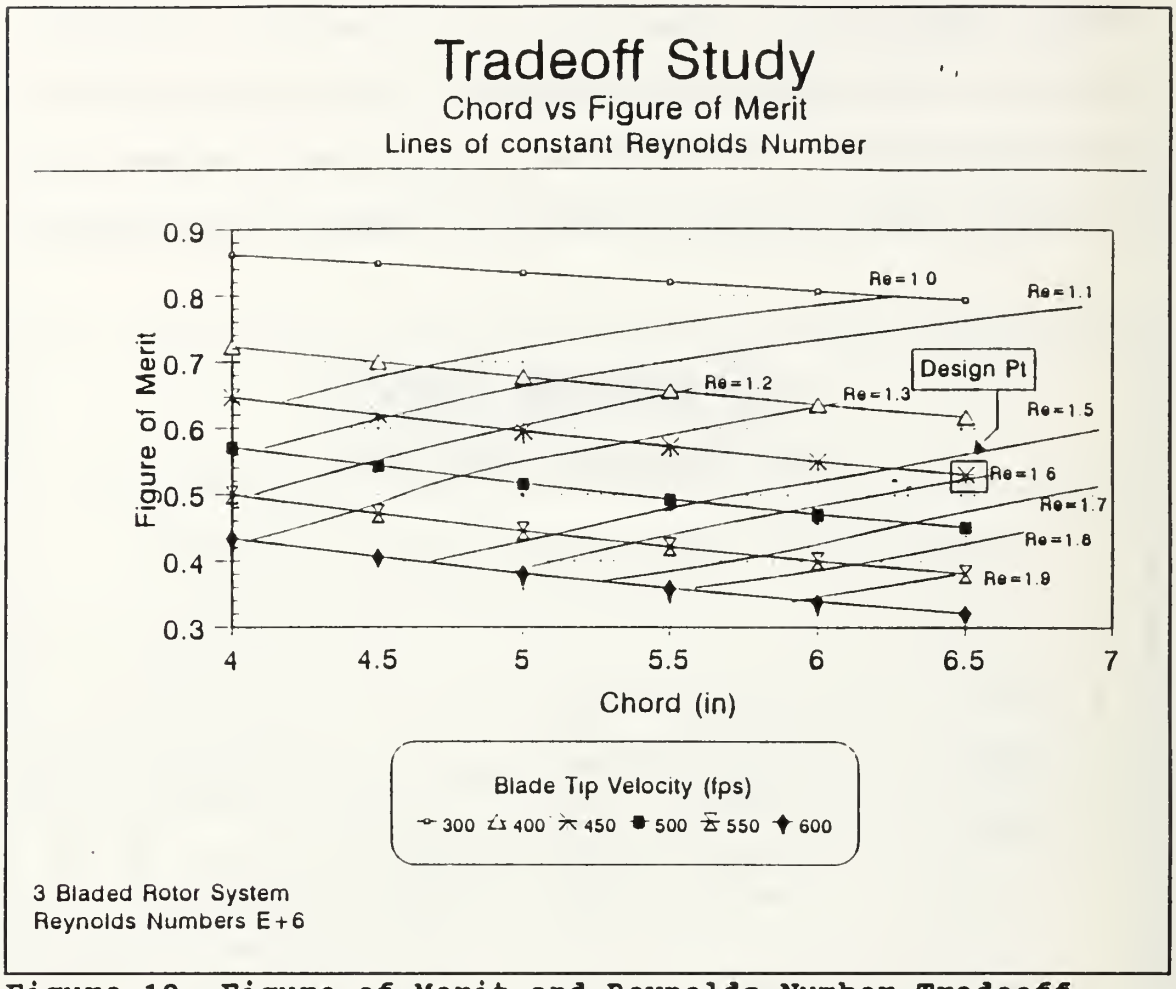

Figure 18 Figure of Merit and Reynolds Number Tradeoff

The stability of the Hummingbird is a critical area that will require additional research. The two proposed modifications to the helicopter significantly alter the stability of the RPV. Eqn. 11 shows that rotor speed and Lock number will affect the damping of the rotor. The rotor blade is not changed; therefore, the Lock number will remain the same. The rotor speed will be increased from 550 rpm to 759 rpm, thus decreasing the effective rotor damping. Ref. 8 states that

In addition to the effects of rotor speed, rotor damping may be increased by the use of devices that act upon the control system in such a manner as to increase the displacement of the rotor from its trim position due to a given rate of roll or pitch. An example of such a device is a rate gyro that would apply opposite control by an amount proportional to the rolling or pitching velocity of the helicopter.

The Bell-Hiller stabilizer bar hub configuration is such a device. Therefore, changing from that type of hub to an articulated hub will significantly decrease the rotor roll and pitch damping and thus the helicopter's handling characteristics. For the 3-bladed Hummingbird, rate gyros may be required in order to have satisfactory flying qualities.

D. BLADE DYNAMICS

1. Introduction

It is very important to consider the vibratory effect on the main rotor blades. High vibrations result in high vibratory shear at the rotor hub, which results in high fuselage vibrations. The high vibrations also cause vibratory shear stress, which reduces the effective life of a rotor blade. The vibratory resonance response also affects dynamic stability of the rotor system.

2. Main Rotor Blades

The following analysis was done on two different rotor blades. The first was termed the "heavy" blade. It had a length of 4 ft 6.25 inches, chord of 6 inches, thickness ratio of 12 percent and a weight of 5.18 lbs. The second blade, termed the "light" blade, has a length of 5 ft, chord of 6.5 inches, thickness ratio of 13 percent and a weight of 4.66 lbs. The length given for the blades above does not include the 8 inch blade offset of the rotor hub, but it was included in the rotor radius when the analysis was performed.

In order to analyze each blade, they were broken up into segments: the heavy blade into 17 segments and the light blade into 24. Fig. 19 and 20 show a schematic for the two blades and how the blades were divided into segments. The analysis for each blade was conducted with the exact same technique, and therefore the discussion will be limited to the heavy blade. The following quantities were required to perform the blade analysis: section radii, chord, segment width, segment volume, segment weight, and area moment of inertia (Ixx), and material modulus of elasticity. The section radii was the distance from the center of rotation to the center point of the segment. The chord was constant for the blade until the small taper at the root. The segment width was constant with the exception

of the tip segment, which was allotted any leftover blade. Fig. 21 shows a cross section of the blade, which was used for area and moment of inertia calculation. For calculations, the airfoil cross section was broken up into three sections and approximated as follows: (1) the nose section by a parabola; (2) the center section by a box; and (3) the tail section by an isosceles triangle.

The cross sectional area of each section was calculated using standard geometric formulas in Eqn. 13.

$$\textit{Parabola}: A = \frac{4ah}{3} \quad \textit{Box}: A = bh \quad \textit{Triangle}: A = \frac{1}{2}bh \tag{13}$$

The area moments of inertia for the box and triangle were

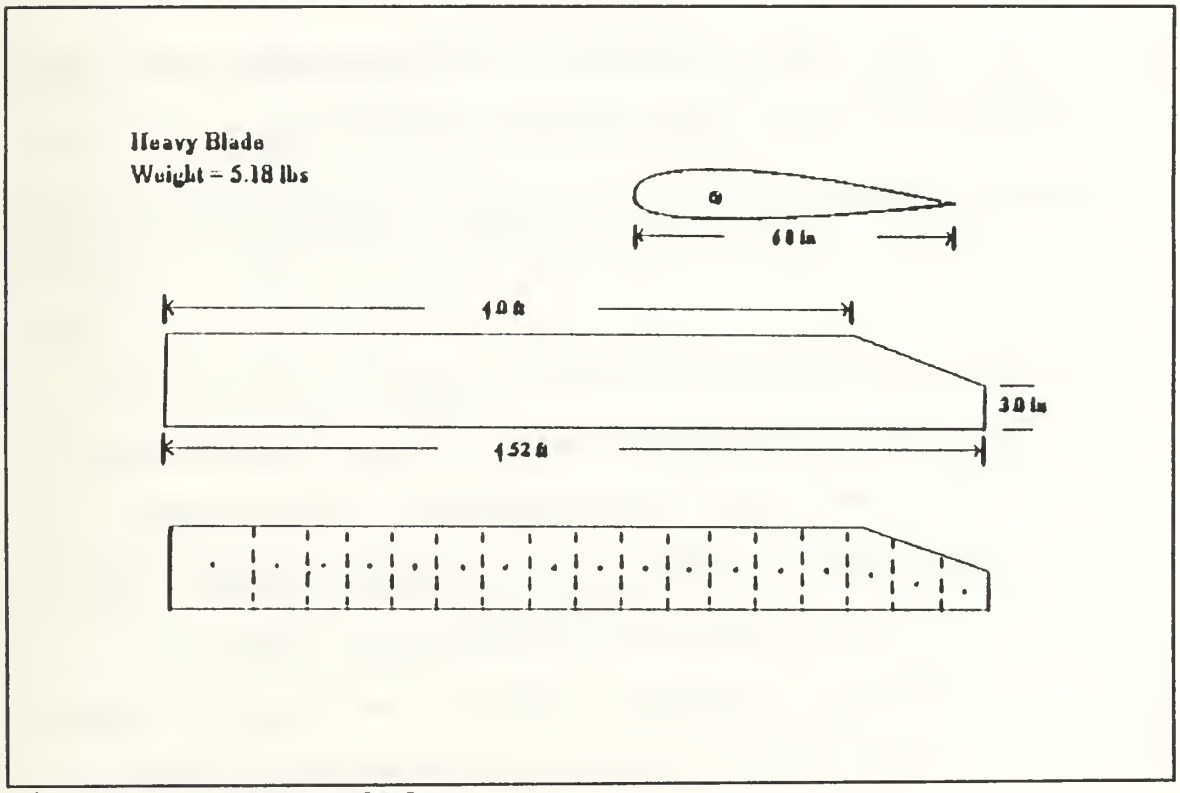

Figure 19 Heavy Blade

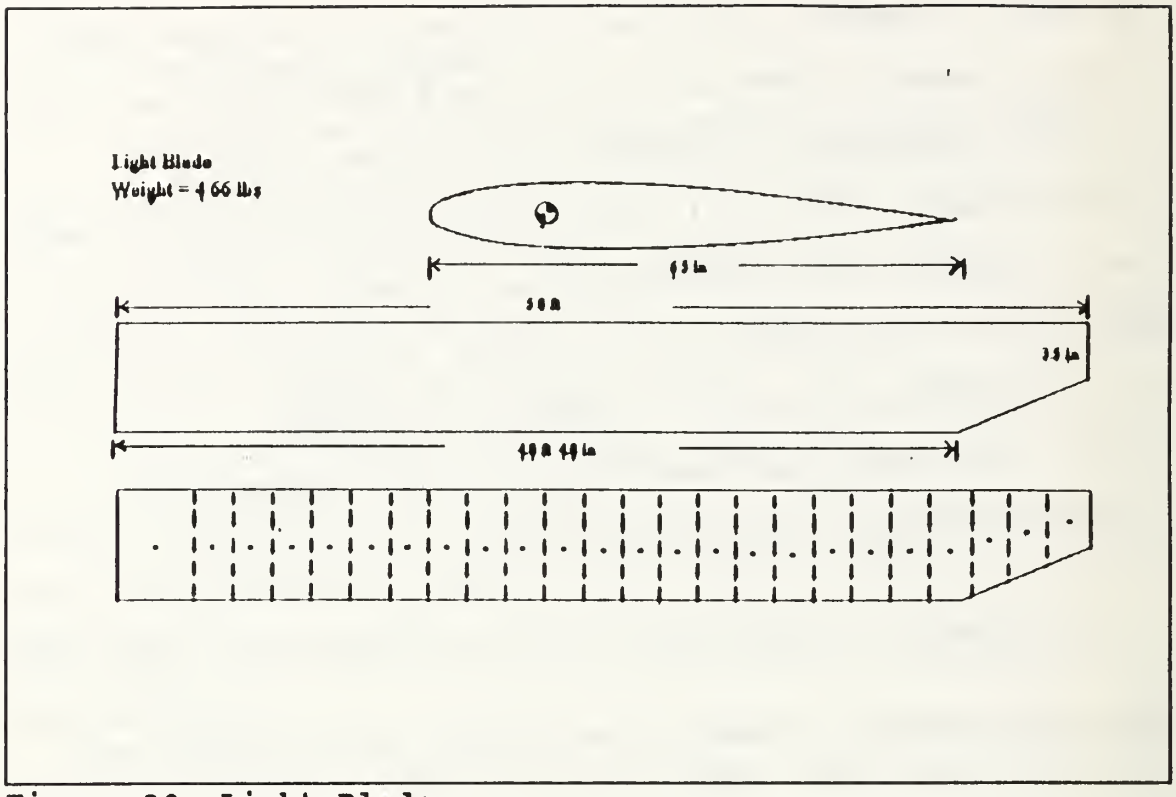

Figure 20 Light Blade

calculated using known formulas, while integration was used to determine the Ixx of the parabola. (Eqn. 14.)

$$Box: Ixx = \frac{1}{12}bh^3 \quad Triangle: Ixx = \frac{1}{12}bh^3 \quad Parabola: Ixx = \int_A y^2 dA$$

(14)

The parabola was approximated by the equation $x = 6.67y^2$.

Using the calculated cross sectional area and the segment width, the volume was calculated. The segment volume was then used to determine the segment weight. The assumption was made that the rotor blade was made of a homogeneous material - spruce. The only variation in these calculations was where the blade was tapered very near the

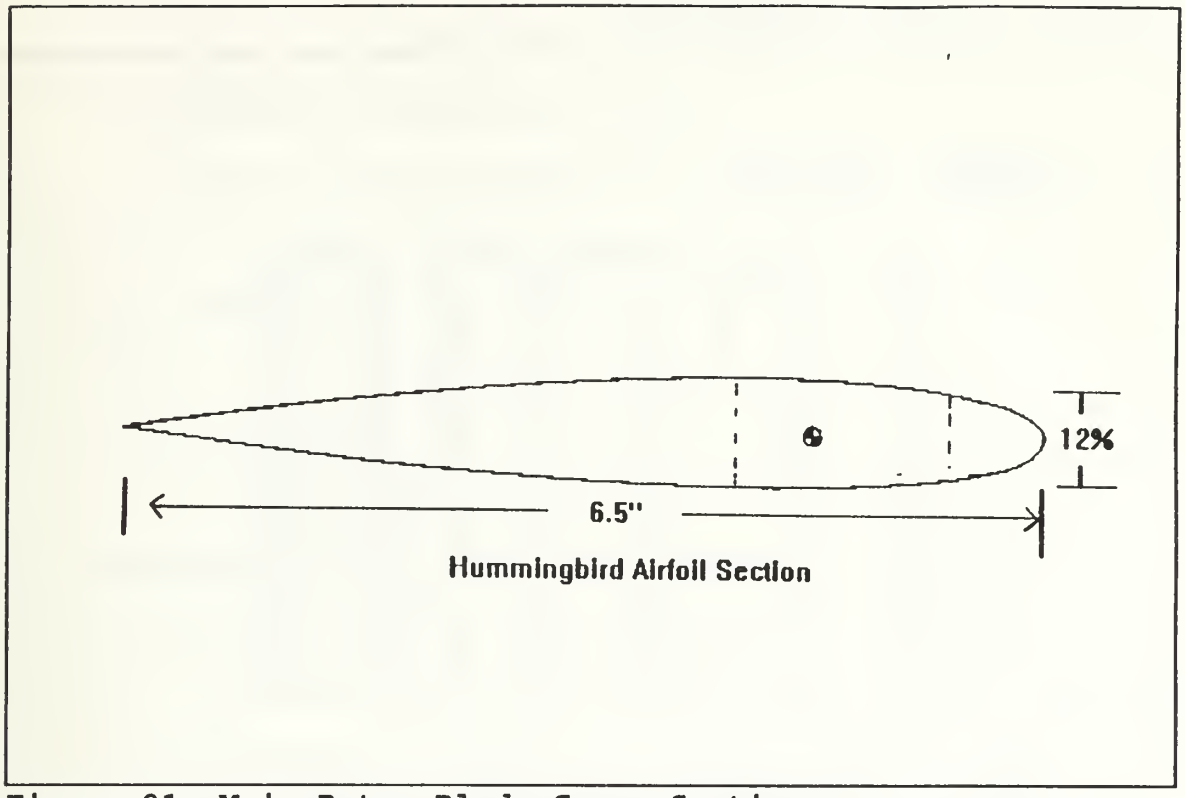

Figure 21 Main Rotor Blade Cross Section

root. This section was no longer an airfoil section, but an inch thick tapered block. The segment weight and Ixx of the root section also included contributions from the blade grip assembly. Table II shows the data for each blade.

Table II BLADE STATION DATA

Heavy Blade Radius = 4 52 ft
Weight 5 18 lbs Chord = 6 in
t/c = 12%

Section	Radii (in)	Chord (in)	Xsec Ar (in^2)	Seg Wd (in)	Volume (in^3)	Seg Wt. (lb)	Ixx (in^4)	Delta Cf (ft lb)
1	59.1	8 0	1 68	6 25	10 50	0.459	0 097	230 85
2	54 5	6 0	1 68	3 00	5 04	0 220	0 097	49 03
3	51.5	6 0	1 68	3 00	5 04	0 220	0 097	46 33
4	48 5	6 0	1 68	3 00	5 04	0 220	0 097	43 63
5	45.5	6 0	1 68	3 00	5 04	0 220	0.097	40 93
6	42.5	6 0	1 68	3 00	5 04	0 220	0 097	38.23
7	39 5	6 0	1 68	3 00	5 04	0 220	0.097	35 53
8	36 5	6 0	1 68	3 00	5 04	0 220	0 097	32 84
9	33 5	6 0	1 68	3 00	5 04	0 220	0 097	30.14
10	30 5	6 0	1 68	3 00	5 04	0 220	0 097	27.44
11	27 5	6 0	1 68	3 00	5 04	0 220	0 097	24 74
12	24 5	6 0	1 68	3 00	5 04	0 220	0 097	22 04
13	21 5	6 0	1 68	3 00	5 04	0 220	0 097	19 34
14	18 5	6 0	1 68	3 00	5 04	0 220	0 097	16 64
15	15 5	5.4	5 40	3 00	16 20	0 708	0.450	44 82
16	12 5	5 0	5 00	3 00	15 00	0 656	0.417	33 47
17	9 5	3 8	3 75	3 00	11 25	0 742	0 808	28 77

Light Blade Radius = 5 0 ft
Weight = 4 66 lbs Chord = 6 5 in
t/c = 13%

Section	Radii (in)	Chord (in)	Xsec Ar (in^2)	Seg Wd (in)	Volume (in^3)	Seg Wt. (lb)	Ixx (in^4)	Delta Cf (ft lb)
1	65 6	6 5	3 37	4 8	16 18	0 353	0 478	151 24
2	62 0	6 5	3 37	2 4	8 09	0 177	0.478	35.74
3	59 6	6 5	3 37	2 4	8 09	0.177	0.478	34.35
4	57 2	6 5	3 37	2 4	8 09	0.177	0.478	32.97
5	54 8	6 5	3 37	2 4	8 09	0.177	0.478	31.59
6	52.4	6 5	3 37	2 4	8 09	0.177	0.478	30.20
7	50 0	6 5	3 37	2.4	8 09	0 177	0.478	28 82
8	47 6	6 5	3 37	2 4	8 09	0.177	0.478	27.44
9	45 2	6 5	3.37	2 4	8.09	0 177	0.478	26.05
10	42 8	6 5	3 37	2 4	8 09	0.177	0.478	24 67
11	40 4	6 5	3 37	2 4	8 09	0 177	0 478	23 29
12	38 0	6 5	3 37	2.4	8 09	0 177	0.478	21.90
13	35 6	6 5	3 37	2.4	8 09	0.177	0.478	20.52
14	33 2	6 5	3 37	2.4	8 09	0 177	0.478	19.14
15	30 8	6 5	3 37	2 4	8 09	0.177	0.478	17.75
16	28 4	6 5	3 37	2.4	8 09	0.177	0.478	16.37
17	26 0	6 5	3 37	2 4	8 09	0.177	0.478	14 99
18	23 6	6 5	3 37	2 4	8 09	0 177	0 478	13 60
19	21 2	6 5	3 37	2 4	8 09	0.177	0.478	12.22
20	18 8	6 5	3 37	2.4	8 09	0 177	0 478	10 84
21	16 4	6 5	3 37	2 4	8 09	0 177	0.478	9 45
22	14 0	5 8	5 76	2 4	13 82	0 302	0.480	13.79
23	11 6	4 8	4 80	2 4	11 52	0 252	0 400	9.52
24	9 2	4 2	4 20	2 4	10 08	0 470	0 845	14.11

3. Myklestad Determinant Method

There are many methods for analyzing vibrations in a rotor blade. Some of these are

- Rayleigh-Ritz
- Holzer
- Myklestad-Prohl
- Matrix iteration

The Myklestad method, which determines the natural frequencies and modes of the blades, was the method of choice. It is especially well suited for vibration analysis of rotor and turbine blades. Dr. Nils Myklestad was a consultant to Bell Helicopter Company for many years. The proper analysis requires considering the coupled flapwise-edgewise-torsional response of the blades. Because the edgewise and torsional stiffness is much greater than the flapwise stiffness and thus has much high frequencies, only the flapwise responses of the blades were considered.

The uncoupled flapwise Myklestad system is shown in Fig. 22.

From this diagram the equations of equilibrium for this n^{th} element can be written.

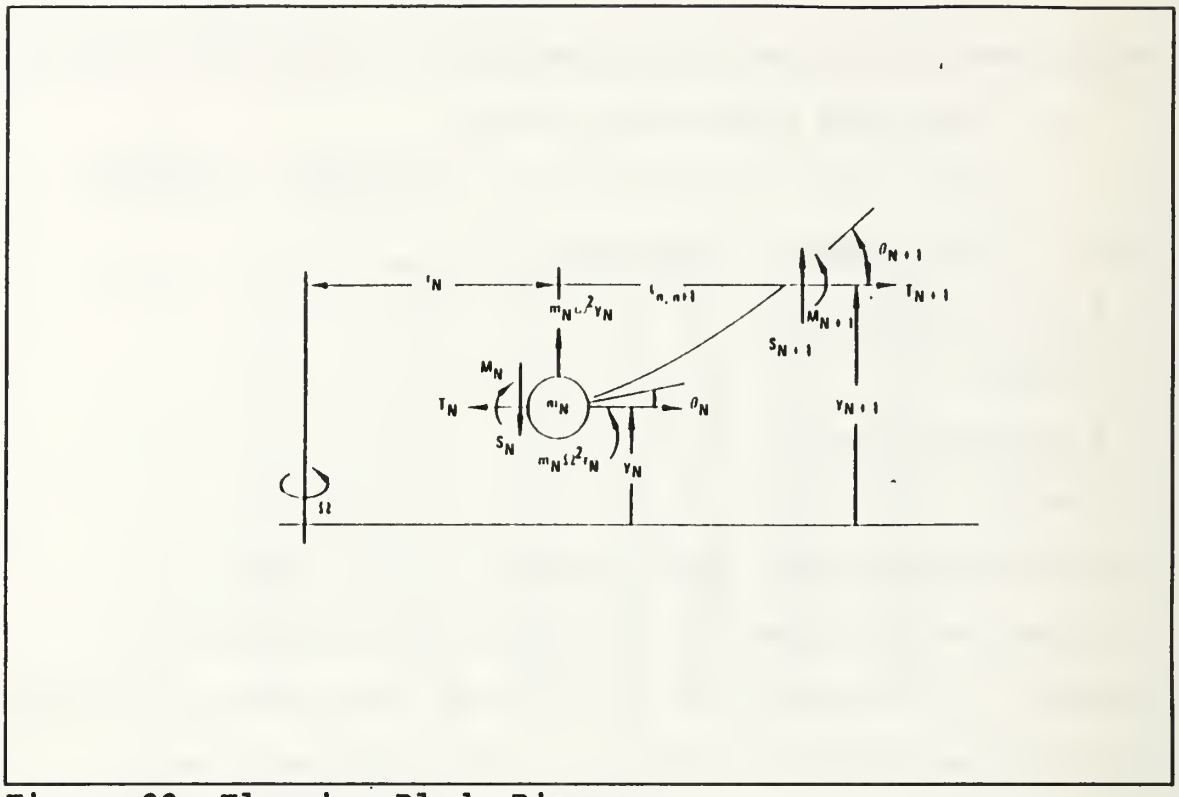

Figure 22 Flapping Blade Diagram

Centrifugal Force:

$$T_N = T_{N+1} + m_N \Omega^2 r_N \tag{15}$$

Shear:

$$S_N = S_{N+1} + m_N \omega^2 y_N \tag{16}$$

Moment:

$$M_N = M_{N+1} + S_{N+1} l_{n,n+1} - T_{N+1}(y_{N+1} - y_N) \tag{17}$$

Slope:

$$\theta_N = \theta_{N+1}\left(1+T_{N+1}\frac{l^2_{n,n+1}}{2EI}\right) - M_{N+1}\frac{l_{n,n+1}}{EI} - S_{N+1}\frac{l^2_{n,n+1}}{2EI} \qquad (18)$$

Deflection:

$$y_N = y_{N+1} - \theta_N l_{n,n+1} + \frac{T_{N+1}\,\theta_{N+1}\,l^3_{n,n+1}}{3EI} - \frac{M_{N+1}\,l^2_{n,n+1}}{2EI} - \frac{S_{N+1}\,l^3_{n,n+1}}{3EI} \qquad (19)$$

The natural frequencies of the system are obtained by assuming a frequency (Ω) and then calculating the centrifugal forces, shears, moments, slopes, and deflections of each blade segment from the blade tip to the blade root. The boundary conditions at the blade tip are

$$S_T = M_T = 0; \quad \theta_T = \theta_T; \quad y_T = y_T$$

At the root of the blade, the two unknowns θ_T and y_T are carried along and the equilibrium equations are written as follows:

$$S_o = A_S y_T + B_S \theta_T$$

$$M_o = A_M y_T + B_M \theta_T$$

$$\theta_o = A_\theta y_T + B_\theta \theta_T$$

$$y_o = A_y y_T + B_y \theta_T$$

In the preceding equation, the coefficients A and B will be calculated as the process proceeds down the blade. They are functions of mass and stiffness properties of the blade, the rotational speed, and the assumed frequency. The boundary conditions at the root of the hinged blade are

$$M_o = y_o = 0$$

or

$$A_M y_T + B_M \theta_T = 0$$

$$A_y y_T + B_y \theta_T = 0$$

These equations can be written in matrix form. The frequencies that satisfy the equation (when the determinant equals zero) are the natural frequencies and can readily be determined.

A Fortran code, Appendix A, was written to solve the Myklestad equations and determine the flapwise natural frequencies of both Hummingbird rotor blades. Fig. 23,24,25, and 26 show a graphical output of the Myklestad determinant for both blades.

The natural frequencies, where the line crosses the x-axis, are clearly seen. Appendix B contains a numerical output of the same data for the different natural frequencies.

A means to verify the accuracy of the code's ability to determine the natural frequencies was to check the ratio of the determinant coefficients. A_y and A_m are the displacement and slope coefficients respectively for the rotor blade root section in response to starting boundary conditions at the blade tip of slope equal zero and deflection equal one. B_y and B_m are similar to A_y and A_m except the starting boundary conditions are slope equals one and displacement equals zero. Knowing that the determinant

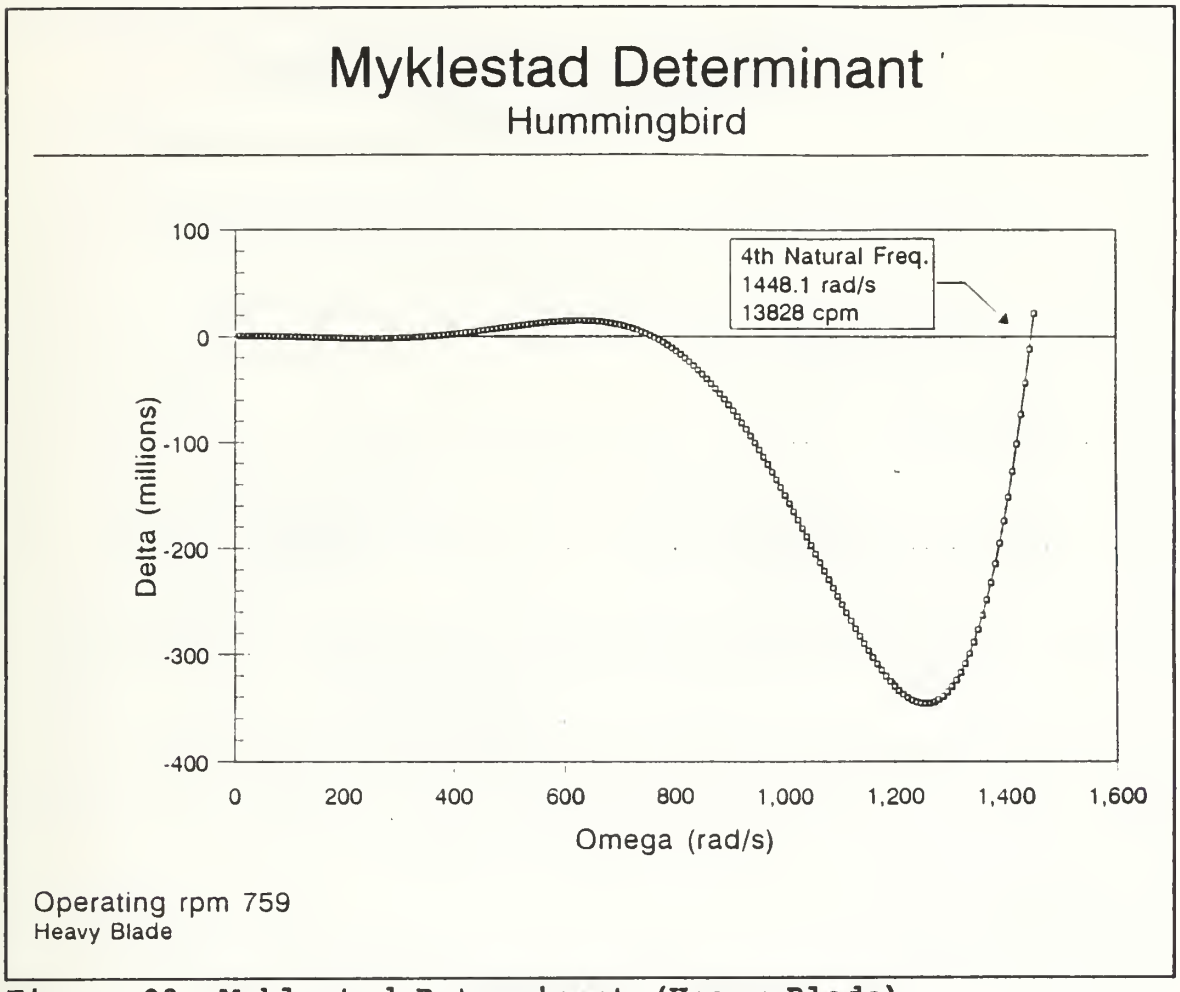

Figure 23 Myklestad Determinant (Heavy Blade)

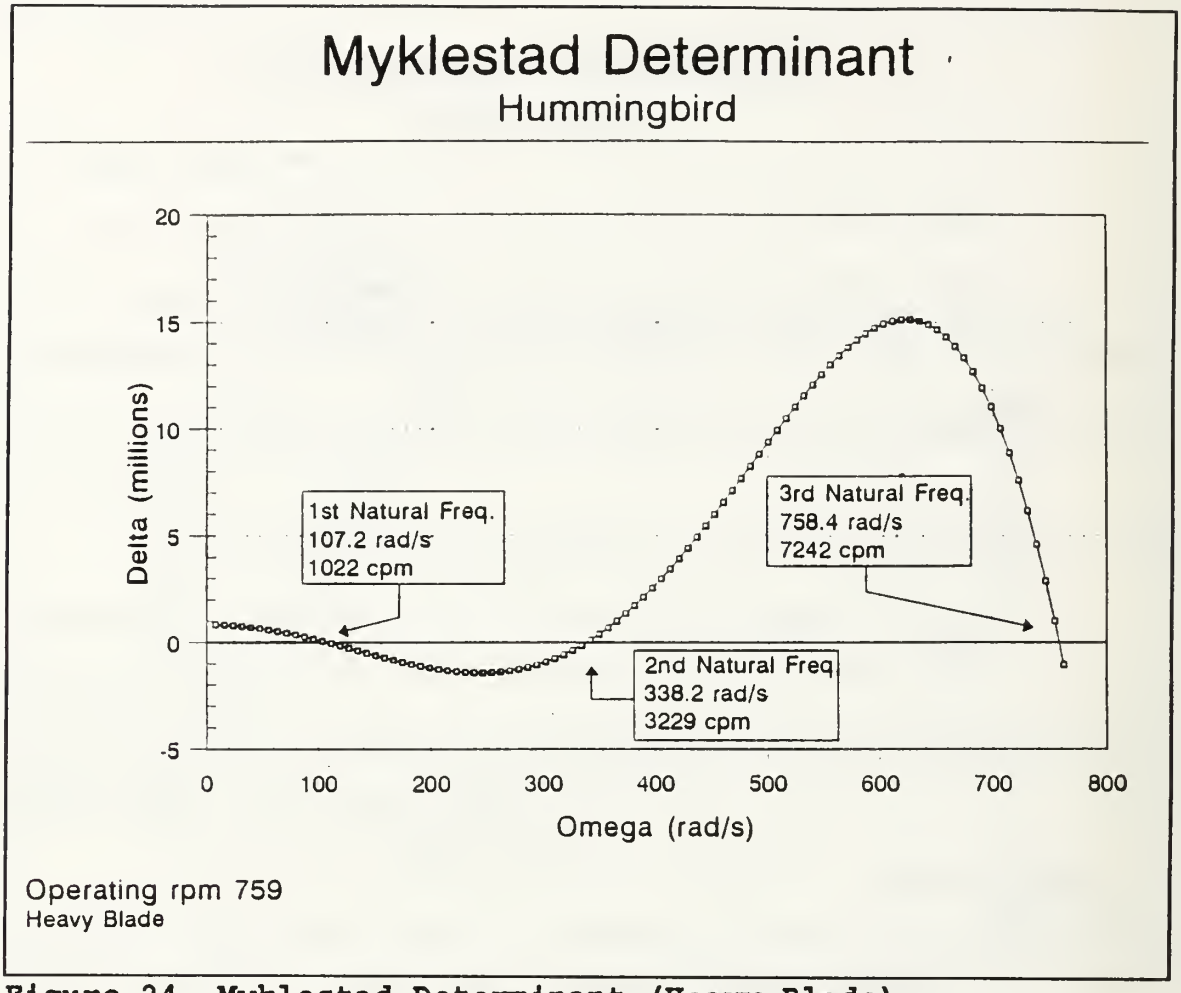

Figure 24 Myklestad Determinant (Heavy Blade)

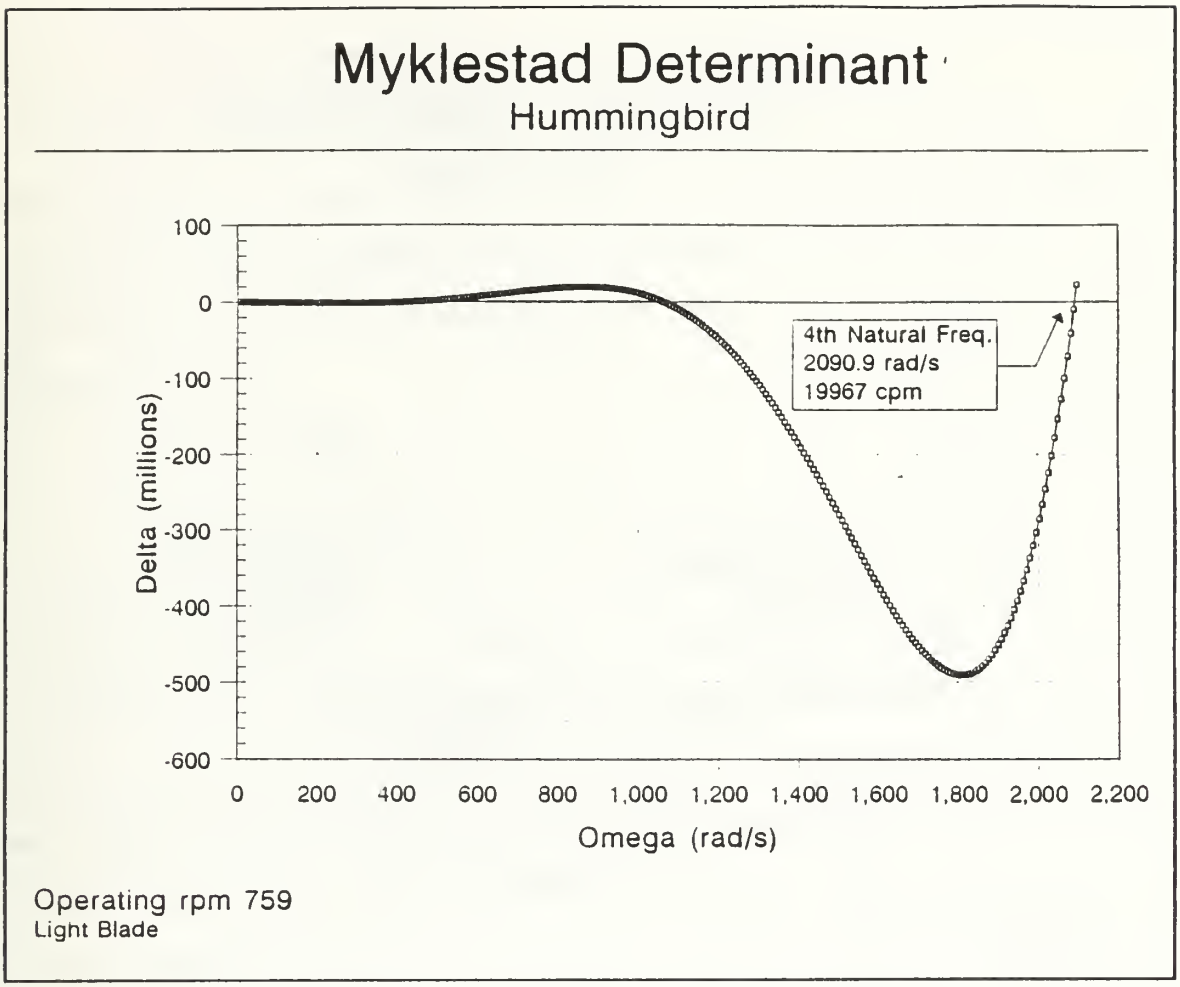

Figure 25 Myklestad Determinant (Light Blade)

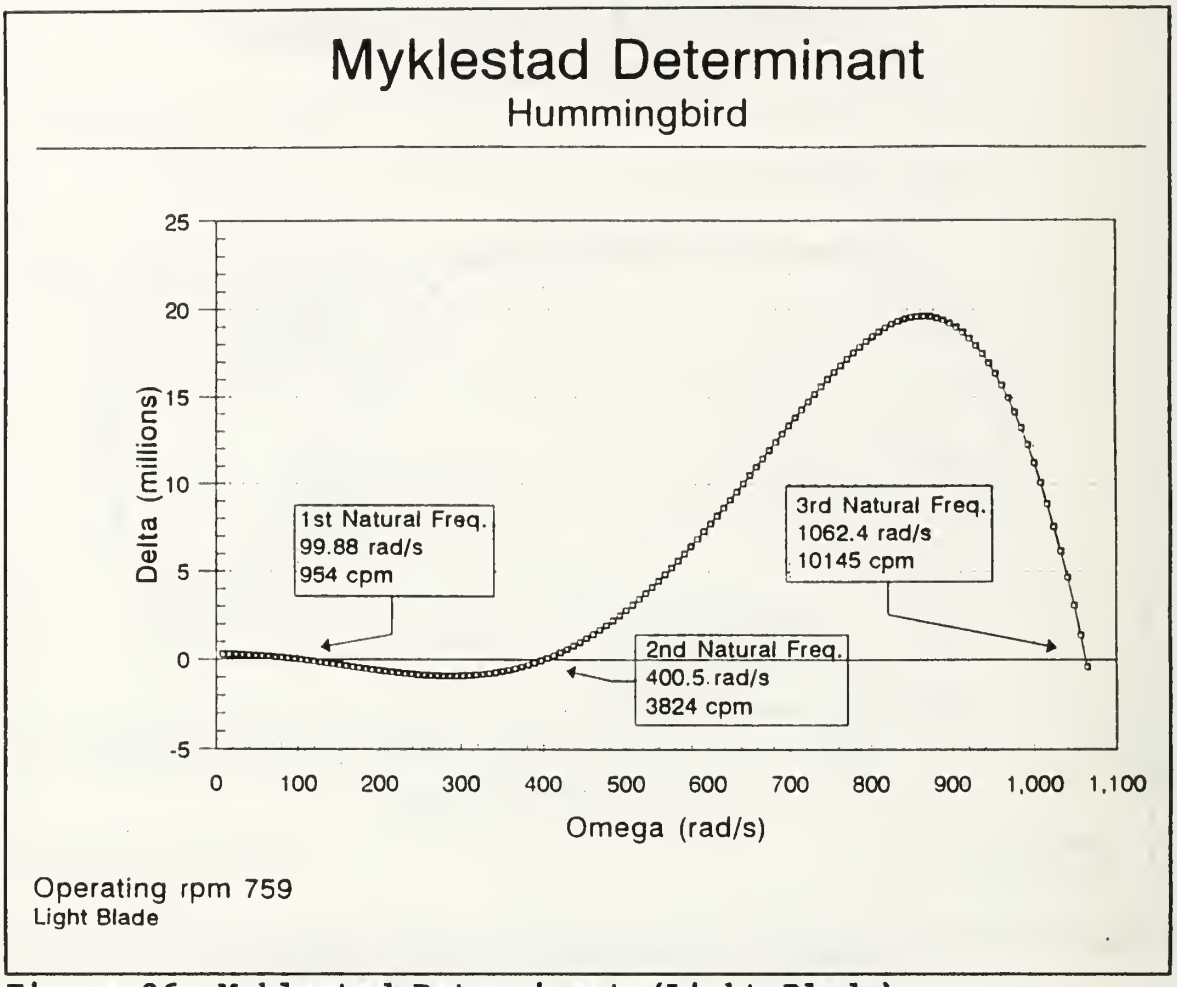

Figure 26 Myklestad Determinant (Light Blade)

equals zero at the natural frequency, the ratio of $-A_y/B_y$ should equal $-A_m/B_m$. Using data in Appendix B for the heavy blade's first natural frequency, the accuracy is seen.

1st Natural freq. = 107.1522 rad/s

A_y= 7.48560 B_y= -469.659

A_m= 1.79121E+04 B_m= -1.12384E+06

$-A_y/B_y$ = 1.593837E-02 $-A_m/B_m$ = 1.593830E-02

It is interesting to note that the natural frequencies are much higher than those of conventional helicopters. This is attributable to the fact that model rotor blades are much shorter and made of solid spruce, which makes them considerably stiffer than full scale blades.

4. Blade Modes

The blade modes were used to verify that the calculated frequencies were in actuality the ascending natural frequencies. Appendix C contains a Fortran code written by Lt. M. Avila that was modified for use on the Hummingbird rotor blades to obtain the rigid and bending flapwise mode shapes. Fig. 27 shows the mode shapes for the heavy blade while Fig. 28 shows the mode shapes for the light blade.

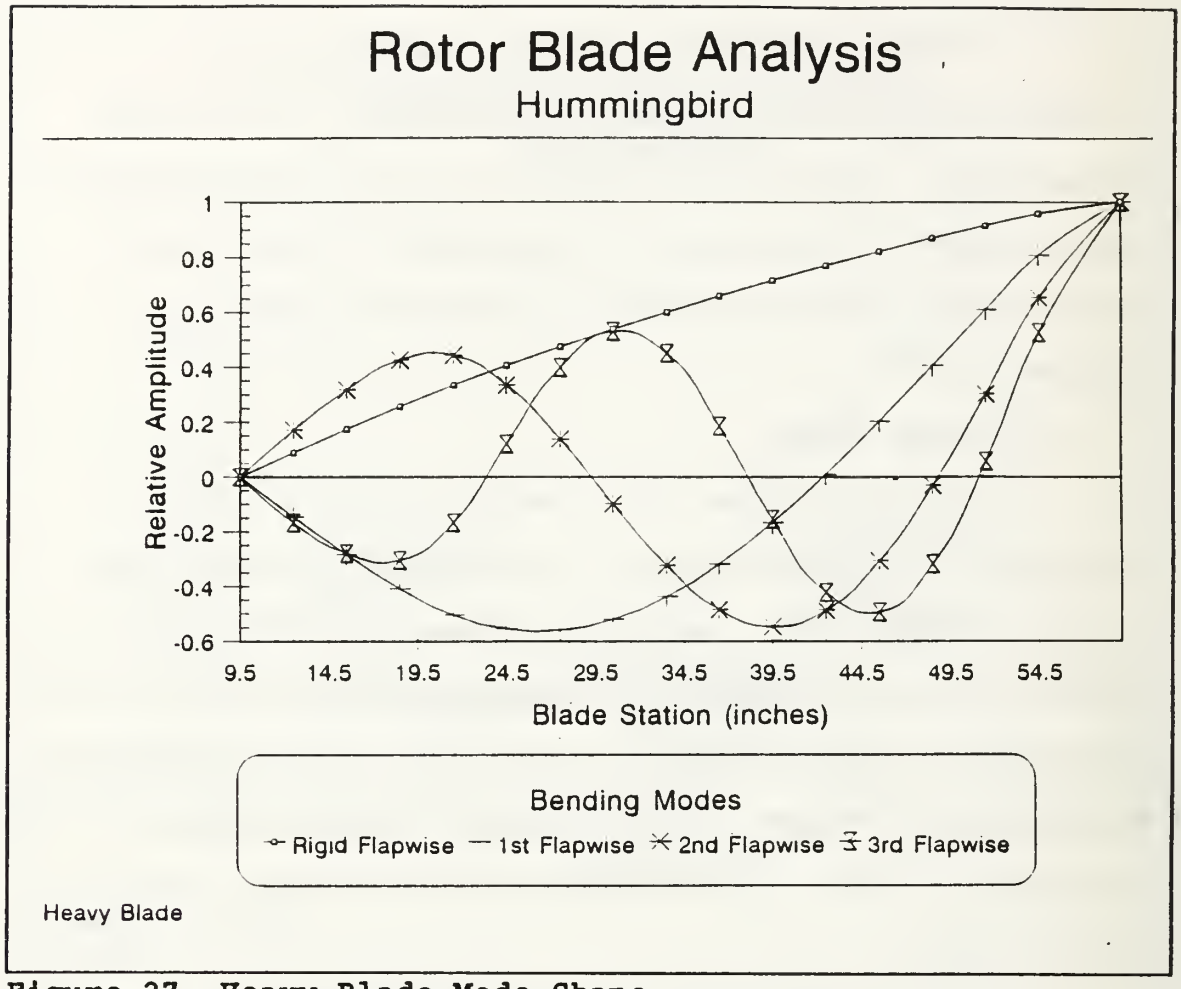

Figure 27 Heavy Blade Mode Shape

5. Southwell Plot

The Southwell plot, also called a Fan plot, is a resonance diagram of the individual blade. It is used to depict the flapwise modes in relation to the integer multiples of the rotor rpm, commonly referred to as 1P, 2P, 3P etc. For a good design, effort should be directed toward keeping the blade natural frequencies away from the 1P,2P, etc. forcing frequencies, since these are the primary

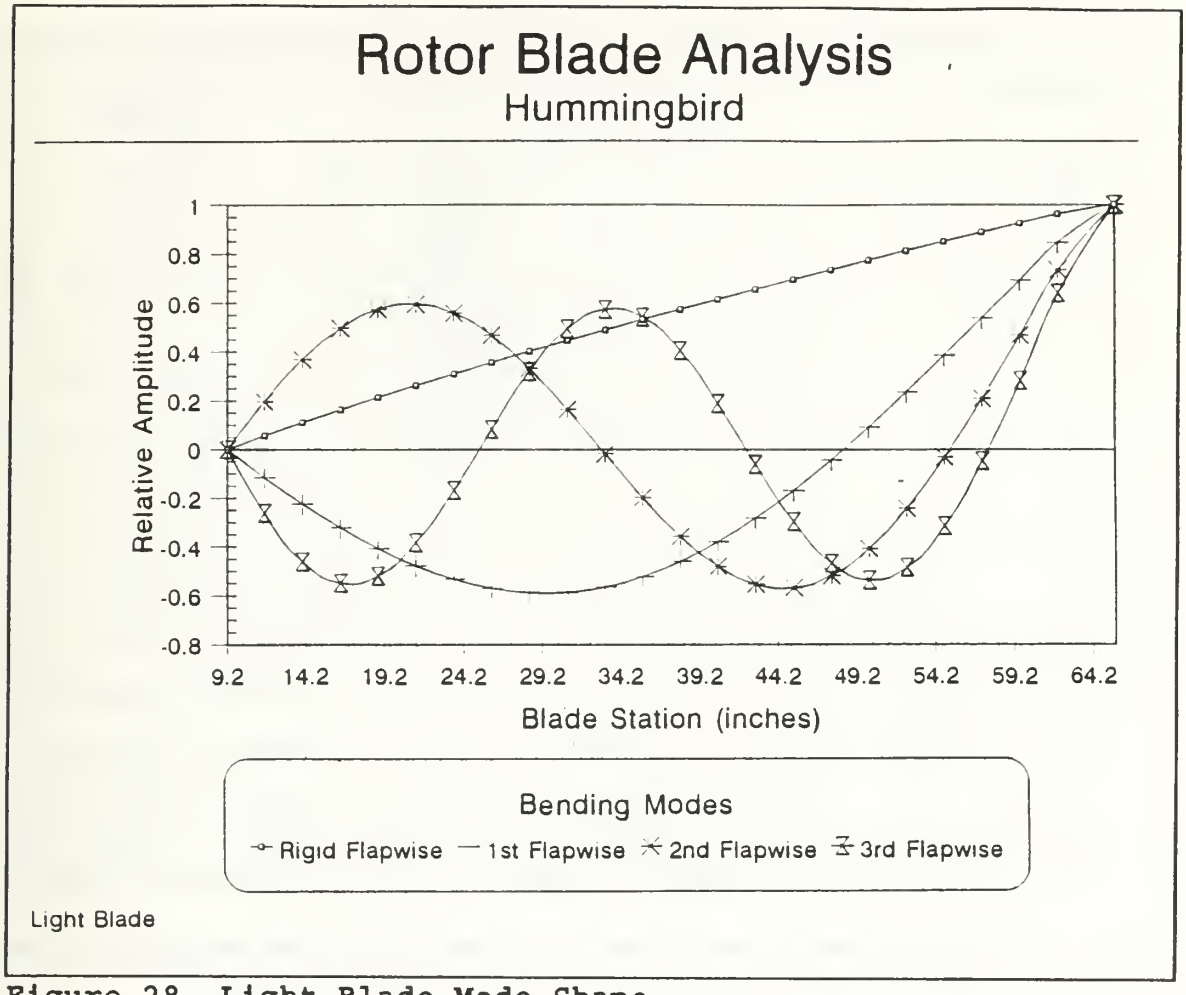

Figure 28 Light Blade Mode Shape

excitations. The Fortran code used for the Myklestad determinant was run for rotor speeds ranging from 0 to 90 rad/s. The results of these runs are shown in Table III. The area of concern is within plus or minus 6 rpm of the operating rpm. Fig. 29 and 30 show the Southwell plot for the heavy blade and light blade respectively.

The rigid mode always lies very near the 1P line. The flapwise bending modes for both blades are much higher than that for full scale blades. Again, this is attributed

Table III BLADE FLAPWISE RESPONSE

Blade		Heavy Blade			Light	
rad/s	rpm	Rigid	1st Bend	2nd Bend	Rigid	1st Bend
		(cpm)	(cpm)	(cpm)	(cpm)	(cpm)
0	0	1.29	1758.9	5757.3	1.19	2876.2
10	95.5	129.9	1791.5	5784.0	119.7	2893.8
20	190	262.6	1887.3	5863.3	240.6	2945.7
30	286.5	390.6	2036.3	5992.7	360.7	3030.0
30	382	517.6	227.9	6169.8	480.9	3144.2
50	477.5	643.6	2452.3	6389.4	601.1	3285.4
60	57.3	774.4	2700.1	6647.3	721.9	3449.2
70	668.5	902.4	2967.4	6939.5	840.9	3634.5
79.42	759	1023.7	3229.2	7241.9	953.7	3824.5
90	859.4	1159.3	3535.2	7608.9	1080	4053.7

to the greatly increased stiffness. The second and third modes for the light blade were higher than those for the heavy blade. This is accounted for by the fact that although the light blade is larger, the lower mass more than offsets the length by increasing the natural frequency. The heavy blade Southwell plot show that there will be no vibratory resonance problems with any of the modes. The first flapwise bending mode of the light blade lies very near the 5P line at the operating frequency. The 5P lies at 62.56 Hz while the second natural frequency lies at 63.74 Hz. The close proximity of the two frequencies should not

be a problem for the Hummingbird, as the critical frequencies occur at the 2P, 3P, and 4P for a three blade rotor system. For a full-scale equivalent 3-bladed helicopter, this near 5P resonance might need to be monitored due to possible high amplification of 5P flapwise blade stresses. In the case of the Hummingbird, the relatively short blades are sufficiently overdesigned to avoid this problem.

Discussion of blade resonance results for the RPH blades would not be complete without comparing these values with values obtained for full-scale helicopters. Here for the light and heavy blades, we find the first rigid mode at 1.26Ω and 1.35Ω respectively. For a uniform articulated blade this would be considerably closer to 1P at 1.02Ω. The first flapwise bending mode for an articulated fullscale blade would be in the vicinity of 2.5Ω, whereas analysis shows in this case that we have much higher frequencies of 5.03Ω and 4.25Ω for the light and heavy blades respectively. Similarly, the second flapwise bending mode for a full-scale articulated blade is about 4.7Ω to 4.9Ω, whereas for the heavy blade, the second flapwise mode occurred much higher, at 9.54Ω. This is even higher than where we would normally expect the frequency of the third flapwise mode to occur for a full-scale rotor. Normally the third mode resonance occurs in the vicinity of 8P.

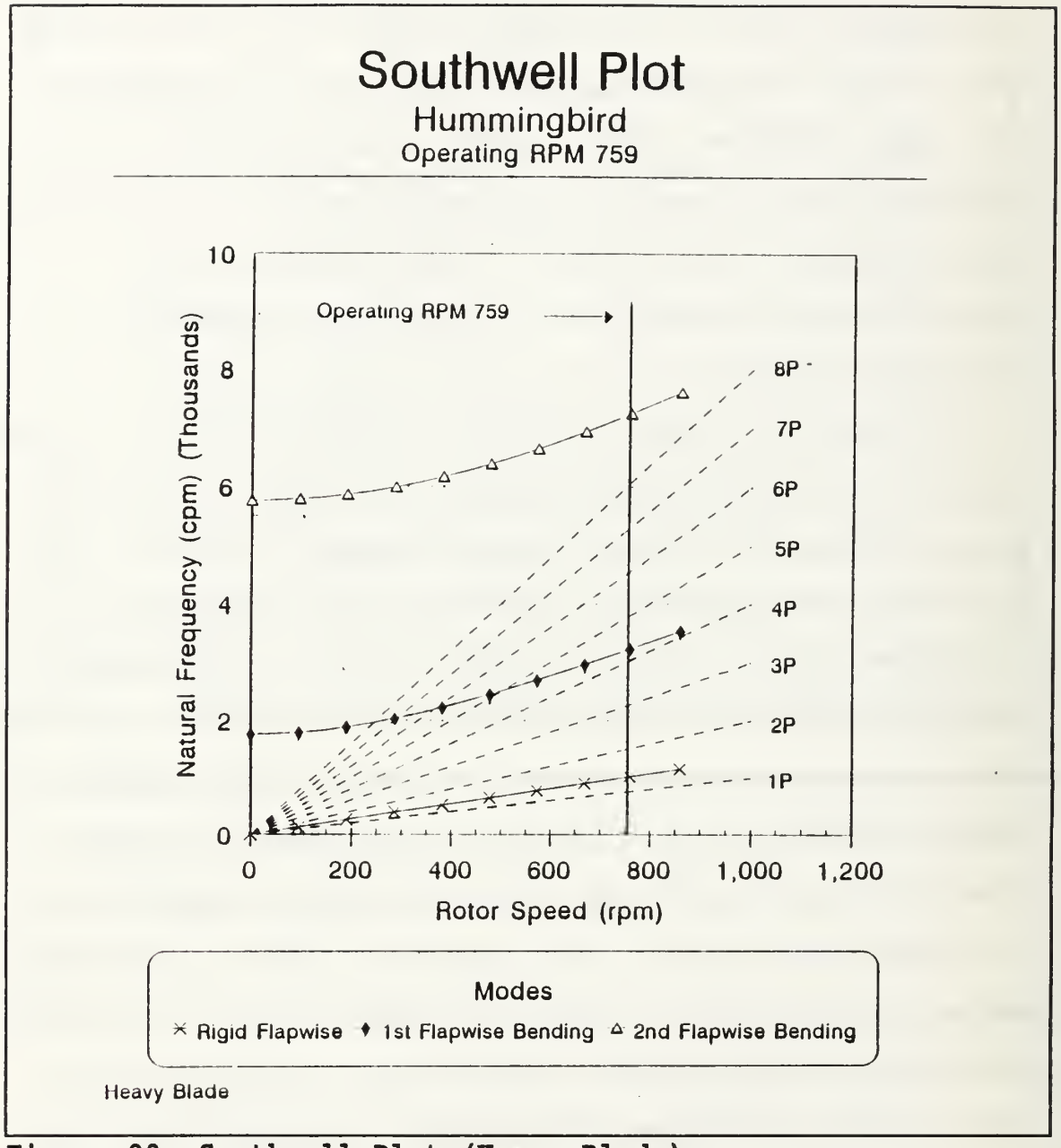

Figure 29 Southwell Plot (Heavy Blade)

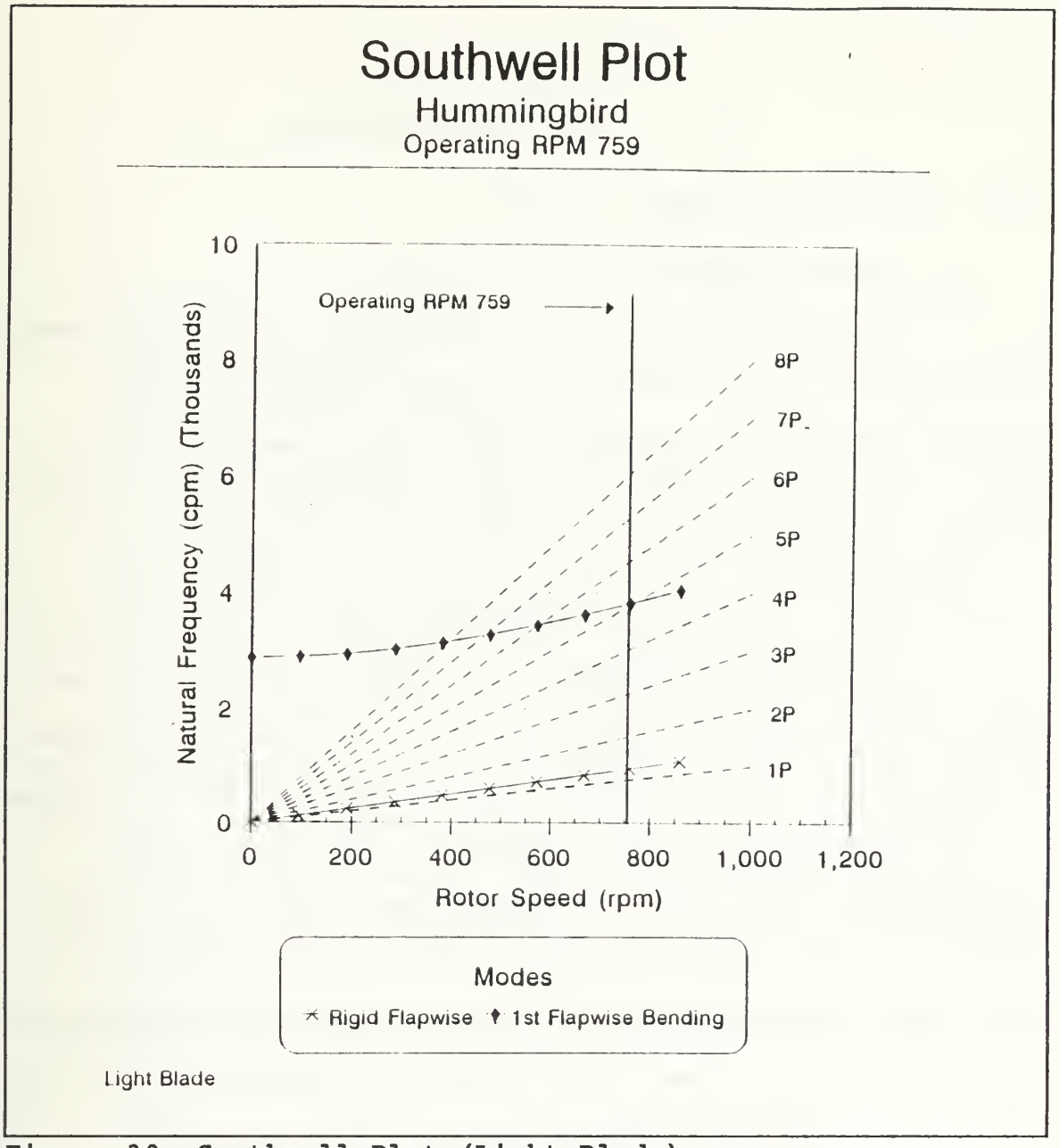

Figure 30 Southwell Plot (Light Blade)

VII. PERFORMANCE ANALYSIS

A. POWER CALCULATIONS

1. Power Required

Using the parameters established in the blade design section and the procedures outlined in Ref. 9, power estimations were calculated. There exist two regimes of operation that establish the power required limits. The first is hover out of ground effect; the second is high speed flight. Since the Hummingbird would not operate in the high speed flight regime, the HOGE was established at the limiting flight condition. Two hover conditions were evaluated: sea level standard day and 4000 ft MSL 95 degrees F. As alluded to earlier, there are three basic power calculations that must be accomplished. They are induced power (P_i), the power required to produce lift; profile power (P_o), the power require to push the blades through the air; and parasite power (P_p), the power required to move the rest of the fuselage through the air. The following formulas were used to calculate these quantities.

$$P_i = \frac{T^{1.5}}{\sqrt{2\rho A}\ B\ 550}\ HP; \quad B = 1 - \frac{(2C_T)^{\frac{1}{2}}}{b} \tag{20}$$

$$P_o = \frac{C_{d_o} \rho \sigma A V_{tip}^3}{4400} \quad HP \tag{21}$$

$$P_p = \frac{\frac{1}{2} \rho f_e V_f^3}{550} \quad HP \tag{22}$$

T = Thrust B = Tip Loss Factor b = Number of blades

A = Rotor Disk Area V_f = Forward Velocity

f_e = Equivalent flat plate area

Using the above formulas, the total power required to hover out of ground effect was calculated. Induced power was 4.95 HP, while profile power was 4.4 HP. The parasite power is equal to zero in the hover case. To calculate the power for the 4000 ft 95 degree F case requires a density correction. The power required to hover in ground effect (HIGE) was also calculated. The induced power ratio equation, based on the a ratio of the rotor height above the ground over the rotor diameter, is used for this calculation, and is shown below:

$$\frac{P_i(IGE)}{P_i(OGE)} = -0.1276\left(\frac{h}{D}\right)^4 + 0.7080\left(\frac{h}{D}\right)^3 - 1.4569\left(\frac{h}{D}\right)^2 + 1.3432\left(\frac{h}{D}\right) + 0.51 \tag{23}$$

The rotor height above the ground (h) equals 2.5 feet. Using the light blades for these calculations, the ratio of h/D equals 0.22. It can be shown that the induced power required to hover IGE is 3.7 HP. These calculations are solely for the main rotor system. The power required for the tailrotor will be included in later calculations. The

final flight regime that must be considered is forward flight. The profile power in forward flight is shown by Eqn. 24.

$$P_{oFlight} = P_{oHover}(1+4.3\mu^2) \quad (24)$$

This equation does not include high speed effects such as compressibility or retreating blade stall, but as stated previously, these will not be factors for the Hummingbird. Power required calculations for velocities ranging from hover to 100 knots are shown in Fig. 31.

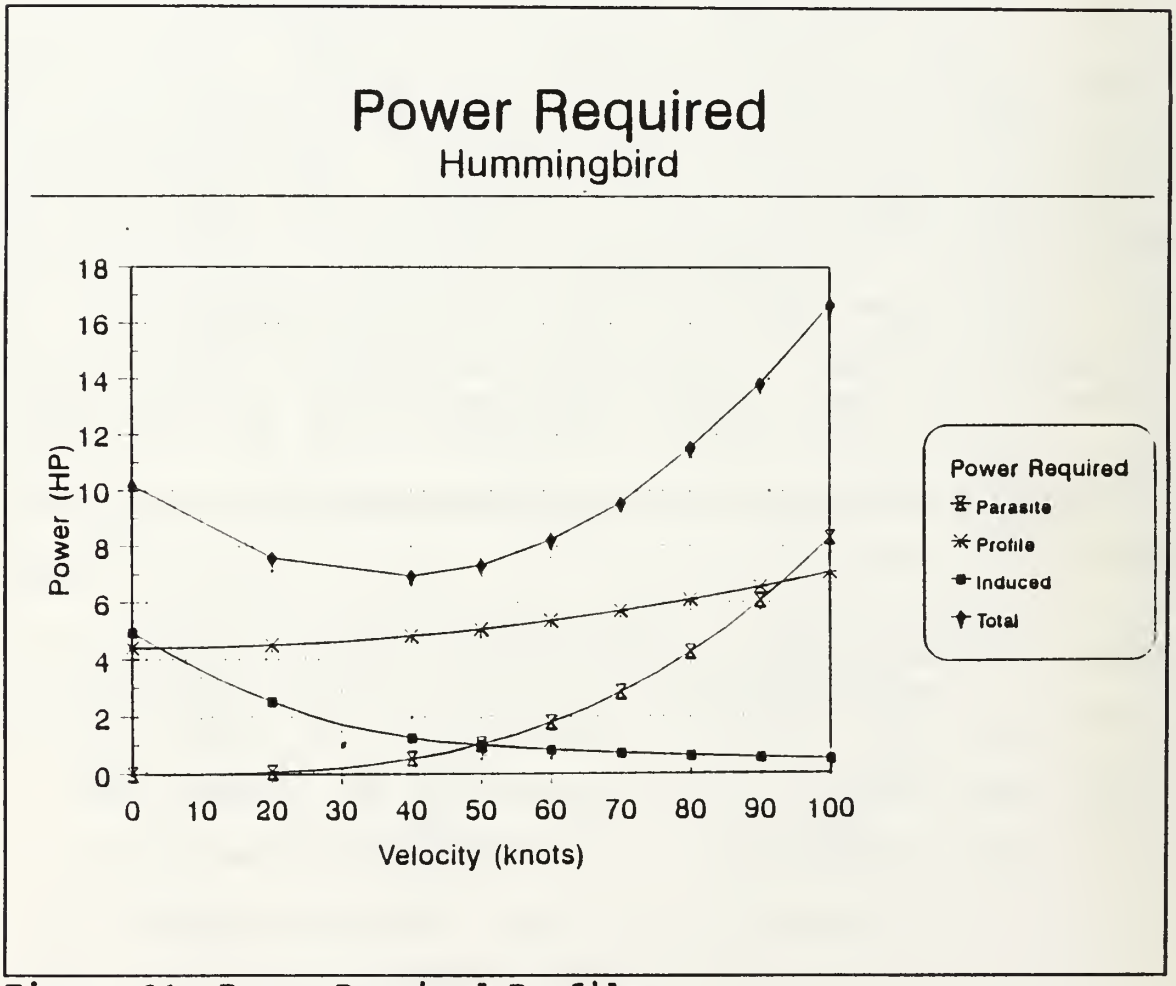

Figure 31 Power Required Profile

Tailrotor power is included in these calculations, assuming that it is nine percent of main rotor in the hover condition, decreasing to three percent at mid-range velocities. Appendix D contains the spreadsheet calculation for all power required calculations.

2. Power Available

The power available curve, Fig. 32, was constructed from data obtained from Ref. 10 and 11. An assumption of near linearity over the entire RPM range was made.

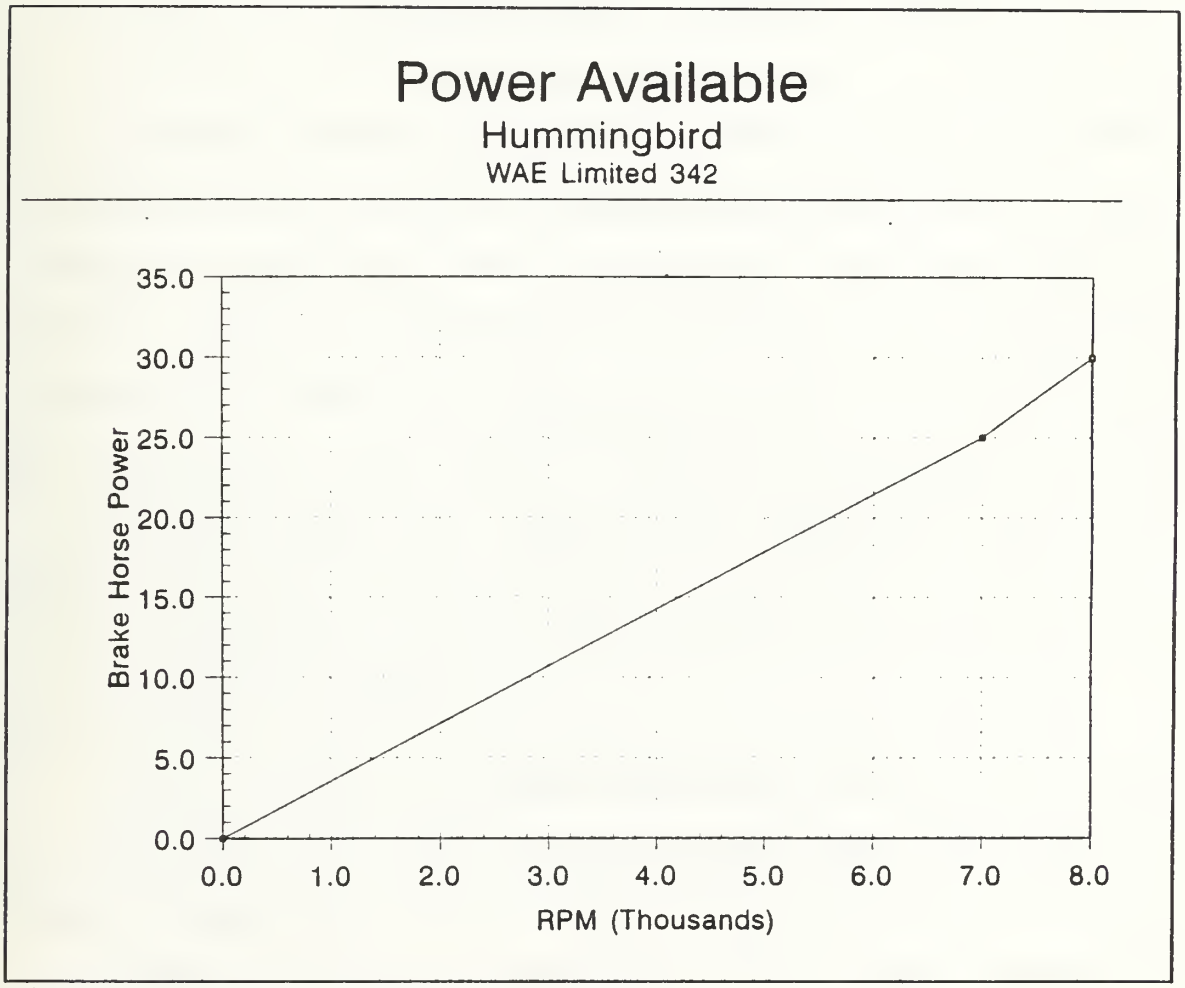

Figure 32 Power Available vs RPM

Fig. 32 will be used again when determining the derated power that will be use in conjunction with resizing of the main rotor drive gear for obtaining desired rotor RPM.

B. RETREATING BLADE STALL

A phenomena that is particular to helicopters is retreating blade stall. It occurs at high forward speeds when the retreating blade is unable to produce the lift required to maintain equilibrium with the advancing blade. This phenomena is due to the great difference in local velocity over the airfoil. The advancing blade encounters the velocity of V_{tip} plus the forward velocity. The retreating blade encounters V_{tip} minus forward velocity. At high forward speeds, the velocity over the retreating blade becomes very small, requiring a very large angle of attack to produce the needed lift for equilibrium. Also, the flow over the inboard part of the retreating blade is reversed, flowing from trailing edge to leading edge. As speed of the helicopter increases this reversed flow region moves out radially along the blade. Typically at cruise speed as much as 30 percent of the blade is experiencing reversed flow.

The total angle of flow can be determined through either of two equations. The first equation is based on the average lift coefficient, which is lift curve slope (a) times the angle of attack, which will be expressed in terms of blade loading (C_T/σ). The second equation is based on

the flapping angle of the blade. Both of these equations are functions of collective pitch angle, θ_0, longitudinal cyclic pitch angle, θ_2, geometric angle of twist, θ_T, and inflow ratio, λ. For each of these two equations, the four parameters are multiplied by coefficients which are functions of the tip loss factor (B), and the advance ratio (μ). The relationship for the first equation is given by Eqn. 25 with the accompanying coefficients given in Eqn. 26, 27, 28 and 29.

$$\frac{2CT}{a} = \lambda T_1 + \theta_0 T_2 + \theta_T T_3 + \theta_2 T_4 \qquad (25)$$

$$T_1 = 0.5(B^2 + 0.5\mu^2) \qquad (26)$$

$$T_2 = 0.33(B^3 + 0.5\mu^2 B) \qquad (27)$$

$$T_3 = 0.25(B^2(B^2 + \mu^2)) \qquad (28)$$

$$T_4 = 0.5\mu(B^2 + 0.25\mu^2) \qquad (29)$$

The second relationship is for the longitudinal flapping coefficient, a_1, which is assumed to be zero or very close to it. The second set of relationships are given in Eqn. 30, 31, 32, 33, and 34.

$$a_1 = 0 = \lambda A_{11} + \theta_0 A_{12} + \theta_T A_{13} + \theta_2 A_{14} \qquad (30)$$

$$A_{11} = \frac{4\left(\frac{\mu B^2}{2} - \frac{3}{8}\right)}{B^2(B^2 - 0.5\mu^2)} \tag{31}$$

$$A_{12} = \frac{8\mu B}{3(B^2 - 0.5\mu^2)} \tag{32}$$

$$A_{13} = \frac{2\mu B^2}{B^2 - 0.5\mu^2} \tag{33}$$

$$A_{14} = \frac{B^2 + 1.5\mu^2}{B^2 - 0.5\mu^2} \tag{34}$$

Solving the two equations simultaneously in terms of the eight coefficients, the collective pitch angle and the longitudinal cyclic pitch angle can be determined. The resulting equations are as follows:

$$\theta_0 = \frac{\theta_T A_{13} + \theta_2 A_{14} + \lambda A_{11}}{A_{12}} \tag{35}$$

$$\theta_2 = \frac{A_{12}\frac{2}{a}\frac{C_T}{\sigma} + \lambda(A_{11}T_2 - A_{12}T_1) + \theta_T(A_{13}T_2 - A_{12}T_3)}{A_{12}T_4 - A_{14}T_2} \tag{36}$$

Using these equations, approximations for the angle of attack of the advancing and retreating blades can be calculated. The equations for the angle of attack are given by Eqn. 37.

$$\alpha_{270} = \theta_0 - \theta_2 + \theta_T + \frac{\lambda}{1+\mu} \qquad \alpha_{90} = \theta_0 + \theta_2 + \theta_T + \frac{\lambda}{1+\mu} \tag{37}$$

Appendix E contains the spreadsheet that was used to calculate the angle of attack for three different blade twist conditions, 0, -4, and -8 degrees of twist. The minus sign indicates that the twist angle decreases from the tip of the blade to the root. Fig. 33, 34, and 35 show the results of these calculations.

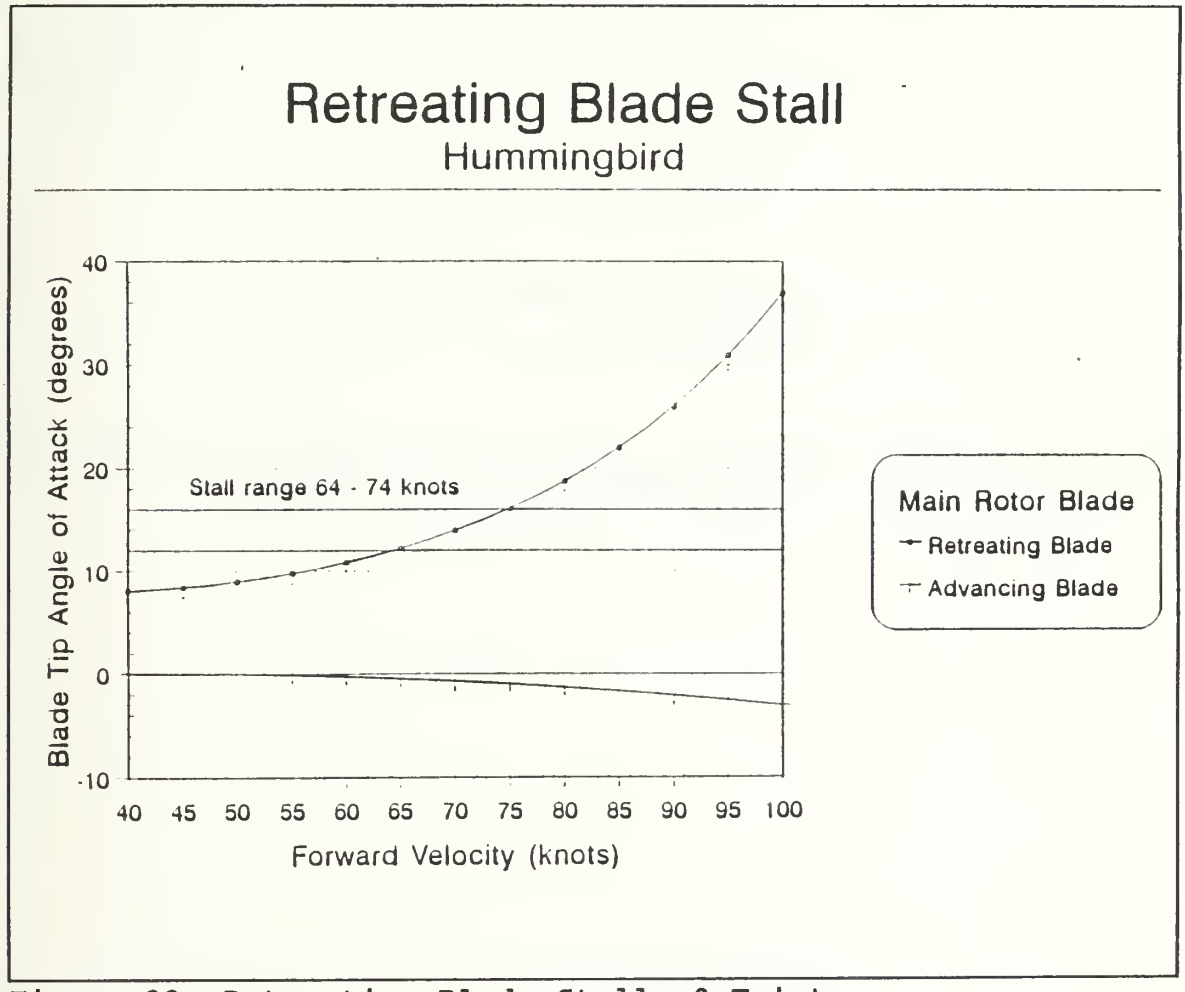

Figure 33 Retreating Blade Stall, 0 Twist

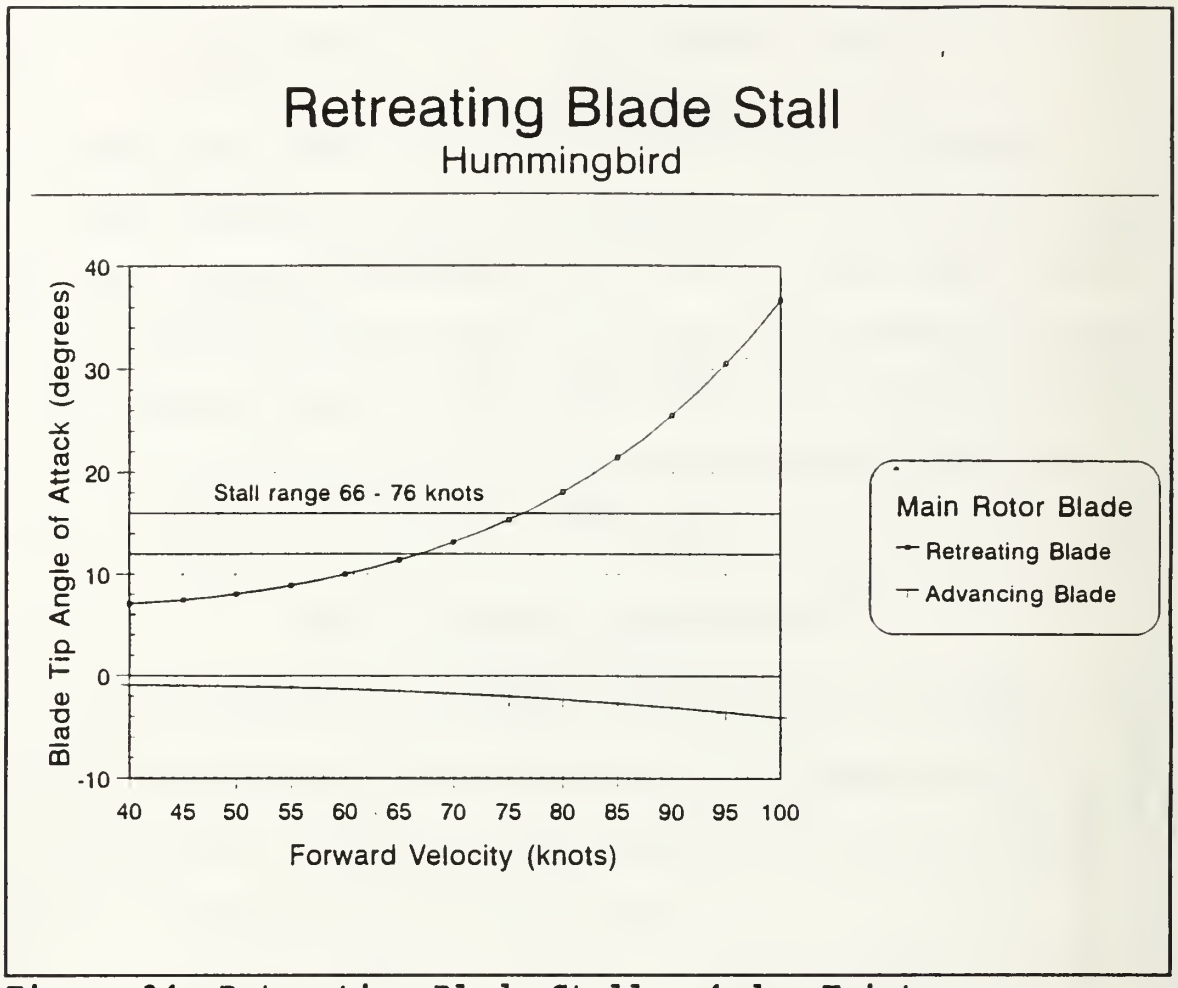

Figure 34 Retreating Blade Stall, -4 deg Twist

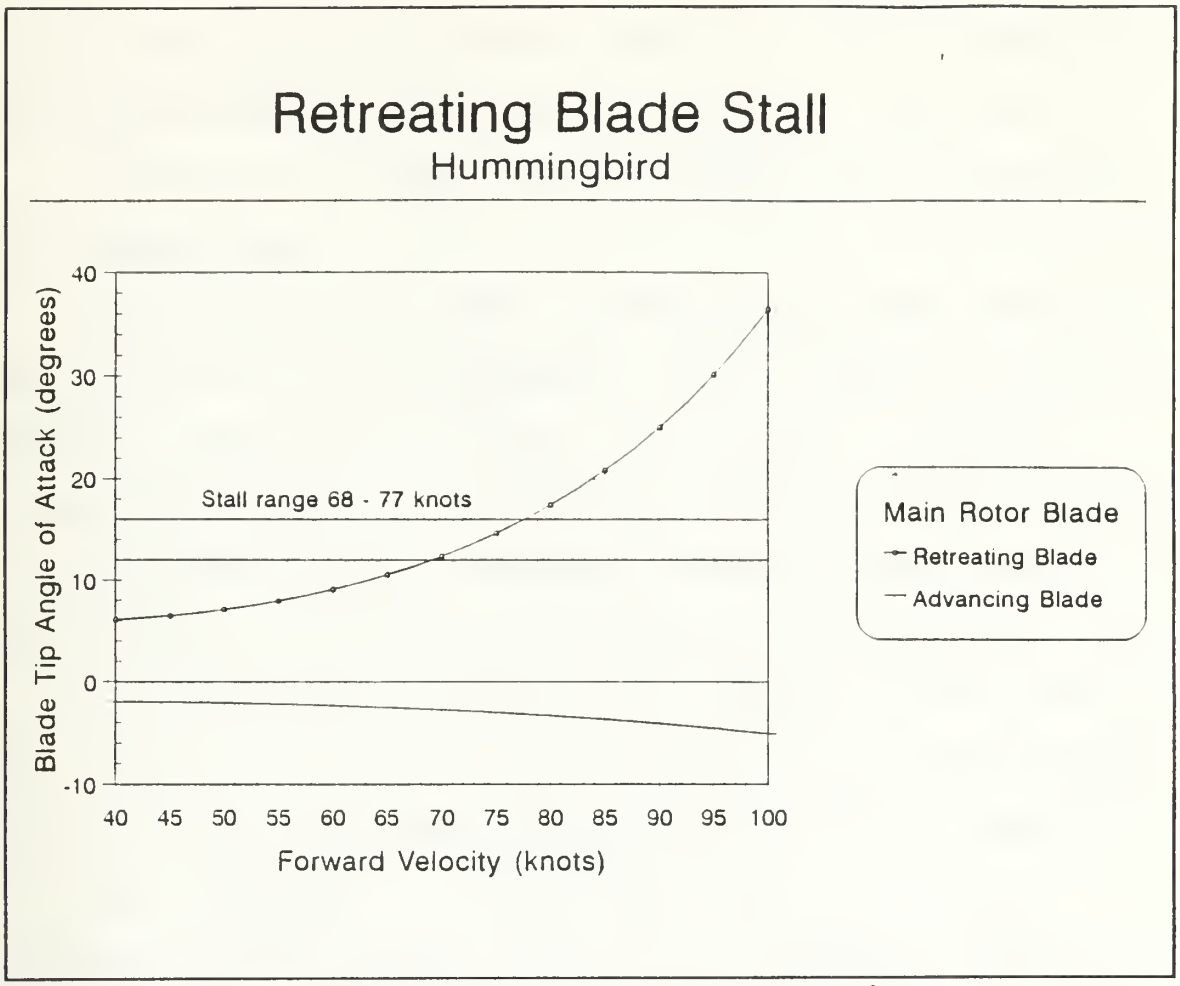

Figure 35 Retreating Blade Stall, -8 deg Twist

According to Ref.8 the blade reaches its operational limit when the angle of attack of the tip of the retreating blade exceeds the stall angle of attack (AOA) of the airfoil section by four degrees [Ref. 8:p. 258]. For the NACA 0012, this AOA would be 16 degrees. There are three areas of interest on these figures: airspeeds which require less than 12 degrees AOA where no stall will be encountered, airspeeds which require between 12 degrees and 16 degrees AOA where a moderate amount of stall is present, and airspeeds which require 16 degrees or greater AOA where the severity of the stall prohibits flight. Two lines are annotated on the above graphs to show the velocity for this stall area. The limiting velocities for the three conditions are 64 & 74, 66 & 76, and 68 & 77 knots respectively. The result agrees with theory, because the increase in twist should increase the stall envelope, which the figures demonstrate.

VIII. MODIFICATIONS

A. LANDING GEAR

The rear landing gear of the Hummingbird has a narrow tread width which is considered to be too narrow in view of takeoff and landing stability. It also has no shock absorption capability, which is critical for avoiding ground resonance. A study was conducted to determine the most advantageous route to take to overcome this challenge. The options were to leave it as it is, replace it with a skid configuration, or a strut configuration. The landing gear was redesigned with a strut configuration to overcome both of these problems. The tread width was widened from 17 inches to 27 inches and an oleo was incorporated. The spring constant of the oleo was chosen so that the Hummingbird could survive a fall from ten feet. Ten feet is approximately one rotor diameter, the height to hover out of ground effect.

B. DRIVE TRAIN MODIFICATIONS

1. Engine to Main Rotor Gear Ratio

Because of the requirement for the main rotor blades to obtain a prescribed Reynolds number range, the rotor rpm had to be increased to achieve the tip velocity required. Before the gearing ratio was chosen, the decision to derate

the engine had to be made. It was shown earlier that for the Hummingbird's range of operation, there would always be excess power available. Based on this fact and the desire to extend the life of the engine, it is recommended that the engine be rated to operate at 18 HP vice 25 HP. Fig. 32 shows that for this horsepower an engine rpm of 5000 is required. The present gear ratio is 10:1 and would have to be lowered to 6.6:1 to achieve a rotor rpm of 759.

2. Freewheeling Unit

The Hummingbird, as stated earlier, has no ability to autorotate. Because of this operating limitation, the Hummingbird is at great risk of loss to an inflight engine failure. It was decided that the most effective way to solve this safety hazard was to incorporate a one-way bearing in the gear that would be changed for the gear ratio change. After examination of the drive train, the last gear in the drive train was selected as the most effective point to make the modification. This point was selected for two reasons. First, because it was the last gear in the drive train, the rotor would have the least mechanical resistance during an autorotation. This point is critical because every rpm gives that much more cushion in the touch down phase of an autorotation, thus increasing the chances of a successful autorotation. Second, this gear has easy accessibility and would simplify the modification process.

IX. CONCLUSIONS AND RECOMMENDATIONS

A. CONCLUSIONS

The goal of this research effort was to design a remotely piloted helicopter (RPH) with the capabilities to meet the expanding needs of the Department of Aeronautics and Astronautics helicopter flight test program. These needs have grown rapidly over the past two years. J. G. Scott stated in his thesis that the "requirements were: (1) a four-bladed rotor head; (2) payload capacity of approximately 15 pounds; and (3) a total system cost of no greater than $10,000." [Ref. 12] Numerous research requirements have arisen since that time, which have expanded the envelope of RPH requirements. Lt. M. Borno's quarter scale NOTAR research requires a platform of greater size and power than is available with any of the department's current assets. Continuing HHC research requires an RPH that will produce blade Reynolds numbers in the range of 1.5 to 1.8 million in order to validate HHC performance enhancements. Based on these two research requirements and the hindsight of how quickly these requirements change, it was imperative to develop an RPH that could meet the existing needs and would be flexible enough to meet future needs.

Upon completion of the initial design phase it was determined that two paths were available: (1) complete the detailed design in house; or (2) search the open market to find an RPH capable of meeting the existing requirements. The second path was chosen and resulted in procurement of the Hummingbird. The Hummingbird possesses the capabilities to meet existing and future requirements with some modifications. The NOTAR requirements are fulfilled in the Hummingbird's present state, but the HHC requirement dictates some modification. These modifications include a new three blade main rotor hub to be used with the existing rotor blades and a change in the engine to main rotor gearing ratio. Two other modifications that would be of great value from a safety standpoint are incorporating a freewheeling unit in the engine drive system and replacing the existing landing gear.

The performance analysis shows that with the main rotor hub change, the Hummingbird will be able to achieve a Reynolds number within the range required for aerodynamic performance comparison with the OH-6A. This change will reduce the Figure of Merit, but due to low disk loading, will have little effect on the Hummingbirds power loading.

The analysis of the Hummingbird also shows that it will have an excess power of nearly 10 HP for HOGE and therefore can be operated at a derated power. This would reduce wear on the engine and thus enhance its life. The decision to

derate the engine should be made prior to changing the engine to main rotor gearing, as it will effect the operating rpm of the engine.

The design improvements; modified landing gear and a freewheeling unit, will provide the capability to safely and successfully recover the Hummingbird from nearly any malfunction over a large flight regime.

The overall analysis of the Hummingbird is that it is an ideal platform for subsequent research. It has the capabilities to meet the existing needs and the flexibility to meet any foreseeable future needs.

B. RECOMMENDATIONS

There is almost unlimited potential for the Hummingbird's use in further RPH research. Two items that need to be undertaken as soon a possible are the design and manufacture of a three blade hub and incorporating a freewheeling unit in the engine drive train. The first is necessary before any HHC work can be undertaken on the Hummingbird. Measurement could then be started on the control system freeplay and torsional constants. The ground work is laid out in Ref. 12 and 13. The second item is primarily for safety reasons and to help protect the investment of the department.

The design of a new main rotor hub could be a thesis in itself. A great source of expertise that could be of help

is Mr. Art Phelps of the Aerostructures Directorate at NASA Langley. His directorate owns an RPH identical to the Hummingbird, and it would be of value to develop the bonds of cooperation that have been established with them.

Two other areas where valuable research could be done is in the design of an improved main rotor blade and the incorporation of a new landing gear design. An improved main rotor blade should be designed to optimize airfoil cross section and blade twist. The manufacture of new landing gear should be a moderately easy job which would greatly enhance the survivability of the Hummingbird.

The final recommendation is made in light of all the current and possible future research that would hinge on the Hummingbird. It is highly recommended that a second Hummingbird be purchased. The reason for this is that concurrent research on the Hummingbird will inevitably require alteration that would adversely affect one or both of the areas of research. A case in point is the hub redesign and how it will affect the NOTAR research. The NOTAR research demands that the rotor operating parameters be constant. This demand would not be feasible in the tradeoffs that occur in the design process. Therefore, having a second helicopter would allow for numerous research projects to be accomplished concurrently without adversely affecting one another.

APPENDIX A: MYKLESTAD FORTRAN CODE

```
C  THIS PROGRAM CALCULATES MYKLESTAD DETERMINANT FOR
C  DETERMINING THE NATURAL FREQUENCY OF A ROTOR BLADE
C
C  THIS PROGRAM IS FOR AN ARTICULATED HUB ONLY
C
C  THE PROGRAM IS SET UP TO TAKE A BLADE OF 17 SEGMENTS.


      IMPLICIT DOUBLE PRECISION (A-H,L,M,O-Z)
      DOUBLE PRECISION T(1:17),SHEAR(1:17),MOM(1:17),SLOPE(1:17),
     %Y(1:17),R(1:17),WT(1:17),DELTA1,XI(1:17),NR,NRSQ,F,WSQ,
     %L(1:17),W,S1,S2,S3,Y1,Y2,Y3,Y4,MOM1,MOM2,BS,BM,DELTA2,
     %BSLOPE,BY,AS,AM,ASLOPE,AY,XPLOT(1:17),YPLOT(1:17)

C*****************************************************************
C VARIABLE DEFINITION
C
C T       - CENTRIFUGAL FORCE
C SHEAR   - SHEAR
C MOM     - MOMENT
C SLOPE   - SLOPE
C Y       - DEFLECTION
C*****************************************************************

C
C  THIS OPENS THE DATA FILE FOR OUTPUT "WOODPTS.DAT"
C
      OPEN (UNIT=35,FILE='WOODPTS.DAT',STATUS='UNKNOWN')
C

C*****************************************************************
C
C  THESE ARE THE INITIAL PARAMETERS TAKEN FROM THE BLADE DATA
C  THEY ARE FROM THE BLADE TIP TO THE BLADE ROOR
C
C  SEGMENT SPACING (IN)
      DATA L/6.25,16*3.0/
C  SEGMENT RADIUS  (IN)
      DATA R/59.1,54.5,51.5,48.5,45.5,42.5,39.5,36.5,33.8,30.5,
     %27.5,24.5,21.5,18.5,15.5,12.5,9.5/
C  SEGMENT WEIGHT (LBS)
      DATA WT/.459,13*.22,.708,.656,.742/
C  SEGMENT FLAPWISE MOMENT OF INERTIA, Ixx (IN^4)
      DATA XI/14*.097,.45,.417,.808/
C*****************************************************************
C  ALLOWS FOR DIFFERENT NR INPUTS WITHOUT RECOMPILING
C
      PRINT *, 'INPUT ROTOR RPM OMEGA'
      READ *, NR
      NRSQ=NR*NR
      E= 1305000          ! MODULUS OF ELASTICITY OF SPRUCE WOOD

C*****************************************************************
C  THIS LOOP FOR F MAY NEED TO BE MODIFIED FOR THE LOWER FREQUENCY
C  RUNS AS YOU DO NOT OBTAIN ENOUGH DATA
C
      DO 400 F=.1,30,.1
      W=(NR*F)
      WSQ=W*W
      I=1.0
```

```
C*********************************************************************
C
C  INITIAL CONDITIONS
C
      SLOPE(1)=1
      Y(1)=0
020   SHEAR(1)=0
      MOM(1)=0
C
C*********************************************************************
C
C  MYKLESTAD METHOD

      T(1)=WT(1)*NRSQ*R(1)/(32.174*12)
      DO 30 J=2,17
      T(J)=T(J-1)+((WT(J)*NRSQ*R(J))/(32.174*12))
      S1=SLOPE(J-1)*(1+((T(J-1)*L(J)*L(J))/(2*E*XI(J))))
      S2=MOM(J-1)*L(J)/(E*XI(J))
      S3=SHEAR(J-1)*L(J)*L(J)/(2*E*XI(J))
      SLOPE(J)=S1-S2-S3
      Y1=SLOPE(J)*L(J)
      Y2=T(J-1)*SLOPE(J-1)*(L(J)**3)/(3*E*XI(J))
      Y3=MOM(J-1)*(L(J)**2)/(2*E*XI(J))
      Y4=SHEAR(J-1)*(L(J)**3)/(3*E*XI(J))
      Y(J)=Y(J-1)-Y1+Y2-Y3-Y4
      SHEAR(J)=SHEAR(J-1)+((WT(J)*WSQ*Y(J))/(32.174*12))
      MOM1=SHEAR(J-1)*L(J)
      MOM2=T(J-1)*(Y(J-1)-Y(J))
      MOM(J)=MOM(J-1)+MOM1-MOM2
030   CONTINUE
      IF(I.EQ.2) GOTO 200
      BS=SHEAR(17)
      BM=MOM(17)
      BSLOPE=SLOPE(17)
      BY=Y(17)
      I=2
C
C*********************************************************************
C  NEW INITIAL CONDITIONS FOR SECOND COEFFICIENTS
      SLOPE(1)=0
      Y(1)=1
C
C*********************************************************************
      GOTO 020
200   AS=SHEAR(17)
      AM=MOM(17)
      ASLOPE=SLOPE(17)
      AY=Y(17)
C
C  DELTA1 VARIABLE IS FOR THE ARTICULATED ROTOR
C  DELTA2 IS FOR THE HINGELESS ROTOR
C
C  WHERE DELTA GOES TO ZERO IS THE NATURAL FREQUENCY
C

      DELTA1=(AM*BY)-(BM*AY)
      DELTA2=(ASLOPE*BY)-(BSLOPE*AY)
C
50    FORMAT (1X,1PE13.6,1X,1PE12.5,1X,1PE12.5,1X,1PE12.5,1X,1PE12.5,
     %1X,1PE12.5)
```

```
51     FORMAT (1X,F10.3,2X,F10.3)
       WRITE(*,50) W,DELTA1,AM,AY,BM,BY
       WRITE(35,50) W,DELTA1,AM,AY,BM,BY
400    CONTINUE
C
       STOP
       END
```

APPENDIX B: MYKLESTAD NATURAL FREQUENCIES

First Natural Frequency

Operating rpm 759 (79.4118 rad/s)

Frequency (rad/s)	Delta	Coefficients			
		Am	Ay	Bm	By
1.071522E+02	6.82392E-01	1.79121E+04	7.48559E+00	-1.12384E+06	-4.69659E+02
1.071522E+02	5.74431E-01	1.79121E+04	7.48560E+00	-1.12384E+06	-4.69659E+02
1.071522E+02	4.66470E-01	1.79121E+04	7.48560E+00	-1.12384E+06	-4.69659E+02
1.071522E+02	3.58510E-01	1.79121E+04	7.48560E+00	-1.12384E+06	-4.69659E+02
1.071522E+02	2.50549E-01	1.79121E+04	7.48560E+00	-1.12384E+06	-4.69659E+02
1.071522E+02	1.42588E-01	1.79121E+04	7.48560E+00	-1.12384E+06	-4.69659E+02
1.071522E+02	3.46273E-02	1.79121E+04	7.48560E+00	-1.12384E+06	-4.69659E+02
1.071522E+02	-7.33335E-02	1.79122E+04	7.48560E+00	-1.12384E+06	-4.69659E+02
1.071522E+02	-1.81294E-01	1.79122E+04	7.48560E+00	-1.12384E+06	-4.69659E+02
1.071522E+02	-2.89255E-01	1.79122E+04	7.48560E+00	-1.12384E+06	-4.69659E+02
1.071522E+02	-3.97216E-01	1.79122E+04	7.48560E+00	-1.12384E+06	-4.69659E+02
1.071522E+02	-5.05177E-01	1.79122E+04	7.48561E+00	-1.12384E+06	-4.69659E+02

Frequency at which Delta = 0

107.1522	0.0	1.79121E+04	7.48560	-1.12384E+06	-4.69659E+02

(1022 rpm)

2nd Natural Frequency

Operating rpm 759 (79.4118 rad/s)

Frequency (rad/s)	Delta	Coefficients			
		Am	Ay	Bm	By
3.381635E+02	-2.15818E+01	3.50008E+05	8.05647E+01	-5.16530E+06	-1.18895E+03
3.381635E+02	-1.90265E+01	3.50008E+05	8.05647E+01	-5.16530E+06	-1.18895E+03
3.381636E+02	-1.64711E+01	3.50008E+05	8.05647E+01	-5.16530E+06	-1.18895E+03
3.381637E+02	-1.39158E+01	3.50009E+05	8.05648E+01	-5.16531E+06	-1.18895E+03
3.381638E+02	-1.13605E+01	3.50009E+05	8.05648E+01	-5.16531E+06	-1.18895E+03
3.381639E+02	-8.80514E+00	3.50009E+05	8.05649E+01	-5.16531E+06	-1.18895E+03
3.381639E+02	-6.24980E+00	3.50010E+05	8.05649E+01	-5.16532E+06	-1.18895E+03
3.381640E+02	-3.69446E+00	3.50010E+05	8.05650E+01	-5.16532E+06	-1.18895E+03
3.381641E+02	-1.13912E+00	3.50010E+05	8.05650E+01	-5.16532E+06	-1.18895E+03
3.381642E+02	1.41623E+00	3.50010E+05	8.05651E+01	-5.16532E+06	-1.18895E+03
3.381643E+02	3.97157E+00	3.50011E+05	8.05651E+01	-5.16533E+06	-1.18895E+03
3.381643E+02	6.52692E+00	3.50011E+05	8.05652E+01	-5.16533E+06	-1.18895E+03
3.381644E+02	9.08227E+00	3.50011E+05	8.05652E+01	-5.16533E+06	-1.18895E+03
3.381645E+02	1.16376E+01	3.50011E+05	8.05652E+01	-5.16534E+06	-1.18895E+03
3.381646E+02	1.41930E+01	3.50012E+05	8.05653E+01	-5.16534E+06	-1.18895E+03
3.381647E+02	1.67483E+01	3.50012E+05	8.05653E+01	-5.16534E+06	-1.18895E+03
3.381647E+02	1.93037E+01	3.50012E+05	8.05654E+01	-5.16534E+06	-1.18895E+03
3.381648E+02	2.18591E+01	3.50012E+05	8.05654E+01	-5.16535E+06	-1.18895E+03
3.381649E+02	2.44144E+01	3.50013E+05	8.05655E+01	-5.16535E+06	-1.18895E+03

Frequency at whci Delta = 0

338.1641	0.0	3.50010E+05	8.05650E+01	-5.16532E+06	-1.18895E+03

(3229 rpm)

3rd Natural Frequency

Operating rpm 759 (79.4118 rad/s)

Frequency (rad/s)	Delta	Coefficients			
		Am	Ay	Bm	By
7.583725E+02	2.20479E+01	8.24037E+06	8.12285E+02	-7.04041E+07	-6.94000E+03
7.583725E+02	2.00033E+01	8.24038E+06	8.12285E+02	-7.04041E+07	-6.94000E+03
7.583725E+02	1.79588E+01	8.24038E+06	8.12286E+02	-7.04041E+07	-6.94000E+03
7.583725E+02	1.59143E+01	8.24038E+06	8.12286E+02	-7.04041E+07	-6.94000E+03
7.583725E+02	1.38698E+01	8.24038E+06	8.12286E+02	-7.04041E+07	-6.94000E+03
7.583725E+02	1.18253E+01	8.24038E+06	8.12286E+02	-7.04041E+07	-6.94000E+03
7.583725E+02	9.78079E+00	8.24038E+06	8.12286E+02	-7.04041E+07	-6.94000E+03
7.583725E+02	7.73628E+00	8.24038E+06	8.12286E+02	-7.04041E+07	-6.94000E+03
7.583725E+02	5.69177E+00	8.24038E+06	8.12286E+02	-7.04041E+07	-6.94000E+03
7.583725E+02	3.64725E+00	8.24038E+06	8.12286E+02	-7.04041E+07	-6.94000E+03
7.583725E+02	1.60272E+00	8.24038E+06	8.12286E+02	-7.04041E+07	-6.94000E+03
7.583725E+02	-4.41768E-01	8.24038E+06	8.12286E+02	-7.04041E+07	-6.94000E+03
7.583726E+02	-2.48627E+00	8.24038E+06	8.12286E+02	-7.04041E+07	-6.94000E+03
7.583726E+02	-4.53081E+00	8.24038E+06	8.12286E+02	-7.04041E+07	-6.94000E+03
7.583726E+02	-6.57532E+00	8.24038E+06	8.12286E+02	-7.04041E+07	-6.94000E+03
7.583726E+02	-8.61982E+00	8.24038E+06	8.12286E+02	-7.04041E+07	-6.94000E+03
7.583726E+02	-1.06643E+01	8.24038E+06	8.12286E+02	-7.04041E+07	-6.94000E+03
7.583726E+02	-1.27089E+01	8.24038E+06	8.12286E+02	-7.04041E+07	-6.94000E+03

Frequency at which Delta = 0

758.3725	0.0	8.24038E+06	8.12286E+02	-7.04041E+07	-6.94000E+03

(7242 rpm)

4th Natural Frequency

Operating rpm 759 (79.4118 rad/s)

Frequency (rad/s)	Delta	Coefficients			
		Am	Ay	Bm	By
1.448090E+03	-4.21455E+04	2.77806E+08	1.18496E+04	-1.75250E+09	-7.47518E+04
1.448091E+03	-3.88022E+04	2.77807E+08	1.18497E+04	-1.75251E+09	-7.47520E+04
1.448092E+03	-3.54589E+04	2.77808E+08	1.18497E+04	-1.75251E+09	-7.47521E+04
1.448092E+03	-3.21156E+04	2.77809E+08	1.18497E+04	-1.75252E+09	-7.47523E+04
1.448093E+03	-2.87722E+04	2.77810E+08	1.18498E+04	-1.75253E+09	-7.47525E+04
1.448094E+03	-2.54288E+04	2.77811E+08	1.18498E+04	-1.75253E+09	-7.47527E+04
1.448095E+03	-2.20854E+04	2.77812E+08	1.18498E+04	-1.75254E+09	-7.47529E+04
1.448096E+03	-1.87420E+04	2.77813E+08	1.18499E+04	-1.75254E+09	-7.47531E+04
1.448096E+03	-1.53985E+04	2.77814E+08	1.18499E+04	-1.75255E+09	-7.47532E+04
1.448097E+03	-1.20551E+04	2.77815E+08	1.18499E+04	-1.75255E+09	-7.47534E+04
1.448098E+03	-8.71160E+03	2.77816E+08	1.18499E+04	-1.75256E+09	-7.47536E+04
1.448099E+03	-5.36809E+03	2.77817E+08	1.18500E+04	-1.75257E+09	-7.47538E+04
1.448100E+03	-2.02456E+03	2.77818E+08	1.18500E+04	-1.75257E+09	-7.47540E+04
1.448100E+03	1.31898E+03	2.77819E+08	1.18500E+04	-1.75258E+09	-7.47542E+04
1.448101E+03	4.66255E+03	2.77820E+08	1.18501E+04	-1.75258E+09	-7.47544E+04
1.448102E+03	8.00613E+03	2.77821E+08	1.18501E+04	-1.75259E+09	-7.47545E+04
1.448103E+03	1.13497E+04	2.77822E+08	1.18501E+04	-1.75259E+09	-7.47547E+04
1.448104E+03	1.46934E+04	2.77822E+08	1.18502E+04	-1.75260E+09	-7.47549E+04

Frequency at which Delta = 0

1448.100	0.0	2.77819E+08	1.18500E+04	-1.75258E+09	-7.47541E+04

(13828 rpm)

First Natural Frequency (Light Blade)

Operating rpm 759 (79.4118 rad/s)

Frequency (rad/s)	Delta	Coefficients			
		Am	Ay	Bm	By
9.987550E+01	3.75536E-01	6.90470E+03	2.51694E+00	-4.13426E+05	-1.50704E+02
9.987551E+01	3.32246E-01	6.90470E+03	2.51694E+00	-4.13426E+05	-1.50704E+02
9.987552E+01	2.88956E-01	6.90470E+03	2.51694E+00	-4.13426E+05	-1.50704E+02
9.987553E+01	2.45666E-01	6.90470E+03	2.51694E+00	-4.13426E+05	-1.50704E+02
9.987553E+01	2.02376E-01	6.90470E+03	2.51694E+00	-4.13426E+05	-1.50704E+02
9.987554E+01	1.59087E-01	6.90471E+03	2.51694E+00	-4.13426E+05	-1.50704E+02
9.987555E+01	1.15797E-01	6.90471E+03	2.51694E+00	-4.13426E+05	-1.50704E+02
9.987556E+01	7.25066E-02	6.90471E+03	2.51694E+00	-4.13426E+05	-1.50704E+02
9.987557E+01	2.92166E-02	6.90471E+03	2.51694E+00	-4.13426E+05	-1.50704E+02
9.987557E+01	-1.40733E-02	6.90471E+03	2.51695E+00	-4.13426E+05	-1.50704E+02
9.987558E+01	-5.73633E-02	6.90471E+03	2.51695E+00	-4.13426E+05	-1.50704E+02
9.987559E+01	-1.00653E-01	6.90471E+03	2.51695E+00	-4.13426E+05	-1.50704E+02
9.987560E+01	-1.43943E-01	6.90471E+03	2.51695E+00	-4.13426E+05	-1.50704E+02

Frequency at which Delta = 0

99.87557	0.0	6.90471E+03	2.51695	-4.13426E+05	-1.50504E+02

(954 rpm)

2nd Natural Frequency (Light Blade)

Operating rpm 759 (79.4118 rad/s)

Frequency (rad/s)	Delta	Coefficients			
		Am	Ay	Bm	By
4.004961E+02	-1.03982E+00	1.91468E+05	3.05355E+01	-2.91981E+06	-4.65656E+02
4.004961E+02	-8.98344E-01	1.91468E+05	3.05355E+01	-2.91981E+06	-4.65656E+02
4.004961E+02	-7.56864E-01	1.91468E+05	3.05355E+01	-2.91981E+06	-4.65656E+02
4.004961E+02	-6.15385E-01	1.91468E+05	3.05355E+01	-2.91981E+06	-4.65656E+02
4.004961E+02	-4.73906E-01	1.91468E+05	3.05355E+01	-2.91981E+06	-4.65656E+02
4.004962E+02	-3.32426E-01	1.91468E+05	3.05355E+01	-2.91981E+06	-4.65656E+02
4.004962E+02	-1.90947E-01	1.91468E+05	3.05355E+01	-2.91981E+06	-4.65656E+02
4.004962E+02	-4.94674E-02	1.91468E+05	3.05355E+01	-2.91981E+06	-4.65656E+02
4.004962E+02	9.20121E-02	1.91468E+05	3.05356E+01	-2.91981E+06	-4.65656E+02
4.004962E+02	2.33492E-01	1.91468E+05	3.05356E+01	-2.91981E+06	-4.65656E+02
4.004962E+02	3.74971E-01	1.91468E+05	3.05356E+01	-2.91981E+06	-4.65656E+02
4.004962E+02	5.16451E-01	1.91468E+05	3.05356E+01	-2.91981E+06	-4.65656E+02
4.004962E+02	6.57930E-01	1.91468E+05	3.05356E+01	-2.91981E+06	-4.65656E+02
4.004962E+02	7.99410E-01	1.91468E+05	3.05356E+01	-2.91981E+06	-4.65656E+02
4.004962E+02	9.40889E-01	1.91468E+05	3.05356E+01	-2.91982E+06	-4.65656E+02
4.004962E+02	1.08237E+00	1.91468E+05	3.05356E+01	-2.91982E+06	-4.65656E+02
4.004962E+02	1.22385E+00	1.91468E+05	3.05356E+01	-2.91982E+06	-4.65656E+02
4.004962E+02	1.36533E+00	1.91468E+05	3.05356E+01	-2.91982E+06	-4.65656E+02

Frequency at which Delta = 0

400.4962	0.0	1.91468E+05	3.05356E+01	-2.91981E+06	-4.65656E+02

(3824 rpm)

3rd Natural Frequency (Light Blade)

Operating rpm 759 (79.4118 rad/s)

Frequency (rad/s)	Delta	Coefficients			
		Am	Ay	Bm	By
1.062360E+03	1.49707E+03	7.06185E+06	4.97993E+02	-6.33427E+07	-4.46686E+03
1.062361E+03	1.31505E+03	7.06187E+06	4.97995E+02	-6.33429E+07	-4.46687E+03
1.062362E+03	1.13303E+03	7.06189E+06	4.97996E+02	-6.33431E+07	-4.46688E+03
1.062362E+03	9.51010E+02	7.06192E+06	4.97997E+02	-6.33433E+07	-4.46689E+03
1.062363E+03	7.68988E+02	7.06194E+06	4.97999E+02	-6.33435E+07	-4.46690E+03
1.062364E+03	5.86965E+02	7.06197E+06	4.98000E+02	-6.33437E+07	-4.46691E+03
1.062365E+03	4.04941E+02	7.06199E+06	4.98001E+02	-6.33439E+07	-4.46692E+03
1.062365E+03	2.22916E+02	7.06201E+06	4.98003E+02	-6.33441E+07	-4.46693E+03
1.062366E+03	4.08897E+01	7.06204E+06	4.98004E+02	-6.33443E+07	-4.46694E+03
1.062367E+03	-1.41137E+02	7.06206E+06	4.98005E+02	-6.33444E+07	-4.46695E+03
1.062368E+03	-3.23166E+02	7.06209E+06	4.98007E+02	-6.33446E+07	-4.46696E+03
1.062369E+03	-5.05195E+02	7.06211E+06	4.98008E+02	-6.33448E+07	-4.46697E+03
1.062369E+03	-6.87225E+02	7.06213E+06	4.98009E+02	-6.33450E+07	-4.46698E+03
1.062370E+03	-8.69256E+02	7.06216E+06	4.98011E+02	-6.33452E+07	-4.46699E+03
1.062371E+03	-1.05129E+03	7.06218E+06	4.98012E+02	-6.33454E+07	-4.46700E+03

Frequency at which Delta = 0

1062.366	0.0	7.06204E+06	4.98004E+02	-6.33443E+07	-4.46694E+03

(10145 rpm)

4th Natural Frequency (Light Blade)

Operating rpm 759 (79.4118 rad/s)

Frequency (rad/s)	Delta	Coefficients			
		Am	Ay	Bm	By
2.090913E+03	-1.47646E+04	2.52950E+08	9.15755E+03	-1.68095E+09	-6.08555E+04
2.090913E+03	-1.15527E+04	2.52951E+08	9.15757E+03	-1.68096E+09	-6.08556E+04
2.090914E+03	-8.34069E+03	2.52952E+08	9.15759E+03	-1.68096E+09	-6.08557E+04
2.090915E+03	-5.12869E+03	2.52952E+08	9.15761E+03	-1.68097E+09	-6.08558E+04
2.090916E+03	-1.91669E+03	2.52953E+08	9.15762E+03	-1.68097E+09	-6.08559E+04
2.090917E+03	1.29533E+03	2.52953E+08	9.15764E+03	-1.68097E+09	-6.08560E+04
2.090917E+03	4.50736E+03	2.52954E+08	9.15766E+03	-1.68098E+09	-6.08561E+04
2.090918E+03	7.71941E+03	2.52955E+08	9.15768E+03	-1.68098E+09	-6.08563E+04
2.090919E+03	1.09315E+04	2.52955E+08	9.15769E+03	-1.68098E+09	-6.08564E+04

Frequency at which Delta = 0

2090.917	0.0	2.52953E+08	9.15764E+03	-1.68097E+09	-60.8560E+04

(19967 rpm)

APPENDIX C: MODE SHAPE FORTRAN CODE

```
*****
* This Program is used to calculate the mode shapes once
* the natural frequencies are determined by the Myklestad
* determinant method
*****
      IMPLICIT DOUBLE PRECISION (A-H,O-Z)
      DOUBLE PRECISION RSTA(24),DMASS(24),EI(24),CENT(24),SHEAR(24)
      DOUBLE PRECISION DMOM(24),SLP(24),DEFL(24),ix(24),dm(24),
     %dx(24),mod,pi,p
      OPEN (101,FILE='MODE.OUT',STATUS='UNKNOWN')

      pi   = 3.141592654              ! PI
      g    = 32.174                   ! GRAVITATIONAL CONSTANT
      e    = 0.133                    ! HINGE OFFSET RATIO
      RAD  = 68.0                     ! ROTOR RADIUS
      R0   = e*RAD                    ! HINGE POINT
      C    = 6.5                      ! CHORD
      t0   = .13                      ! ROOT SECTION THICKNESS (t/c)
      tt   = .13                      ! TIP SECTION THICKNESS (t/c)
      p    = .0                       ! DENSITY OF SPRUCE lbm/in^3
      mod =  1305000.0                ! MODULUS OF ELASTICITY SPRUCE

      PRINT *,'ENTER ROTOR RPM AND NATURAL FREQUENCY'
      READ *,rpm,wrpm
      RV=rpm*2.0*pi/60.0
      w=wrpm*2.0*pi/60

! THE FOLLOWING ARRAYS ARE NUMBERED FROM BLADE TIP TO ROOT:

! SEGMENT RADIUS (IN)
      DATA RSTA/65.6,62.0,59.6,57.2,54.8,52.4,50.0,47.6,45.2,42.8,
     %40.4,38.0,35.6,33.2,30.8,28.4,26.0,23.6,21.2,18.8,16.4,14.0,
     %11.6,9.2/

! SEGMENT SPACING (IN)
      DATA dx/4.8,23*2.4/

! SEGMENT WEIGHT (LBS)
      DATA dm/.353,20*.177,.302,.252,.470/

! SEGMENT FLAPWISE MOMENT OF INERTIA, IXX (IN^4)
      DATA ix/21*.478,.48,.400,.845/



C      DO 10 J=24,1,-1
C         x = (J-1)*dx(LL)+0.5*dx(LL)
C         RSTA(25-J)= x
C         t = ((RAD-R0-x)*(t0-tt)/(RAD-R0)+tt)*C
C         dm  = (2.0*6.60*0.2850+2.0*t*0.1250)*p*dx(LL)
C         DMASS(25-J) = dm/g
C         i  = (2.0*6.85*.2850)*((.5*(t-.1425))**2.0)
C         EI(25-J) = i*mod
C10    CONTINUE

! CENTRIFUGAL FORCES COMPUTED ALONG THE BLADE

      DMASS(1)=dm(1)/g

      CENT(1)=DMASS(1)*(R0+RSTA(1))*(RV**2)/12
```

```
      DO 30 J=2,24
         DMASS(J)=dm(J)/G
         EI(J)=ix(J)*mod
         CENT(J)=CENT(J-1)+DMASS(J)*(RO+RSTA(J))*(RV**2)/12
30    CONTINUE

! ITERATION LOOP
         SLP(1)    = 0.0          ! BC'S AT TIP FOR Ay AND Am
         DEFL(1)   = 1.0
         DMOM(1)   = 0.0
         SHEAR(1)  = 0.0
      DO 40 KK=1,2
      DO 50 LL=2,24               ! MYKLESTAD INTEGRATION
         SLP1=SLP(LL-1)*(1+CENT(LL-1)*(dx(LL)**2)/2/EI(LL))
         SLP2=DMOM(LL-1)*dx(LL)/EI(LL)
         SLP3=SHEAR(LL-1)*(dx(LL)**2)/2/EI(LL)
         SLP(LL)=SLP1-SLP2-SLP3
         DEFL1=SLP(LL)*dx(LL)
         DEFL2=CENT(LL-1)*SLP(LL-1)*(dx(LL)**3)/3/EI(LL)
         DEFL3=DMOM(LL-1)*(dx(LL)**2)/2/EI(LL)
         DEFL4=SHEAR(LL-1)*(dx(LL)**3)/3/EI(LL)
         DEFL(LL)=DEFL(LL-1)-DEFL1+DEFL2-DEFL3-DEFL4
         SHEAR(LL)=SHEAR(LL-1)+DMASS(LL)*(w**2)*DEFL(LL)/12
         DMOM1=SHEAR(LL-1)*dx(LL)
         DMOM2=CENT(LL-1)*(DEFL(LL-1)-DEFL(LL))
         DMOM(LL)=DMOM(LL-1)+DMOM1-DMOM2
50    CONTINUE
      IF (KK.EQ.1) THEN           ! COEF. COMPUTATION
         Ay=DEFL(24)
         Am=DMOM(24)
      ELSE
         By=DEFL(24)
         Bm=DMOM(24)
      END IF
      SLP(1)=1.0                  ! BC'S FOR By AND Bm
      DEFL(1)=0.0
40    CONTINUE                    ! LOOP FOR By AND Bm
      DET=Am*By-Ay*Bm
      PRINT *,DET

         SLP(1)    = -Ay/By
         DEFL(1)   = 1.0
         DMOM(1)   = 0.0
         SHEAR(1)  = 0.0
      DO 60 LL=2,24               ! MYKLESTAD INTEGRATION
         SLP1=SLP(LL-1)*(1+CENT(LL-1)*(dx(LL)**2)/2/EI(LL))
         SLP2=DMOM(LL-1)*dx(LL)/EI(LL)
         SLP3=SHEAR(LL-1)*(dx(LL)**2)/2/EI(LL)
         SLP(LL)=SLP1-SLP2-SLP3
         DEFL1=SLP(LL)*dx(LL)
         DEFL2=CENT(LL-1)*SLP(LL-1)*(dx(LL)**3)/3/EI(LL)
         DEFL3=DMOM(LL-1)*(dx(LL)**2)/2/EI(LL)
         DEFL4=SHEAR(LL-1)*(dx(LL)**3)/3/EI(LL)
         DEFL(LL)=DEFL(LL-1)-DEFL1+DEFL2-DEFL3-DEFL4
         SHEAR(LL)=SHEAR(LL-1)+DMASS(LL)*(w**2)*DEFL(LL)/12
         DMOM1=SHEAR(LL-1)*dx(LL)
         DMOM2=CENT(LL-1)*(DEFL(LL-1)-DEFL(LL))
         DMOM(LL)=DMOM(LL-1)+DMOM1-DMOM2
60    CONTINUE
```

```
      DO 100 J=1,24
         WRITE (101,*)J,RSTA(25-J),DEFL(25-J)
100   CONTINUE
*********************************************************************
*
*  This program was written by Lt Matt Avila
*  Modifications were made by Lt J.L. Vandiver
*
*********************************************************************


      END
```

APPENDIX D: PRELIMINARY POWER CALCULATIONS

Thesis Helicopter Design

Preliminary Power Calculations

Variables and constants from Mainrotor worksheet link

R =	8 67	ft	Wg =	150 00	lbs		
c =	0 5417	ft	Vtip =	266 82	knots	450 00	fps
b =	3		Vf =	40 00	knots	67 61	fps
A =	100 84	ft ^ 2	AR =	10 48			
sigma =	0 08133		omega	76 41	rad/s	758	rpm
DL =	1 48	psf	Ct =	3 09E 03			
BL =	0 03362		CL (avg) =	0 20			
Mu =	0 15003		rho =	2 36E 03			
Re =	1 58E + 06		@4000 ft	1 85E 03			

NACA0012	CLmax	Cdo	CLalpha	Mcr	Alpha (stall)
	1 25	0 0087	5 73	0 71	12

Power required to Hover OGE

Pi = (T ^ 1 5)/(2*rho*A) ^ 5) /B/550 HP B = Tip loss factor

B = 1 (2*Ct) ^ 5/b

B = 0 9738

Pi = 4 953 HP B(Alt) = 0 9708 Must correct the rho in Ct

Pi (alt) = 5 533 HP

Used new B and rho correction

Po = Cdo*rho*sigma*A*Vtip ^ 3/4400 HP

Po = 4 399 HP

Figure of Merit

FM = ideal pwr/ actual pwr

FM = Pi\(Pi Po)

FM = 0 53 FM range 7 to 8

This value is a low due to high tip speed and low AR It is related to DL and BL

Power required to hover IGE (ESL)

Pi(IGE)/Pi(OGE) = (0 1278*(h/D) ^ 4 + 0 7080*(h/D) ^ 3 1 4589*(h/D) ^ 2 + 1 3432*(h/D) + 0 5147)

h = height of the rotor above the surface

h = 2 5 ft

D = rotor diameter h/D = 0 2208

D = 11 33 ft

Pi(IGE)/Pi(OGE) = 0 74738

Pi(IGE) = 3 70 HP

Parasite Drag of the Fuselage

Equivalent Flat Plate Area

fe = 0 8 This was determined by a chart from a Sikorsky Study

Parasite Power (Pp) = 0 5*rho*fe*Vf ^ 3

Pp = 0 53 HP Tail rotor power req =

9% *Pi (rotor) at a hover and

3% *Pi (rotor) in midrange fwd vel

Po(flight) = Po(hover)*(1 + 4 3*Mu ^ 2)

Pi(flight) = W ^ 2/(rho*A*Vf)

Vel (knots)	Vel (fps)	Parasite	Profile	Induced	T/R pwr	Total	Adv Bld Mach
0	0 00	0 00	4 40	4 66	0 84	10 10	0 40
20	33 76	0 07	4 51	2 53	0 50	7 60	0 43
40	67 51	0 53	4 83	1 28	0 33	6 95	0 46
50	84 38	1 04	5 06	1 01	0 21	7 33	0 48
60	101 27	1 80	5 38	0 84	0 24	8 24	0 48
70	118 15	2 86	5 70	0 72	0 28	9 58	0 51
80	135 02	4 28	6 10	0 63	0 55	11 54	0 52
90	151 90	6 06	6 58	0 56	0 66	13 84	0 54
100	168 78	8 32	7 06	0 51	0 78	16 68	0 55

4000 ft 95 deg F = > rho = 0 001817

Altitude corrections

Parasite	Profile	Induced	T/R pwr	Total	Adv Blade Mach No	
0 00	3 56	6 18	0 87	10 58	0 41	Pi(alt) = Pi(sl)*(rho(sl)/rho(alt))
0 05	3 63	3 13	0 48	7 30	0 44	Po(alt) = Po(sl)*rho(alt)/rho(sl)
0 43	3 89	1 57	0 29	6 18	0 47	Pp(alt) = Pp(sl)*rho(alt)/rho(sl)
0 84	4 08	1 25	0 18	6 36	0 48	Pi hover used different correction
1 45	4 32	1 04	0 20	7 02	0 50	It incorporated change in Ct = >
2 30	4 80	0 90	0 23	8 03	0 52	
3 43	4 92	0 78	0 48	9 58	0 53	
4 88	5 28	0 70	0 54	11 41	0 55	
6 70	5 69	0 63	0 65	13 67	0 56	

APPENDIX E: BLADE TIP PITCH ANGLE WORKSHEET

Thesis RPV Helicopter Design

Pitch Angle Determination.

Inflow ratio Lam = ((Pp/W W/(rho*A*Vt))/Vtip)
Advance Ratio Mu = Vt/Vtip
Parasite Power (Pp) = 0 5*rho*fe*Vt ^ 3
Pp = 0 33 HP

Variables and constants from Mainrotor worksheet link

R =	5 67	ft	Wg =	150 00	lbs		
c =	0 5417	ft	Vtip =	264 82	knots	450 00	fps
b =	3		Vt =	40 00	knots	67 61	fps
A =	100 84	ft ^ 2	AR =	10 46			
sigma =	0 09133		omega	78 41	rad/s	750	rpm
DL =	1 487494	psf	Ct =	0 00308			
BL =	0 033824		Cl (avg) =	0 20			
Mu =	0 15003		fe =	0 80			

NACA0012 Clmax Cdo Cl alpha Mcr Alpha(stall)
1 25 0 0097 5 73 0 71 13 ThetaT = twist

Vt(knots)	Vt(fps)	Vtip (fps)	Pp (HP)	Mu	Lam	Ct	B	sigma	c	Twist(rad)
40	67 61	450 00	0 83	0 1500	-0 0248	0 0031	0 9738	0 0913	5 73	0 00
45	73 95	450 00	0 76	0 1868	-0 0243	0 0031	0 9738	0 0913	5 73	0 00
50	84 39	450 00	1 04	0 1875	-0 0249	0 0031	0 9738	0 0913	5 73	0 00
55	92 83	450 00	1 38	0 2063	-0 0283	0 0031	0 9738	0 0913	5 73	0 00
60	101 27	450 00	1 80	0 2250	-0 0284	0 0031	0 9738	0 0913	5 73	0 00
65	109 71	450 00	2 28	0 3438	-0 0313	0 0031	0 9738	0 0913	5 73	0 00
70	118 13	450 00	2 85	0 2625	0 0350	0 0031	0 9738	0 0913	5 73	0 00
75	126 58	450 00	3 31	0 2813	0 0396	0 0031	0 9738	0 0913	5 73	0 00
80	135 03	450 00	4 26	0 3001	-0 0450	0 0031	0 9738	0 0913	5 73	0 00
85	143 46	450 00	5 11	0 3188	-0 0513	0 0031	0 9738	0 0913	5 73	0 00
90	151 90	450 00	6 08	0 3376	0 0585	0 0031	0 9738	0 0913	5 73	0 00
95	160 34	450 00	7 13	0 3563	-0 0668	0 0031	0 9738	0 0913	5 73	0 00
100	168 78	450 00	8 32	0 3751	0 0760	0 0031	0 9738	0 0913	5 73	0 00

T1 = 0 5*(B ^ 3 + 0 5*Mu ^ 2)
T2 = 0 33*(B ^ 3 + 06*Mu ^ 2*B)
T3 = 0 25*(B ^ 2*(B ^ 3 + Mu ^ 2))
T4 = 0 5*Mu*(B ^ 2 + 0 25*Mu ^ 2)

A11 = (4*(Mu*B ^ 2/2 3/8))/(B ^ 2(B ^ 3 0 5*Mu ^ 2))
A12 = (6*Mu*B)/(3*(B ^ 3 0 3*Mu ^ 2))
A13 = (2*Mu*B ^ 2)/(B ^ 3 0 5Mu ^ 3)
A14 = (B ^ 3 + 1 5*Mu ^ 2)/(B ^ 3 0 5*Mu ^ 2)

T1	T2	T3	T4	A11	A12	A13	A14
0 4786	0 3084	0 2301	0 0718	1 3878	0 4158	0 3037	1 0480
0 4613	0 3083	0 2316	0 0808	1 3321	0 4692	0 3427	1 0810
0 4629	0 3104	0 2331	0 0897	1 2986	0 5233	0 3822	1 0758
0 4648	0 3116	0 2349	0 0988	1 2813	0 5776	0 4220	1 0816
0 4668	0 3128	0 2368	0 1081	1 2263	0 6333	0 4624	1 1097
0 4690	0 3143	0 2389	0 1174	1 1012	0 6892	0 5034	1 1284
0 4714	0 3158	0 2412	0 1267	1 1564	0 7461	0 5449	1 1508
0 4738	0 3174	0 2438	0 1362	1 1316	0 8039	0 5871	1 1743
0 4767	0 3193	0 2463	0 1458	1 0866	0 8626	0 6300	1 1993
0 4796	0 3211	0 2488	0 1553	1 0521	0 9225	0 6737	1 2265
0 5028	0 3230	0 2516	0 1648	1 0173	0 9835	0 7183	1 2557
0 5058	0 3251	0 2546	0 1746	0 9823	1 0457	0 7638	1 2870
0 5093	0 3273	0 2582	0 1844	0 9473	1 1094	0 8102	1 3206

Two equations two unknowns
3(Cl/sigma)/a = LamT1 + Theta0*T2 + ThetaT*T3 + Theta2*T4
Lam*A11 + Theta0*A12 + ThetaT*A13 + Theta2*A14 = 0
Solving for Theta0 and Theta2

Theta0 = -(ThetaT*A13 + Theta2*A14 + Lam*A11)/A12
Theta2 = (A12*(2(Cl/sigma)/a-Lam*T1 ThetaT*T3) + T2*ThetaT*A13 + Lam*A11*T2)/(T4*A13 A14*T2)

Theta2	Theta0	alpha270	alpha90	alpha(270) = Theta0 Theta2 + ThetaT + Lam/(1 + Mu)
-0 07	0 08	6 08	0 12	alpha(90) = Theta0 + Theta2 + ThetaT + Lam/(1 + Mu)
0 07	0 10	6 43	0 08	
-0 08	0 10	0 00	0 00	
0 09	0 11	6 80	0 13	
0 10	0 13	10 84	0 28	
0 11	0 13	13 23	0 46	
0 13	0 14	13 95	0 73	
0 15	0 16	16 11	0 98	
0 18	0 18	18 77	1 31	
0 21	0 22	22 04	1 67	
0 25	0 25	26 06	2 08	
0 29	0 30	30 87	2 55	

Thesis RPV Helicopter Design

Pitch Angle Determination.

Inflow ratio Lam= ((Pp/W W/(rho*A*Vt))/Vtip)
Advance Ratio Mu = Vt/Vtip
Parasite Power (Pp) = 0 5*rho*fe*Vt ^ 3
Pp= 0 53 HP

Variables and constants from Mainrotor worksheet link

R=	5 67	ft	Wg=	150 00	lbs		
c=	0 5417	ft	Vtip=	266 92	knots	450 00	fps
b=	3		Vt=	40 00	knots	67 51	fps
A=	100 84	ft ^ 2	AR=	10 49			
sigma=	0 08133		omega	79 41	rad/s	758	rpm
DL=	1 487484	psf	Ct=	0 00309			
BL=	0 033624		CL(avg)=	0 20			
Mu=	0 15003		fe=	0 80			

NACA0012	CLmax	Cdo	CLalpha	Mcr	Alpha(stall)		
	1 25	0 0097	5 73	0 71	12	ThetaT = twist	-4

Vt(knots)	Vt(fps)	Vtip (fps)	Pp (HP)	Mu	Lam	Ct	B	sigma	a	Twist(rad)
40	67 51	450 00	0 53	0 1500	0 0249	0 0031	0 9738	0 0813	5 73	-0 07
45	75 95	450 00	0 76	0 1688	-0 0243	0 0031	0 9738	0 0813	5 73	-0 07
50	84 38	450 00	1 04	0 1875	-0 0249	0 0031	0 9738	0 0813	5 73	-0 07
55	92 83	450 00	1 38	0 2063	-0 0262	0 0031	0 9738	0 0813	5 73	-0 07
60	101 27	450 00	1 80	0 2250	-0 0284	0 0031	0 9738	0 0813	5 73	-0 07
65	109 71	450 00	2 28	0 2438	-0 0313	0 0031	0 9738	0 0813	5 73	-0 07
70	118 15	450 00	2 83	0 2625	-0 0350	0 0031	0 9738	0 0813	5 73	-0 07
75	126 58	450 00	3 31	0 2813	-0 0396	0 0031	0 9738	0 0813	5 73	-0 07
80	135 02	450 00	4 26	0 3001	-0 0450	0 0031	0 9738	0 0813	5 73	-0 07
85	143 46	450 00	5 11	0 3188	-0 0513	0 0031	0 9738	0 0813	5 73	-0 07
90	151 90	450 00	6 06	0 3376	-0 0585	0 0031	0 9738	0 0813	5 73	0 07
95	160 34	450 00	7 13	0 3563	-0 0666	0 0031	0 9738	0 0813	5 73	0 07
100	168 78	450 00	8 32	0 3751	0 0760	0 0031	0 9738	0 0813	5 73	0 07

T1 = 0 5*(B ^ 2 + 0 5*Mu ^ 2)
T2 = 0 33*(B ^ 3 + 05*Mu ^ 2*B)
T3 = 0 25*(B ^ 2*(B ^ 2 + Mu ^ 2))
T4 = 0 5*Mu*(B ^ 2 + 025*Mu ^ 2]

A11 = (4*(Mu*B ^ 2/2 3/8))/(B ^ 2(B ^ 2 0 5*Mu ^ 2)]
A12 = (5*Mu*B)/(3*(B ^ 2 0 3*Mu ^ 2))
A13 = (2*Mu*B ^ 2)/(B ^ 2 0 5Mu ^ 2)
A14 = (B ^ 2 + 1 5*Mu ^ 2)/(B ^ 2 0 5*Mu ^ 2)

T1	T2	T3	T4	A11	A12	A13	A14
0 4786	0 3084	0 2301	0 0716	1 3879	0 4158	0 3037	1 0480
0 4813	0 3093	0 2319	0 0808	-1 3321	0 4682	0 3427	1 0810
0 4839	0 3104	0 2331	0 0897	-1 2966	0 5232	0 3822	1 0758
0 4849	0 3119	0 2349	0 0988	-1 2813	0 5778	0 4220	1 0919
0 4868	0 3128	0 2366	0 1081	-1 2292	0 6332	0 4624	1 1067
0 4890	0 3143	0 2388	0 1174	-1 1912	0 6892	0 5034	1 1284
0 4914	0 3158	0 2412	0 1267	-1 1564	0 7491	0 5449	1 1508
0 4938	0 3174	0 2438	0 1362	-1 1219	0 8039	0 5871	1 1742
0 4967	0 3192	0 2462	0 1456	-1 0868	0 8628	0 6300	1 1993
0 4996	0 3211	0 2489	0 1552	-1 0521	0 9226	0 6737	1 2266
0 5028	0 3230	0 2516	0 1646	1 0172	0 9835	0 7183	1 2557
0 5058	0 3251	0 2540	0 1740	0 9823	1 0457	0 7636	1 2870
0 5093	0 3273	0 2582	0 1844	0 9473	1 1094	0 8102	1 3205

Two equations two unknowns
2(Ct/sigma)/a = LamT1 + Theta0*T2 + ThetaT*T3 + Theta2*T4
Lam*A11 + Theta0*A12 + ThetaT*A13 + Theta2*A14 = 0
Solving for Theta0 and Theta2

Theta0 = (ThetaT*A13 + Theta2*A14 + Lam*A11)/A12
Theta2 = [A12*(2(Ct/sigma)/a-Lam*T1-ThetaT*T3) + T2*ThetaT*A13 + Lam*A11*T2]/(T4*A12 A14*T2]

Theta2	Theta0	alpha270	alpha90	alpha(270) = Theta0 Theta2 + ThetaT + Lam/(1 + Mu]
-0 07	0 19	7 10	-0 92	alpha(90) = Theta0 + Theta2 + ThetaT + Lam/(1 + Mu]
-0 07	0 15	7 47	-0 95	
-0 08	0 15	8 08	-1 03	
-0 09	0 16	8 89	-1 13	
-0 10	0 17	9 99	1 30	
-0 11	0 18	11 40	-1 50	
-0 13	0 20	13 17	-1 73	
-0 15	0 22	15 38	2 01	
-0 18	0 24	18 11	2 32	
-0 21	0 27	21 49	2 88	
-0 25	0 31	25 58	3 09	
0 30	0 35	30 58	3 55	

Thesis RPV Helicopter Design

Pitch Angle Determination.

Inflow ratio Lam = ((Pp/W W/(rho*A*Vtip))/Vtip)
Advance Ratio Mu = Vt/Vtip
Parasite Power (Pp) = 0 5*rho*fe*Vt ^ 3
Pp = 0 83 HP

Variables and constants from Mainrotor worksheet link

R =	5 67	ft	Wg =	150 00	lbs		
c =	0 5417	ft	Vtip =	288 82	knots	450 00	fps
b =	3		Vt =	40 00	knots	67 51	fps
A =	100 64	ft ^ 2	AR =	10 48			
sigma =	0 08133		omega	79 41	rad/s	758	rpm
DL =	1 487494	psf	Ct =	0 00309			
BL =	0 033824		Cl (avg) =	0 20			
Mu =	0 15003		fe =	0 80			

NACA0012 Cl max 1 25 | Cdo 0 0097 | Cl alpha 5 73 | Mcr 0 71 | Alpha(stall) 12 | ThetaT = twist

Vt(knots)	Vt(fps)	Vtip (fps)	Pp (HP)	Mu	Lam	Ct	B	sigma	a	Twist(rad)
40	67 51	450 00	0 53	0 1500	0 0246	0 0031	0 9738	0 0813	5 73	-0 14
45	75 95	450 00	0 78	0 1688	-0 0245	0 0031	0 9738	0 0813	5 73	0 14
50	84 39	450 00	1 04	0 1875	-0 0248	0 0031	0 9738	0 0813	5 73	-0 14
55	92 83	450 00	1 38	0 2063	-0 0282	0 0031	0 9738	0 0813	5 73	-0 14
60	101 27	450 00	1 80	0 2250	-0 0284	0 0031	0 9738	0 0813	5 73	-0 14
65	109 71	450 00	2 28	0 2438	0 0313	0 0031	0 9738	0 0813	5 73	-0 14
70	118 15	450 00	2 85	0 2625	0 0350	0 0031	0 9738	0 0813	5 73	-0 14
75	126 59	450 00	3 51	0 2813	-0 0398	0 0031	0 9738	0 0813	5 73	-0 14
80	135 02	450 00	4 28	0 3001	0 0450	0 0031	0 9738	0 0813	5 73	-0 14
85	143 46	450 00	5 11	0 3188	-0 0513	0 0031	0 9738	0 0813	5 73	-0 14
90	151 90	450 00	6 09	0 3376	-0 0585	0 0031	0 9738	0 0813	5 73	-0 14
95	160 34	450 00	7 13	0 3563	-0 0666	0 0031	0 9738	0 0813	5 73	-0 14
100	168 78	450 00	8 32	0 3751	0 0760	0 0031	0 9738	0 0813	5 73	-0 14

T1 = 0 5*(B ^ 2 + 0 5*Mu ^ 2)
T2 = 0 33*(B ^ 2 + 05*Mu ^ 2*B)
T3 = 0 25*(B ^ 2*(B ^ 2 + Mu ^ 2))
T4 = 0 5*Mu*(B ^ 2 + 025*Mu ^ 2)

A11 = (4*(Mu*B ^ 2/2 3/8))/(B ^ 2(B ^ 2-0 5*Mu ^ 2))
A12 = (6*Mu*B)/(3*(B ^ 2 0 5*Mu ^ 2))
A13 = (2*Mu*B ^ 2)/(B ^ 2 0 5Mu ^ 2)
A14 = (B ^ 2 + 1 5*Mu ^ 2)/(B ^ 2 0 5*Mu ^ 2)

T1	T2	T3	T4	A11	A12	A13	A14
0 4798	0 3084	0 2301	0 0718	1 3878	0 4158	0 3037	1 0480
0 4813	0 3093	0 2318	0 0808	-1 3321	0 4692	0 3427	1 0610
0 4828	0 3104	0 2331	0 0897	-1 2966	0 5232	0 3822	1 0756
0 4846	0 3116	0 2349	0 0989	-1 2813	0 5778	0 4220	1 0918
0 4868	0 3128	0 2368	0 1081	-1 2262	0 6332	0 4624	1 1097
0 4890	0 3143	0 2389	0 1174	1 1812	0 6892	0 5034	1 1294
0 4914	0 3158	0 2412	0 1267	-1 1584	0 7461	0 5449	1 1508
0 4938	0 3174	0 2438	0 1362	1 1218	0 8039	0 5871	1 1742
0 4967	0 3192	0 2462	0 1456	1 0888	0 8626	0 6300	1 1993
0 4998	0 3211	0 2488	0 1552	-1 0521	0 9225	0 6737	1 2265
0 5028	0 3230	0 2518	0 1648	-1 0172	0 9835	0 7183	1 2557
0 5058	0 3251	0 2548	0 1748	-0 9823	1 0457	0 7638	1 2870
0 5083	0 3273	0 2582	0 1844	-0 9473	1 1094	0 8102	1 3206

Two equations two unknowns
2(Cl/sigma)/a = Lam*T1 + Theta0*T2 + ThetaT*T3 + Theta2*T4
Lam*A11 + Theta0*A12 + ThetaT*A13 + Theta2*A14 = 0
Solving for Theta0 and Theta2

Theta0 = (ThetaT*A13 + Theta2*A14 + Lam*A11)/A12
Theta2 = (A12*(2(Cl/sigma)/a Lam*T1 ThetaT*T3) + T2*ThetaT*A13 + Lam*A11*T2)/(T4*A12 A14*T2)

Theta2	Theta0	alpha270	alpha90
-0 07	0 20	5 12	-1 98
0 07	0 20	8 51	1 98
0 04	0 20	7 13	-2 09
0 09	0 21	7 98	2 17
-0 10	0 22	9 12	2 32
0 11	0 24	10 57	2 52
0 13	0 25	12 39	2 75
0 15	0 27	14 85	-3 02
0 18	0 30	17 45	-3 33
0 21	0 33	20 87	3 69
0 25	0 37	25 07	4 10
0 30	0 41	30 19	4 58

alpha(270) = Theta0 Theta2 + ThetaT + Lam/(1 + Mu)
alpha(90) = Theta0 + Theta2 + ThetaT + Lam/(1 + Mu)

LIST OF REFERENCES

1. McGovern, J.J., Flight Operations for Higher Harmonic Control Research, Master's Thesis, Naval Postgraduate School, Monterey, California, March 1991.

2. Seddon, J., Basic Helicopter Aerodynamics, American Institute of Aeronautics and Astronautics, Inc.,1990.

3. Prouty, R.W., Helicopter Performance, Stability, and Control, PWS Publishers,1986.

4. Prouty, R.W., "The Preliminary Design Process," not dated.

5 U.S. Army Transportation Research Command, Report 64-15, Parametric Investigation of the Aerodynamic and Aeroelastic Characteristics of Articulated and Rigid (Hingeless) Helicopter Rotor Systems, by E.R. Wood and A.C. Buffalano, p. 35, April 1964.

6. Wood, E.R., "An Introduction to Helicopter Dynamics," Lecture notes from the Department of Aeronautics and Astornautics at the Naval Postgraduate School, Monterey, California, not dated.

7. Kuethe, A.M., and Chow, C., Foundations of Aerodynamics: Bases of Aerodynamic Design, 3rd ed., pp. 303-305, John Wiley & Sons, Inc., 1976.

8. Gessow, A., and Myer, G.C., Aerodynamics of the Helicopter, Frederick Ungar Publishing Co.,1967.

9. Layton, D.M., "Helicopter Conceptual Design," Lecture notes from the Department of Aeronautics and Astornautics at the Naval Postgraduate School, Monterey, California, June 1988.

10. Westlake Aeromarine Engines Limited, "Operators Handbook for WAE Limited 342 Engine Series 2100D," Normalair-Garrett, Ltd., 1985.

11. Taylor, John W.R., ed., Janes's All The Worlds Aircraft 1981-82, p. 758, Jane's Publishing Inc., 1982.

12. Scott, J.G., Establishment of a Remotely Piloted Helicopter Test Flight Program for Higher Harmonic Control Research, Master's Thesis, Naval Postgraduate School, Monterey, California, June 1990.

13. Webb, C.D., Initial Design Study of Existing Flight Control Systems of RPH and Feasibility Study of Implementing HHC on the SH-60B, Master's Thesis, Naval Postgraduate School, Monterey, California, September 1990.

INITIAL DISTRIBUTION LIST

		No. of Copies
1.	Defense Technical Information Center Cameron Station Alexandria, Virginia 22304-6145	2
2.	Library, Code 52 Naval Postgraduate School Monterey, California 93943-5000	2
3.	Professor E. Roberts Wood, Code AA/Wd Department of Aeronautics and Astronautics Naval Postgraduate School Monterey, California 93943-5000	6
4.	Professor Ramesh Kolar, Code AA/Kj Department of Aeronautics and Astronautics Naval Postgraduate School Monterey, California 93943-5000	2
5.	LT James L. Vandiver 729 G Avenue Coronado, California 92118	2

Thesis
V162527 Vandiver
c.1 RPH preliminary design, trend analysis and initial analysis of the NPS Hummingbird.